SPINTRONICS

Jacek.Szczytko@fuw.edu.pl

(Yatzek Schtchitko)

Faculty of Physics, University of Warsaw

University of Warsaw

inżynieria nanostruktur

ELBYSIER

Electronics Beyond Silicon Era

Google: Jacek Szczytko

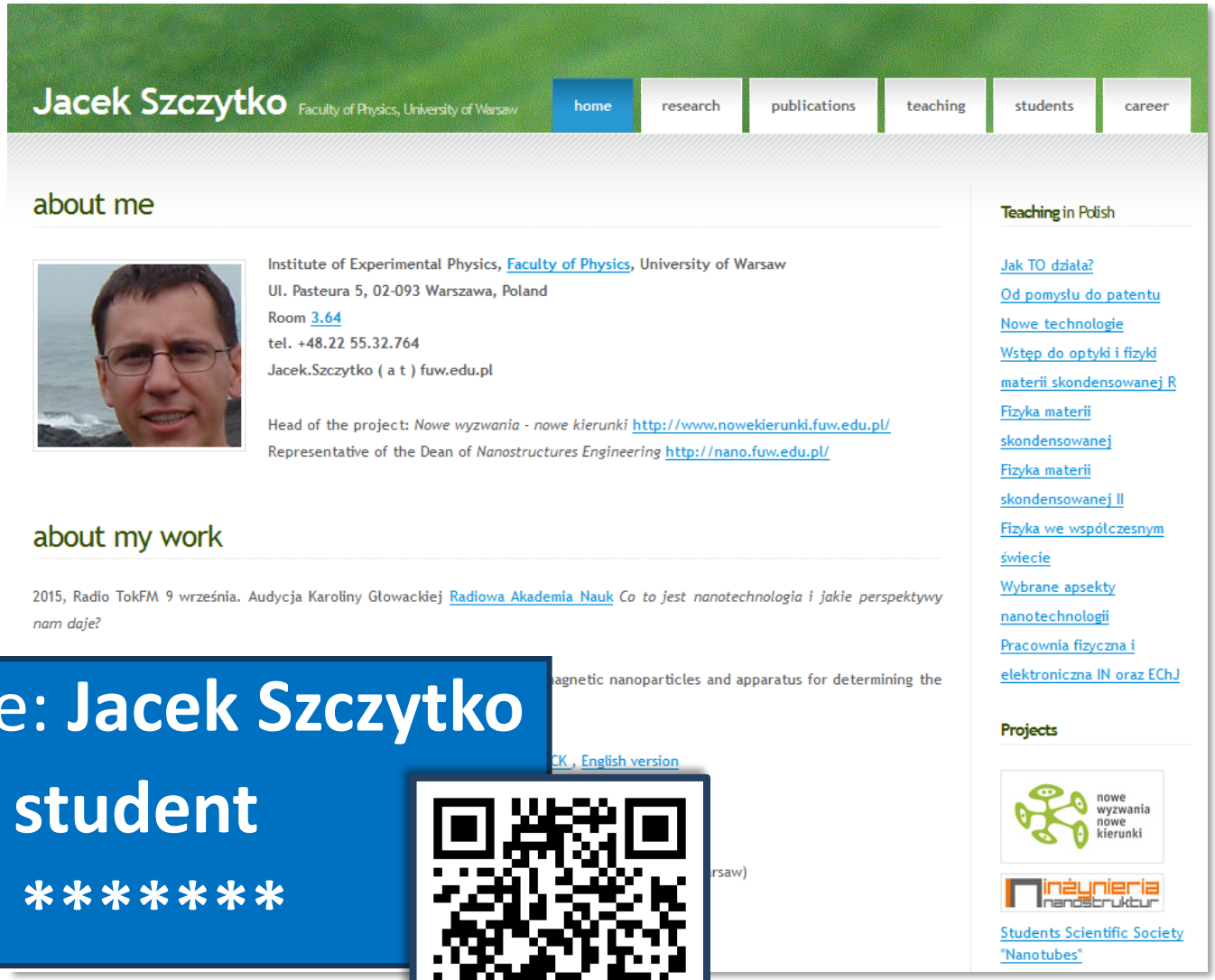

Google: **Jacek Szczytko**

Login: **student**

Hasło: *******

Faculty of Physics, University of Warsaw

Hoża 69: 1921-2014 r.

WYDZIAŁ FIZYKI
UNIWERSYTET WARSZAWSKI

INFRASTRUKTURA I ŚRODOWISKO
NARODOWA STRATEGIA SPÓJNOŚCI

UNIA EUROPEJSKA
EUROPEJSKI FUNDUSZ ROZWOJU REGIONALNEGO

The polariton laboratory

attocube CFM
1.5-320K, 0.0-9.0T
700-1000nm
420nm, 532nm, 633nm…

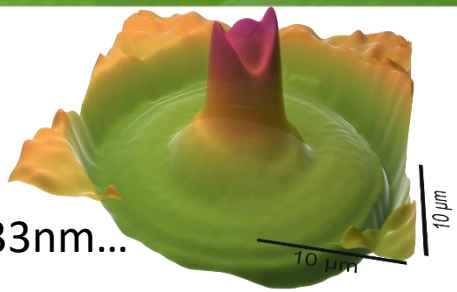

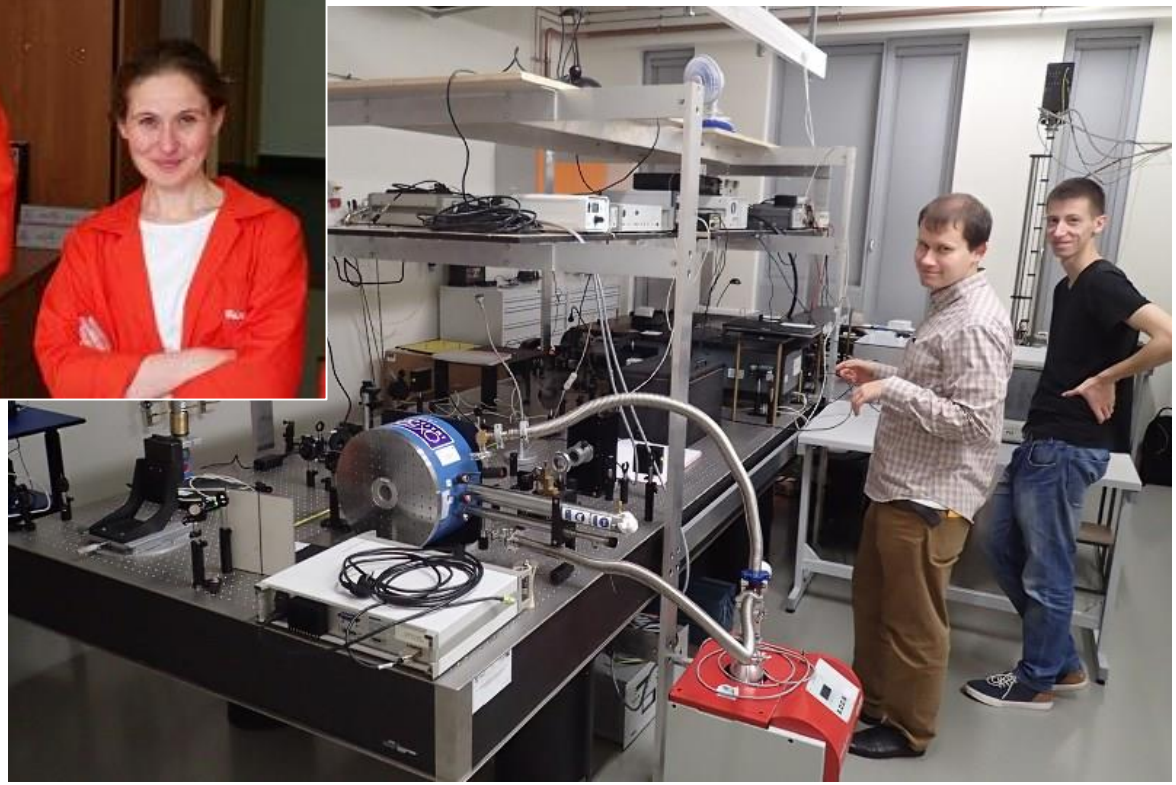

Kasia Lekenta

Dr Barbara Piętka

Mateusz Król

Rafał Mirek

The polariton laboratory

Appl. Phys. Lett. 107, 201109 (2015)

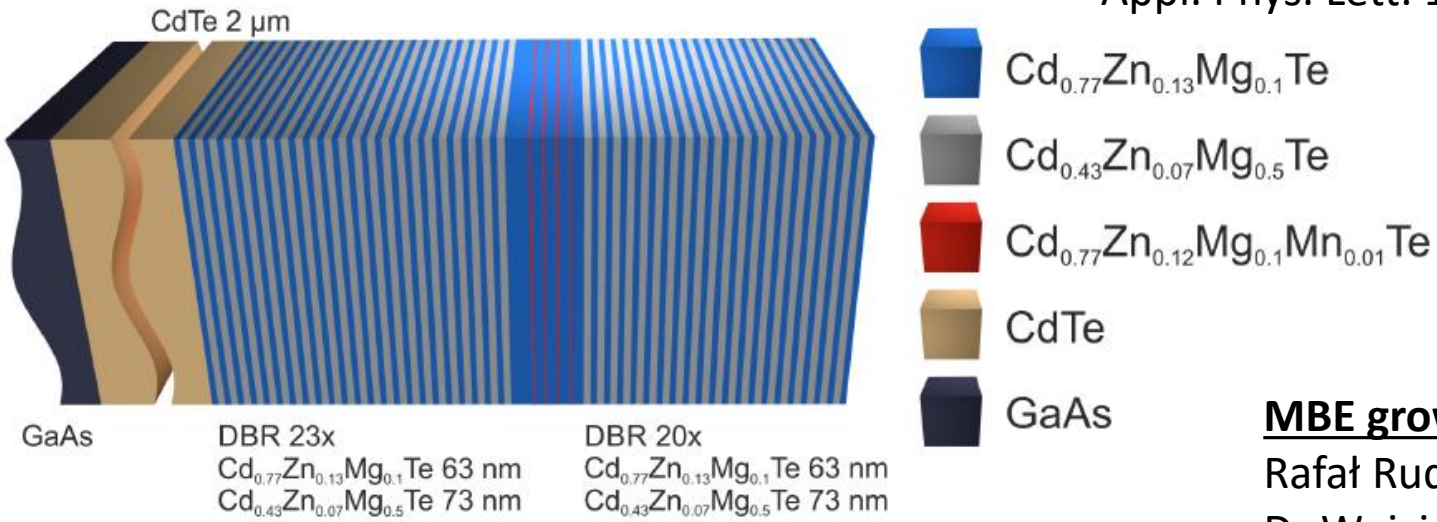

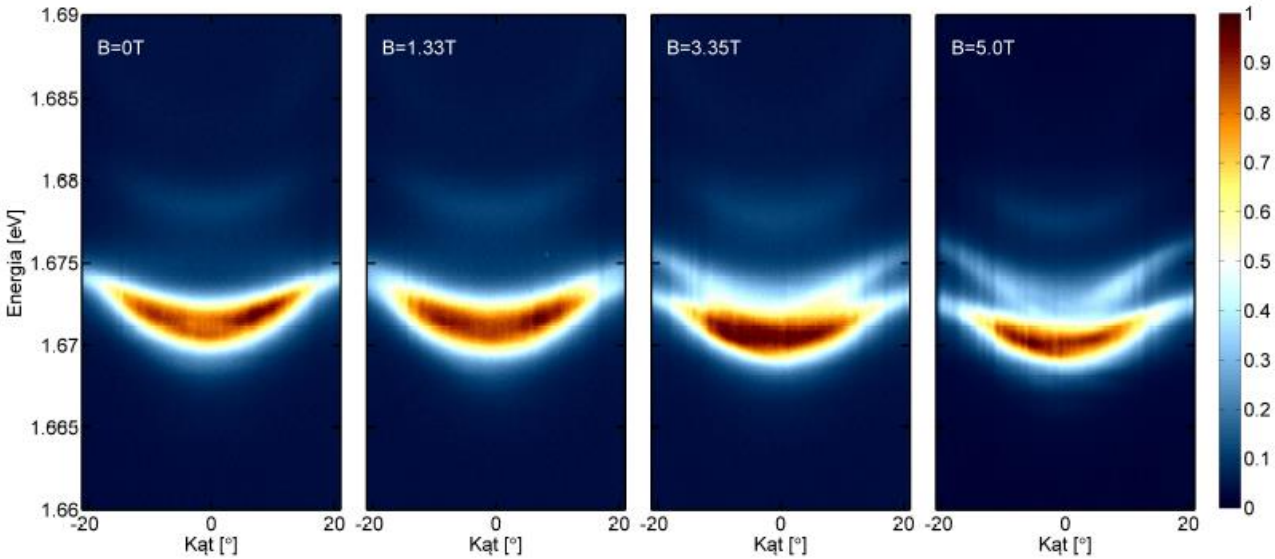

MBE growth:
Rafał Rudniewski,
Dr Wojciech Pacuski,
Jean-Guy Rousset

Magneto-optical properties
Rafał Mirek
Katarzyna Lekenta
Mateusz Król
Dr Barbara Piętka

Laboratory of SQUID magnetometry

Andrzej Twardowski
Andrzej Majhofer
Anita Gardias
Jarosław Rybusiński
Maciej Marchwiany (Monte Carlo)

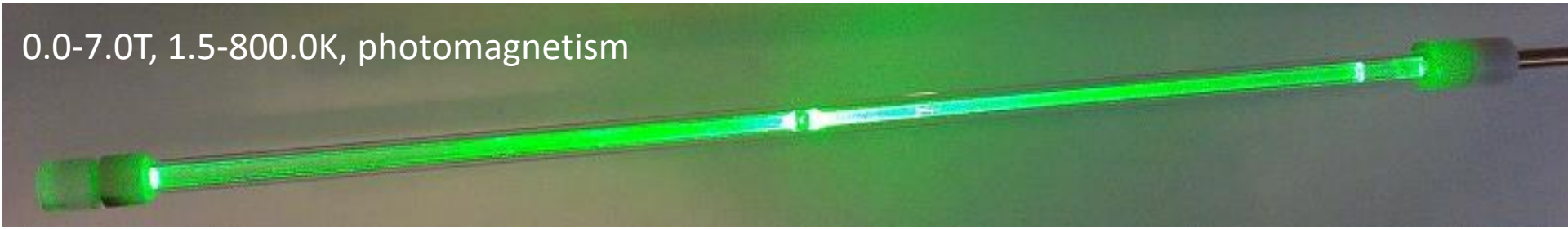

Magnetic nanoparticles

BioMACROMOLECULES

Article

pubs.acs.org/Biomac

Magnetic-Nanoparticle-Decorated Polypyrrole Microvessels: Toward Encapsulation of mRNA Cap Analogues

Krystyna Kijewska,[†] Anita Jarzębińska,[†] Joanna Kowalska,[‡] Jacek Jemielity,[‡,§] Daria Kępińska,[†] Jacek Szczytko,[∥] Marcin Pisarek,[⊥] Katarzyna Wiktorska,[¶] Jarosław Stolarski,[#] Paweł Krysiński,[†] Andrzej Twardowski,[∥] and Maciej Mazur*,[†]

THE JOURNAL OF PHYSICAL CHEMISTRY C

Adsorption of Doxorubicin onto Citrate-Stabilized Magnetic Nanoparticles

Krzysztof Nawara,[†] Jerzy Romiszewski,[†] Krystyna Kijewska,[†] Jacek Szczytko,[‡] Andrzej Twardowski,[‡] Maciej Mazur,[†] and Paweł Krysinski*,[†]

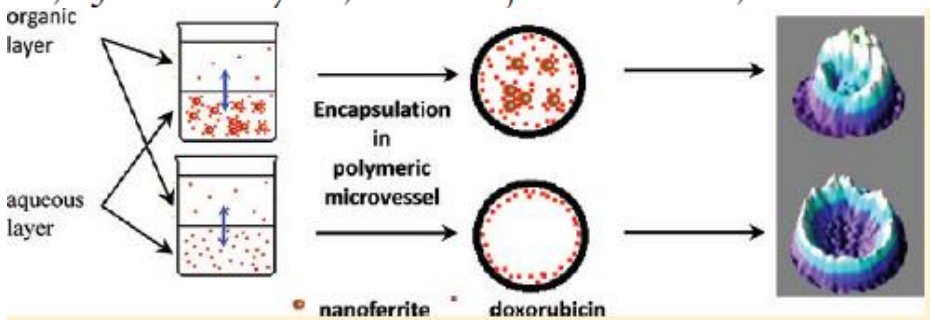

Magnetic Organic LC

Piotr Kaszyński (Univ. Vanderbilt USA, The Centre of Molecular and Macromolecular Studies, Lodz, Poland)
Ewa Górecka (Faculty of Chemistry, University of Warsaw)
Damian Pociecha (Faculty of Chemistry, University of Warsaw)

Piotr

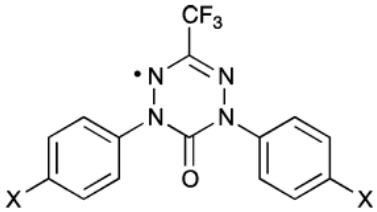

Ewa

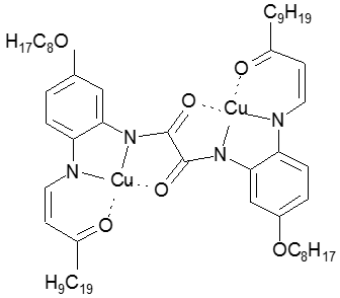

Magnetic Organic LC

JACS
JOURNAL OF THE AMERICAN CHEMICAL SOCIETY
Communication
pubs.acs.org/JACS

Photoconductive Liquid-Crystalline Derivatives of 6-Oxoverdazyl

Aleksandra Jankowiak,[†] Damian Pociecha,[‡] Jacek Szczytko,[§] Hirosato Monobe,[∥] and Piotr Kaszyński*[,†,⊥]

[†]Organic Materials Research Group, Department of Chemistry, Vanderbilt University, Nashville, Tennessee 37235, United States
[‡]Department of Chemistry, University of Warsaw, 02-089 Warsaw, Poland
[§]Institute of Experimental Physics, Faculty of Physics, University of Warsaw, Hoża 69, 00-681 Warsaw, Poland
[∥]Research Institute for Ubiquitous Energy Devices, National Institute of Advanced Industrial Science and Technology, AIST Kansai Centre, Ikeda, Osaka 563-8577, Japan
[⊥]Faculty of Chemistry, University of Łódź, Tamka 12, 91-403 Łódź, Poland

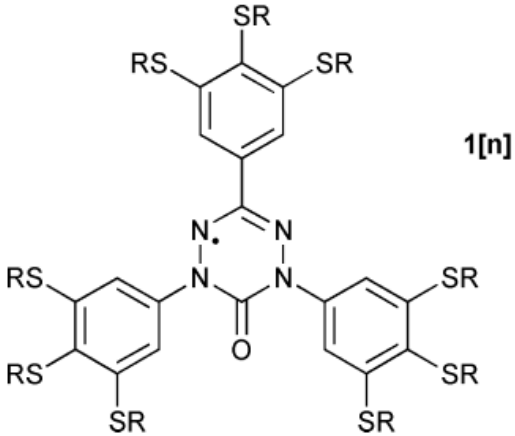

JACS
JOURNAL OF THE AMERICAN CHEMICAL SOCIETY
Communication
pubs.acs.org/JACS

Tetragonal Phase of 6-Oxoverdazyl Bent-Core Derivatives with Photoinduced Ambipolar Charge Transport and Electrooptical Effects

Marcin Jasiński,[†] Damian Pociecha,[‡] Hirosato Monobe,[§] Jacek Szczytko,[∥] and Piotr Kaszyński*[,†,⊥]

[†]Faculty of Chemistry, University of Łódź, Tamka 12, 91403 Łódź, Poland
[‡]Department of Chemistry, University of Warsaw, 02-089 Warsaw, Poland
[§]Research Institute for Ubiquitous Energy Devices, National Institute of Advanced Industrial Science and Technology (AIST), Ikeda, Osaka 563-8577, Japan
[∥]Institute of Experimental Physics, Faculty of Physics, University of Warsaw, Hoża 69, 00-681 Warsaw, Poland
[⊥]Organic Materials Research Group, Department of Chemistry, Vanderbilt University, Nashville, Tennessee 37235, United States

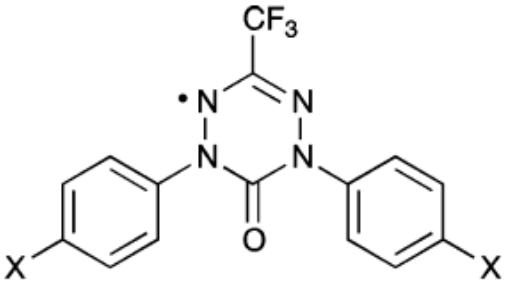

ORGANIC SPINTRONICS

1. Magnetic field and spin
2. Exchange interactions
3. Magnetism of matter
4. Spintronics
5. Organics spintronics
   a. Magnetism
   b. Transport
   c. Light
   d. Liquid crystals

S. Harris

ELBYSIER
Electronics Beyond Silicon Era

Hamiltonian

$$\left\{\frac{1}{2m}\hat{p}^2 + U(\vec{r},t)\right\}\psi(\vec{r},t) = i\hbar\frac{d}{dt}\psi(\vec{r},t)$$

kinetic energy

$$E_k = \frac{mv^2}{s} = \frac{p^2}{2m}$$

potential energy

time evolution

Homogenous magnetic field

The Landau gauge solution

$$\left\{\frac{1}{2m}\left[\hat{p} - q\,\vec{A}(\vec{r},t)\right]^2 + q\varphi(\vec{r},t) + U(\vec{r},t)\right\}\psi(\vec{r},t) = i\hbar\frac{d}{dt}\psi(\vec{r},t)$$

„free electron” $(U(x,y,z) = U(z)) \Rightarrow$ **Landau levels**

Homogenous magnetic field

The Landau gauge solution

$$\left\{\frac{1}{2m}\left[\hat{p} - q\,\vec{A}(\vec{r},t)\right]^2 + q\varphi(\vec{r},t) + U(\vec{r},t)\right\}\psi(\vec{r},t) = i\hbar\frac{d}{dt}\psi(\vec{r},t)$$

Landau gauge: magnetic field $\vec{B} = (0,0,B_z) \Rightarrow B_z = \frac{\partial A_y}{\partial x} - \frac{\partial A_x}{\partial y}$ (unfortunately distinguishes direction)

$\vec{A} = [0, B_z x, 0]$ czyli $A_y = B_z x \stackrel{\text{def}}{=} Bx$ $\qquad q = -e$

We assume that in a plane xy there is no other potential

$$\left\{\frac{1}{2m}\left[-\hbar^2\frac{\partial^2}{\partial x^2} + \left(-i\hbar\frac{\partial}{\partial y} + eBx\right)^2 - \hbar^2\frac{\partial^2}{\partial z^2}\right] + U(z)\right\}\psi(\vec{r}) = E\psi(\vec{r})$$

Which gives: $$\left[-\frac{\hbar^2}{2m}\nabla^2 - \frac{ie\hbar}{m}Bx\frac{\partial}{\partial y} + \frac{(eBx)^2}{2m} + U(z)\right]\psi(\vec{r}) = E\psi(\vec{r})$$

The evidence of the Lorentz force

Parabolic potential!

„free electron" $(U(x,y,z) = U(z)) \Rightarrow$ **Landau levels**

Homogenous magnetic field

The Landau gauge solution

$$\left\{\frac{1}{2m}\left[\hat{p} - q\,\vec{A}(\vec{r},t)\right]^2 + q\varphi(\vec{r},t) + U(\vec{r},t)\right\}\psi(\vec{r},t) = i\hbar\frac{d}{dt}\psi(\vec{r},t)$$

Landau gauge: magnetic field $\vec{B} = (0,0,B_z) \Rightarrow B_z = \frac{\partial A_y}{\partial x} - \frac{\partial A_x}{\partial y}$ (unfortunately distinguishes direction)

$\vec{A} = [0, B_z x, 0]$ czyli $A_y = B_z x \stackrel{\text{def}}{=} Bx$ $\qquad q = -e$

[illegible] that in a plane xy [illegible]here is no other potential

But in chemistry (usually) we have no free electrons

$$\left\{\frac{1}{2m}\left[-\hbar^2\frac{\partial^2}{\partial x^2} + \left(-i\hbar\frac{\partial}{\partial}\right.\right. \qquad \frac{\partial}{\partial z^2}\right] + U(z)\right\}\psi(\vec{r}) = E\psi(\vec{r})$$

Which gives: $\left[-\frac{\hbar^2}{2m}\nabla^2 - \frac{ie\hbar}{m}Bx\frac{\partial}{\partial y} + \frac{(eBx)^2}{2m} + U(z)\right]\psi(\vec{r}) = E\psi(\vec{r})$

The evidence of the Lorentz force

Parabolic potential!

„free electron" $(U(x,y,z) = U(z)) \Rightarrow$ **Landau levels**

Hamiltonian

$$\left\{\frac{1}{2m}\hat{p}^2 + U(\vec{r},t)\right\}\psi(\vec{r},t) = i\hbar\frac{d}{dt}\psi(\vec{r},t)$$

Coulomb potential

$$U(r) = -\frac{e^2}{4\pi\varepsilon_r\varepsilon_0}\frac{1}{r}$$

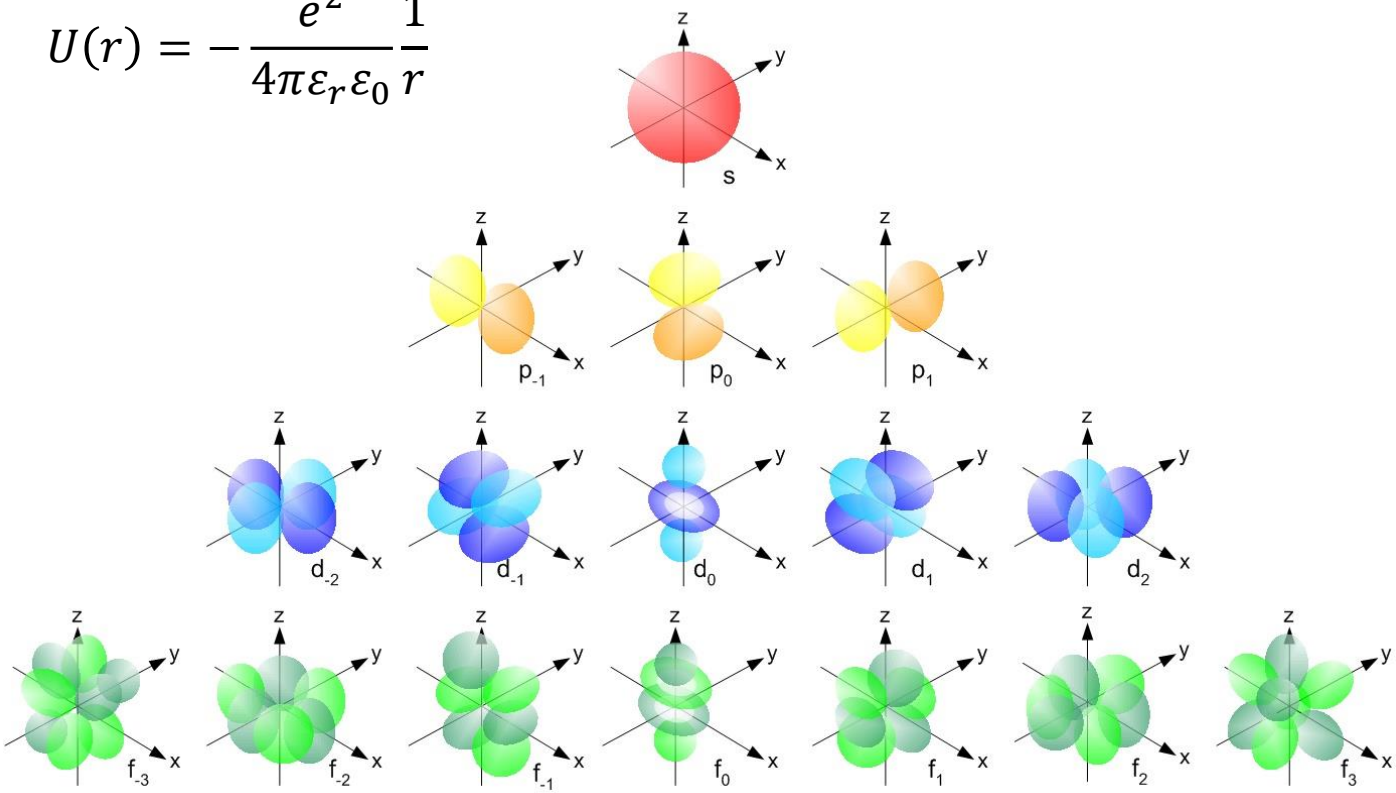

Coulomb potential

FIRST:

Coulomb potential in 3D in the semiconductor of dielectric constant ε_r, effective mass m^*:

$$U(r) = -\frac{e^2}{4\pi\varepsilon_r\varepsilon_0}\frac{1}{r}$$

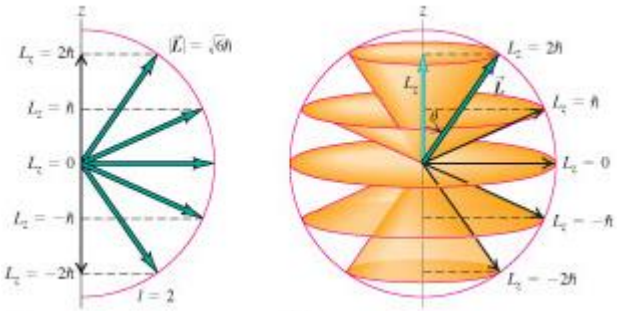

$$Ry = \left(\frac{e^2}{4\pi\varepsilon_0}\right)^2 \frac{m}{2\hbar^2} = \frac{\hbar^2}{2ma_B^2} = \frac{1}{2}\frac{e^2}{4\pi\varepsilon_0 a_B} = 13.6\ \text{eV}$$

$$a_B = \frac{4\pi\varepsilon_0\hbar^2}{m_0 e^2} = 0.5\ \text{Å}$$

$$L^2 = -\hbar^2\left(\frac{1}{\sin\theta}\frac{\partial}{\partial\theta}\left(\sin\theta\frac{\partial}{\partial\theta}\right) + \frac{1}{\sin^2\theta}\frac{\partial^2}{\partial\phi^2}\right)$$

$l = 0,1,2 \ldots$

$$E_n = -Ry\frac{1}{n^2} \qquad \Rightarrow \ |n, l, m_l\rangle$$

$$E_n = -\left(\frac{m^*}{m_0}\right)\frac{1}{\varepsilon_r^2}Ry\frac{1}{n^2}$$

$$a_B^* = \frac{4\pi\varepsilon_r\varepsilon_0\hbar^2}{m_0 e^2}\left(\frac{m_0}{m^*}\right) = a_B\varepsilon_r\left(\frac{m_0}{m^*}\right)$$

principal, angular, magnetic

Magnetic field and spin

Magnetic field:

$$H' = -\vec{m}\vec{B}$$

Here $\vec{m}$ is magnetic moment

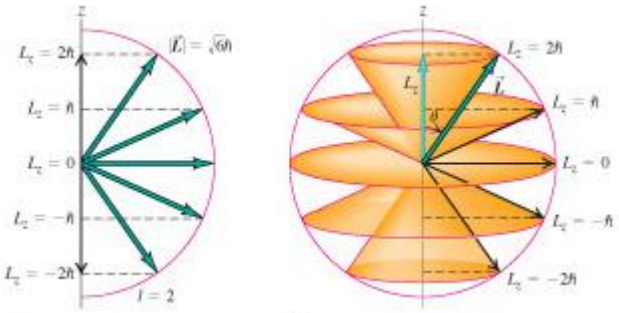

clasically:

$$|\vec{m}| = |I\vec{S}| = \frac{e}{T}\pi r^2 = \frac{e}{2\pi r/v}\pi r^2 = \frac{e}{2}rv \quad [\mathrm{Am}^2]$$

thus: $\vec{m} = -\frac{e}{2m_0}\vec{L} = -\frac{\mu_B}{\hbar}\hat{L}$

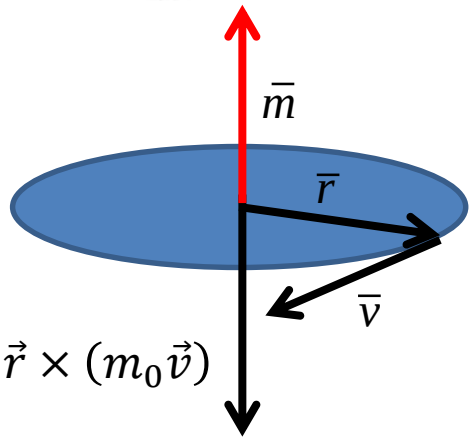

Bohr magneton $\mu_B = \frac{\hbar e}{2m_0}$

$\mu_B = 9{,}274009994(57)\times10^{-24}$ J/T

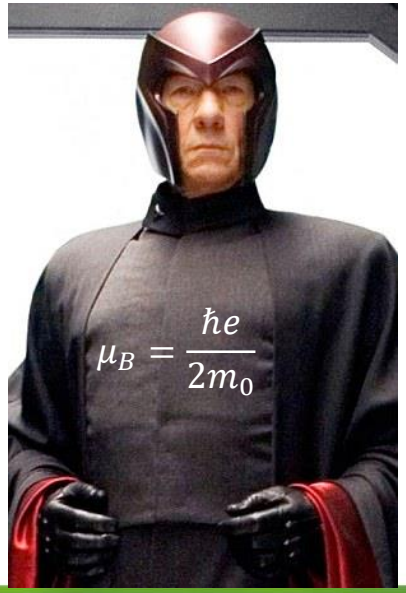

$$\vec{L} = \vec{r} \times (m_0\vec{v})$$

$$H' = -\vec{m}\vec{B} = \frac{\mu_B}{\hbar}\hat{L}\vec{B}$$

$$\hat{L} = (\hat{L}_x, \hat{L}_y, \hat{L}_z)$$

circumference of a circle

Magnetic field and spin

Magnetic field:

$$H' = -\vec{m}\vec{B} = \frac{\mu_B}{\hbar}\hat{L}\vec{B}$$

Here $\vec{m}$ is magnetic moment

for $\vec{B} = (0,0,B_z)$

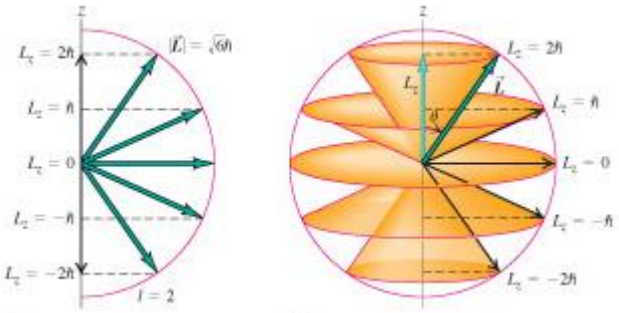

we have: $H' = \frac{\mu_B}{\hbar}\hat{L}_z B_z = \mu_B B_z m$

where $m = -l, -l+1, \dots l-1, l$

Here m is NOT a magnetic moment
(it is a magnetic quantum number)

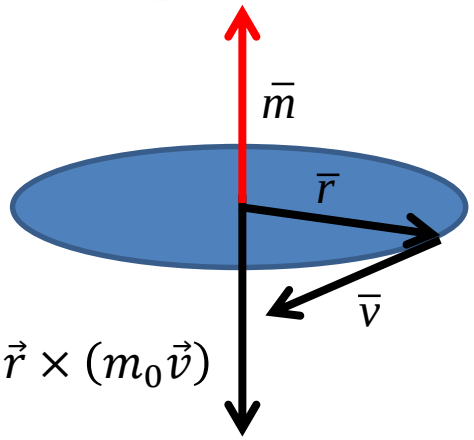

the base: $|l,m\rangle$

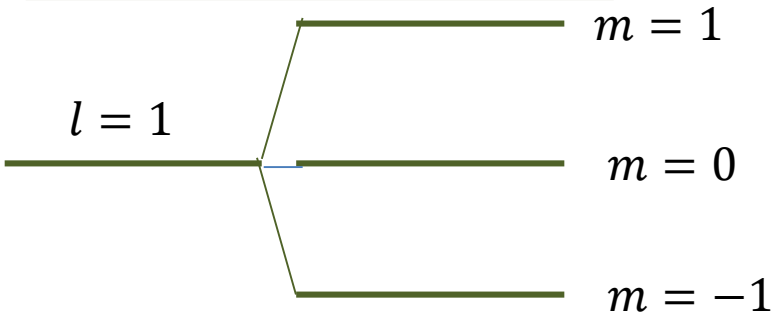

$\vec{L} = \vec{r} \times (m_0\vec{v})$

$B = 0$ $\quad$ $B \neq 0$

$\hat{L} = (\hat{L}_x, \hat{L}_y, \hat{L}_z)$

Magnetic field and spin

Magnetic field:

$$H' = -\vec{m}\vec{B} = \frac{\mu_B}{\hbar}\hat{L}\vec{B}$$

Here $\vec{m}$ is magnetic moment

for $\vec{B} = (0,0,B_z)$

we have: $H' = \frac{\mu_B}{\hbar}\hat{L}_z B_z = \mu_B B_z m$

where $m =$

Does it mean that for s-state(l=0) there is no splitting in magnetic field B?

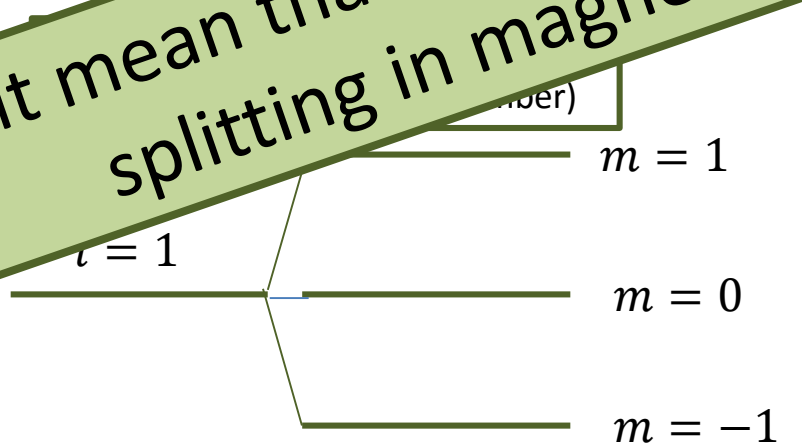

the b

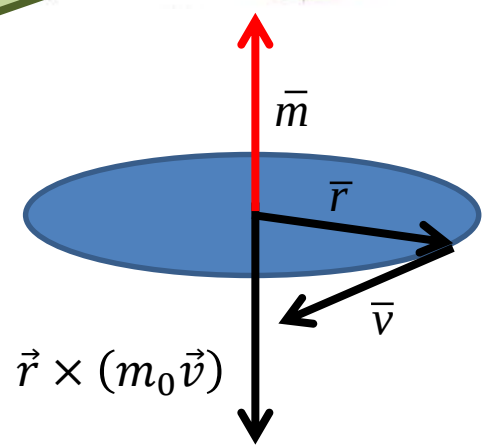

$\vec{L} = \vec{r} \times (m_0\vec{v})$

$\hat{L} = (\hat{L}_x, \hat{L}_y, \hat{L}_z)$

Magnetic field and spin

Stern-Gerlach experiment (1922 r.)

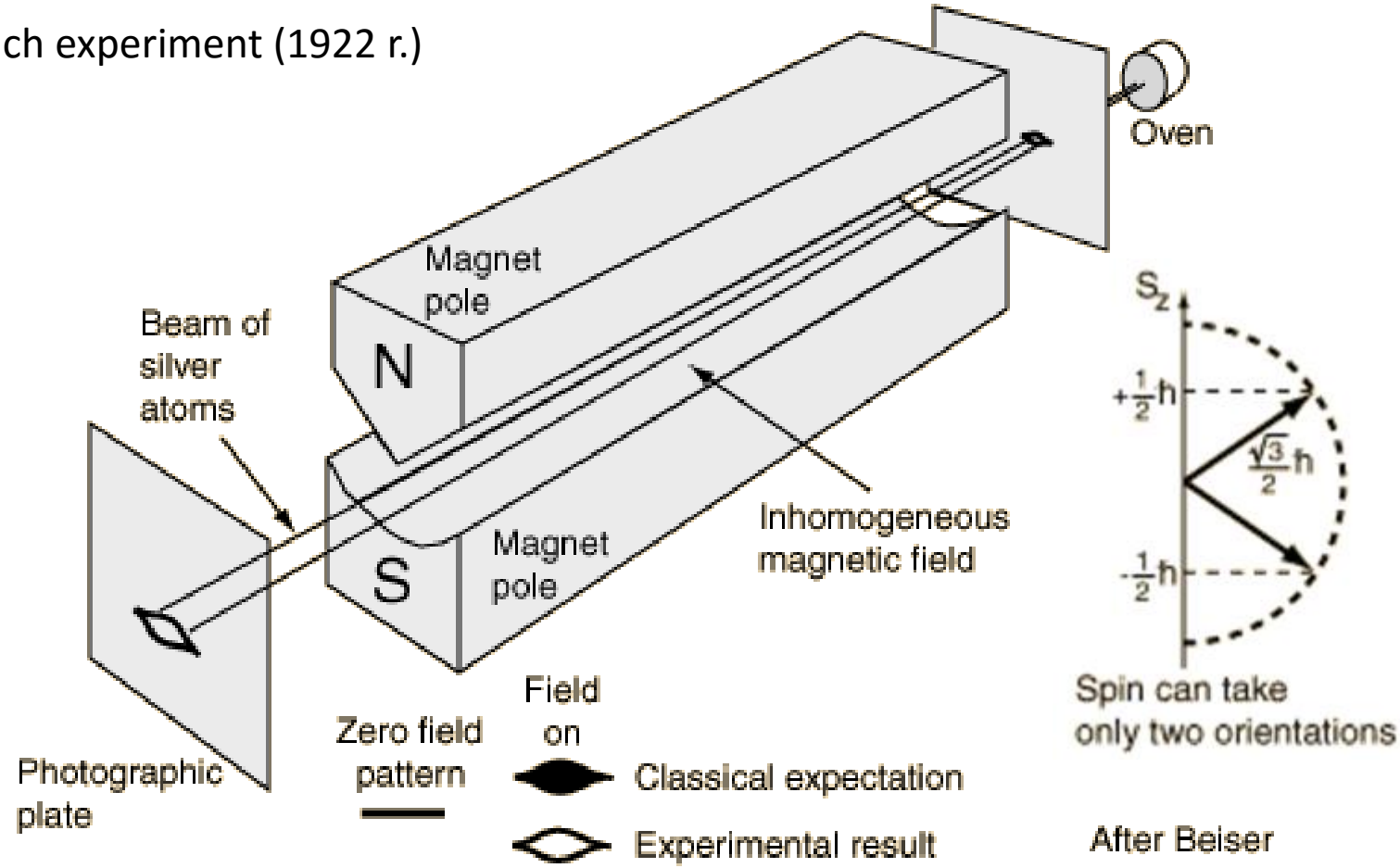

http://hyperphysics.phy-astr.gsu.edu

What is the „spin”?

- What is „mass”?

$$\vec{F} = m\vec{a}$$

$$F = G\frac{m_1 m_2}{r^2}$$

Mariusz Pudzianowski http://www.pudzian.pl/

What is the „spin”?

- What is the „momentum”?

$$\vec{p} = m\vec{v}$$

What is the „spin”?

- What is the „angular momentum”?

$$\vec{L} = \vec{r} \times \vec{p}$$

What is the „spin”?

- What is the „charge”?

$$F = k\frac{q_1 q_2}{r^2}$$

What is the „spin”?

- Spin?

http://www.floridahistory.com/us@1570.html

Sebastian Münster, Cosmographia in 1544

Disney

Magnetic field and spin

Spin, spin-orbit interaction

Spin operators $\hat{S}_x, \hat{S}_y, \hat{S}_z, \hat{S}^2$

$$\psi(\vec{r}, S_z) = \psi(\vec{r})\chi(S_z)$$

Spinor

$$[\hat{S}_x, \hat{S}_y] = i\hbar\hat{S}_z, \text{ etc.}$$

Pauli matrices: $\sigma_x, \sigma_y, \sigma_z$

$$\hat{S}_x = \frac{1}{2}\hbar\sigma_x = \frac{1}{2}\hbar\begin{bmatrix} 0 & 1 \\ 1 & 0 \end{bmatrix}$$

$$\hat{S}_y = \frac{1}{2}\hbar\sigma_y = \frac{1}{2}\hbar\begin{bmatrix} 0 & -i \\ i & 0 \end{bmatrix}$$

$$\hat{S}_x = \frac{1}{2}\hbar\sigma_z = \frac{1}{2}\hbar\begin{bmatrix} 1 & 0 \\ 0 & -1 \end{bmatrix}$$

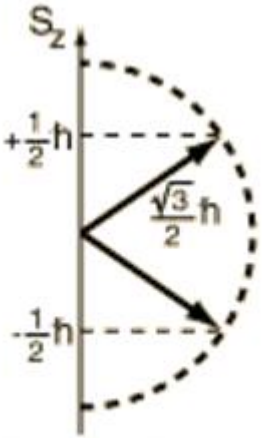

Spin can take only two orientations

projections of the spin on the axis z

$$\chi_\uparrow = \begin{pmatrix} 1 \\ 0 \end{pmatrix}, \chi_\downarrow = \begin{pmatrix} 0 \\ 1 \end{pmatrix}$$

Magnetic field and spin

Spin, spin-orbit interaction

Spin operators $\hat{S}_x, \hat{S}_y, \hat{S}_z, \hat{S}^2$

$$H' = \frac{\mu_B}{\hbar}(\hat{L} + g\hat{S})\vec{B}$$

g-factor for the agreement with experiments

$$[\hat{S}_x, \hat{S}_y] = i\hbar\hat{S}_z, \text{ etc.}$$

Pauli matrices: $\sigma_x, \sigma_y, \sigma_z$

$$\hat{S}_x = \frac{1}{2}\hbar\sigma_x = \frac{1}{2}\hbar\begin{bmatrix} 0 & 1 \\ 1 & 0 \end{bmatrix}$$

$$\hat{S}_y = \frac{1}{2}\hbar\sigma_y = \frac{1}{2}\hbar\begin{bmatrix} 0 & -i \\ i & 0 \end{bmatrix}$$

$$\hat{S}_x = \frac{1}{2}\hbar\sigma_z = \frac{1}{2}\hbar\begin{bmatrix} 1 & 0 \\ 0 & -1 \end{bmatrix}$$

projections of the spin on the axis z

$$\chi_\uparrow = \begin{pmatrix} 1 \\ 0 \end{pmatrix}, \chi_\downarrow = \begin{pmatrix} 0 \\ 1 \end{pmatrix}$$

Magnetic field and spin

Spin, spin-orbit interaction

Spin operators $\hat{S}_x, \hat{S}_y, \hat{S}_z, \hat{S}^2$

$$H' = \frac{\mu_B}{\hbar}(\hat{L} + g\hat{S})\vec{B}$$

g-factor for the agreement with experiments

$$[\hat{S}_x, \hat{S}_y] = i\hbar\hat{S}_z, \text{ etc.}$$

Pauli matrices: $\sigma_x, \sigma_y, \sigma_z$

$$\hat{S}_x = \frac{1}{2}\hbar\sigma_x = \frac{1}{2}\hbar\begin{bmatrix} 0 & 1 \\ 1 & 0 \end{bmatrix}$$

$$g = -2.00231930436182 \pm 0.00000000000052$$

$$\hat{S}_y = \frac{1}{2}\hbar\sigma_y = \frac{1}{2}\hbar\begin{bmatrix} 0 & -i \\ i & 0 \end{bmatrix}$$

$$\hat{S}_x = \frac{1}{2}\hbar\sigma_z = \frac{1}{2}\hbar\begin{bmatrix} 1 & 0 \\ 0 & -1 \end{bmatrix}$$

projections of the spin on the axis z

$$\chi_\uparrow = \begin{pmatrix} 1 \\ 0 \end{pmatrix}, \chi_\downarrow = \begin{pmatrix} 0 \\ 1 \end{pmatrix}$$

QED – Quantum ElectroDynamics

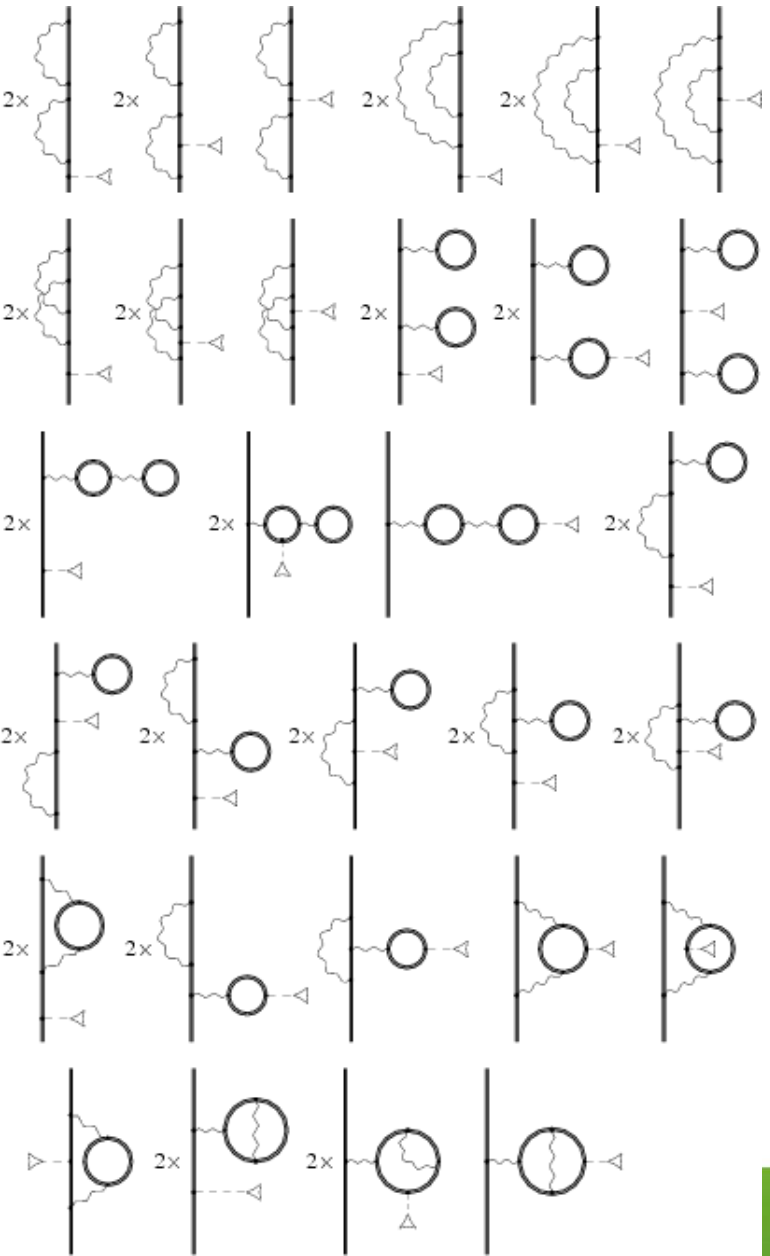

$$g = -2.00231930436182 \pm 0.00000000000052$$

There is the „spin”

The consequences?

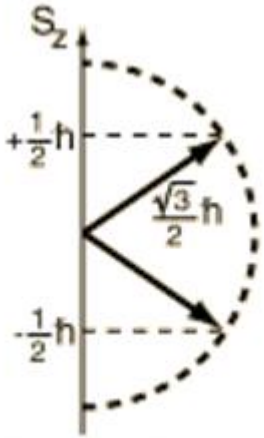

Spin can take
only two orientations

Magnetic field and spin

Spin, spin-orbit interaction

Spin operators $\hat{S}_x, \hat{S}_y, \hat{S}_z, \hat{S}^2$

$$H' = \frac{\mu_B}{\hbar}(\hat{L} + g\hat{S})\vec{B}$$

g-factor for the agreement with experiments

Total angular momentum operator $\hat{J} = \hat{L} + \hat{S}$, the base $|j, m_j\rangle$

Total magnetic moment $\widehat{M} = \widehat{M}_L + \widehat{M}_S = -g_L \frac{\mu_B}{\hbar}\hat{L} - g_S \frac{\mu_B}{\hbar}\hat{S}$

g_L ↑ =1, g_S ↑ =2

$\widehat{M} \neq \hat{J}$ - magnetic anomaly of spin

Magnetic field and spin

Spin-orbit interaction $\hat{H}_{SO} = \lambda \hat{L}\hat{S}$ with the base $|n, l, s, m_l, m_s\rangle$

For s-states $\hat{L} = 0 \Rightarrow \hat{L}\hat{S} = 0$

Total angular momentum operator $\hat{J} = \hat{L} + \hat{S}$, the base $|j, m_j\rangle$

$$\hat{H}_{SO} = \lambda \hat{L}\hat{S} = \lambda \frac{1}{2}\left(J^2 - L^2 - S^2\right) = \lambda\left(L_z S_z + \frac{1}{2}(L_+ S_- + L_- S_+)\right)$$

$$\lambda = hc\, A = \frac{Z\alpha^2}{2}\left\langle \frac{1}{r^3} \right\rangle$$

fine-structure constant

$$\alpha = \frac{e^2}{4\pi\varepsilon_0 \hbar c} \approx \frac{1}{137.037}$$

$$Ry = hcR_\infty$$
$$R_\infty = \frac{m_e e^4}{8\varepsilon_0^2 h^3 c}$$
$$R_\infty = 1{,}097 \times 10^7 \mathrm{m}^{-1}$$

$$E_{SO} = \int \psi^* H_{SO} \psi \, dV = \frac{Z}{2(137)^2} \int \psi^* \frac{\hat{L}\hat{S}}{r^3} \psi \, dV$$

e.g. for ψ_{210} we get $\left\langle \frac{1}{r^3} \right\rangle = \frac{1}{24}\left(\frac{Z}{a_0}\right)^3$ and for general n (principal quantum number)

$$E_{SO} = \frac{Z^4}{2(137)^2 a_0^3 n^3}\left(\frac{j(j+1) - l(l+1) - s(s+1)}{2l(l+1/2)(l+1)}\right)$$

Magnetic field and spin

Spin-orbit interaction $\widehat{H}_{SO} = \lambda \hat{L}\hat{S}$ with the base $|n, l, s, m_l, m_s\rangle$

For s-states $\hat{L} = 0 \Rightarrow \hat{L}\hat{S} = 0$

Total angular momentum operator $\hat{J} = \hat{L} + \hat{S}$, the base $|j, m_j\rangle$

$$\bar{L}\bar{S} = \frac{1}{2}(\bar{J}^2 - \bar{L}^2 - \bar{S}^2) = L_z S_z + \frac{1}{2}(L_+ S_- + L_- S_+)$$

$\hat{L} = 1;\ \hat{S} = \frac{1}{2}$

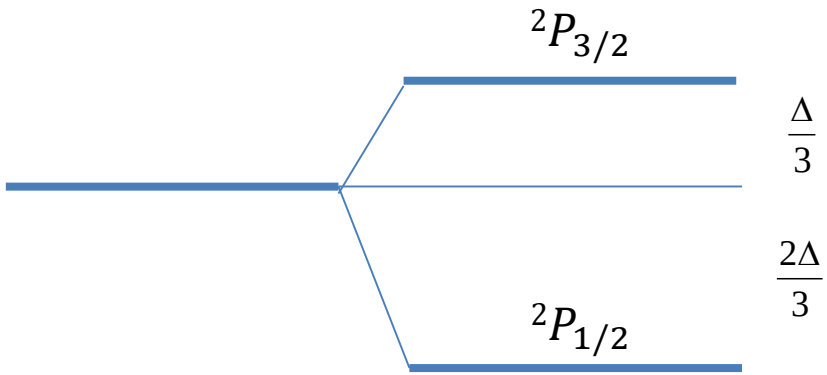

the base: $|n, l, s, j, m_j\rangle$

shortly: $|j, m_j\rangle$

Multi-electron atom

Term symbol $^{2S+1}L_J$

an abbreviated description of the angular momentum quantum numbers in a multi-electron atom

Total wavefunction must be antisymmetric (under interchange of any pair of particle)

$$\psi(\vec{r}, S_z) = \psi(\vec{r})\chi(S_z)$$

Orbital part **Spin part**

Multi-electron wavefunction:

$$\psi(\vec{r}_1, \dots, \vec{r}_N, \vec{S}_1, \dots, \vec{S}_N) = \psi(\vec{r}_1, \dots, \vec{r}_N)\chi(\vec{S}_1, \dots, \vec{S}_N)$$

Antisymmetric wavefunction + Pauli exclusion principle + Coulomb interaction =

Exchange interaction

Exchange interaction

Antisymmetric wavefunction + Pauli exclusion principle + Coulomb interaction =

Exchange interaction

$$\Psi = \varphi_{orbital} \times \chi_{spin}$$ <u>Antisymmetric!</u>

<u>Example:</u>

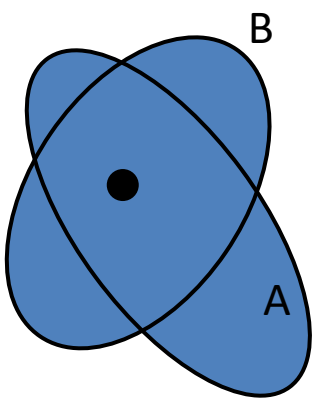

Two electrons localized on one centrum

$$\mathcal{H}(1,2) = H_0(1) + H_0(2) + \frac{e^2}{r_{12}}$$

Exchange interaction

Antisymmetric wavefunction + Pauli exclusion principle + Coulomb interaction =

Exchange interaction

$$\Psi = \varphi_{orbital} \times \chi_{spin}$$ <u>Antisymmetric!</u>

Hund's rules, $E_T < E_S$

$$\frac{1}{\sqrt{2}}\left[\varphi_A(1)\varphi_B(2) - \varphi_A(2)\varphi_B(1)\right] \times \begin{bmatrix} \chi_\uparrow(1)\chi_\uparrow(2) \\ \frac{1}{\sqrt{2}}\left[\chi_\uparrow(1)\chi_\downarrow(2) + \chi_\downarrow(1)\chi_\uparrow(2)\right] \\ \chi_\downarrow(1)\chi_\downarrow(2) \end{bmatrix}$$

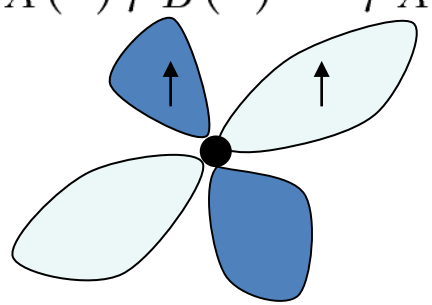

$$\frac{1}{\sqrt{2}}\left[\varphi_A(1)\varphi_B(2) + \varphi_A(2)\varphi_B(1)\right] \quad \frac{1}{\sqrt{2}}\left[\chi_\uparrow(1)\chi_\downarrow(2) - \chi_\downarrow(1)\chi_\uparrow(2)\right]$$

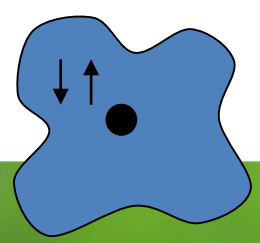

Exchange interaction

Antisymmetric wavefunction + Pauli exclusion principle + Coulomb interaction =

Exchange interaction

$$\Psi = \varphi_{orbital} \times \chi_{spin}$$ <u>Antisymmetric!</u>

<u>Example:</u>

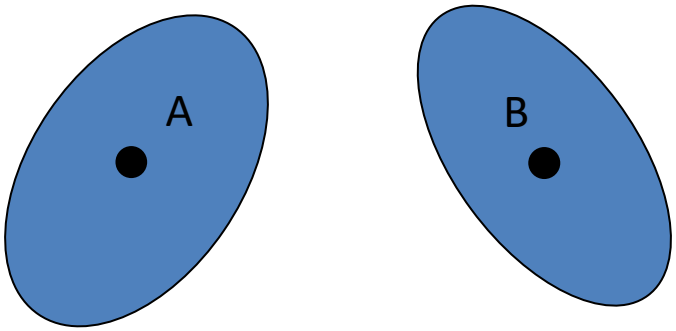

Two electrons localized on two centres

$$\mathcal{H}(1,2) = H_0^A(1) + H_0^B(2) + \frac{e^2}{r_{12}}$$

Exchange interaction

Antisymmetric wavefunction + Pauli exclusion principle + Coulomb interaction =

Exchange interaction

$$\Psi = \varphi_{orbital} \times \chi_{spin}$$

$$\frac{1}{\sqrt{2}}\left[\varphi_A(1)\varphi_B(2) - \varphi_A(2)\varphi_B(1)\right] \times \begin{bmatrix} \chi_\uparrow(1)\chi_\uparrow(2) \\ \frac{1}{\sqrt{2}}\left[\chi_\uparrow(1)\chi_\downarrow(2) + \chi_\downarrow(1)\chi_\uparrow(2)\right] \\ \chi_\downarrow(1)\chi_\downarrow(2) \end{bmatrix}$$

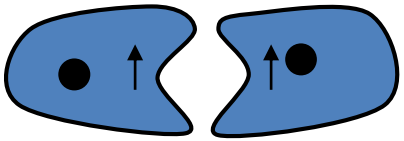

$$\frac{1}{\sqrt{2}}\left[\varphi_A(1)\varphi_B(2) + \varphi_A(2)\varphi_B(1)\right] \quad \frac{1}{\sqrt{2}}\left[\chi_\uparrow(1)\chi_\downarrow(2) - \chi_\downarrow(1)\chi_\uparrow(2)\right]$$

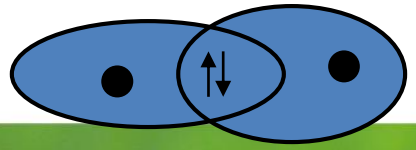

Chemical bonds, $E_S < E_T$

Exchange interactions

Exchange interaction = Coulomb interaction + Pauli principle

$\Psi = \varphi_{orbital} \times \chi_{spin}$ <u>Antisymmetric!</u>

$$\mathcal{H}(1,2) = H_0^A(1) + H_0^B(2) + \frac{e^2}{r_{12}}$$

This was the DIRECT EXCHANGE

depends on the
orientation of the spins.
The effect is purely electrostatic!

$$\mathcal{H}_{i,j} = -2\ J_{ij}\ \overline{\mathbf{S}_i} \circ \overline{\mathbf{S}_j}$$

Heisenberg Hamiltonian

$$J_{ij} = J_{ij}(r_{ij})$$

$J > 0$ ferro

$J < 0$ antiferro

Exchange interactions

Kinetic exchange

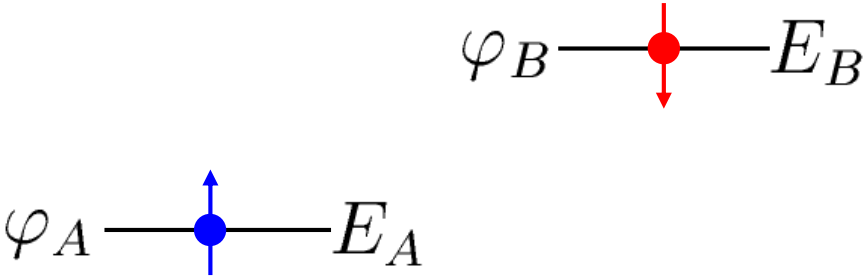

Exchange interactions

Kinetic exchange

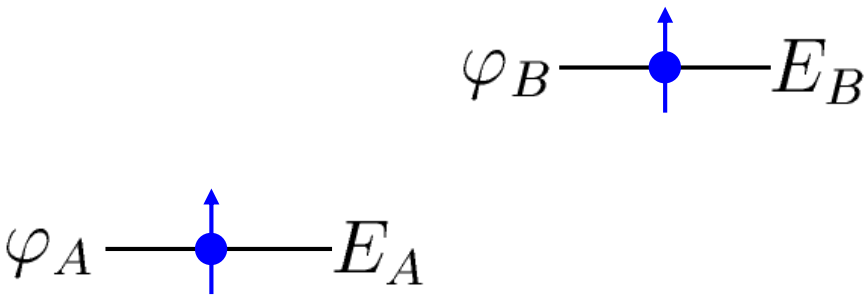

triplet

$$E = E_A + E_B$$

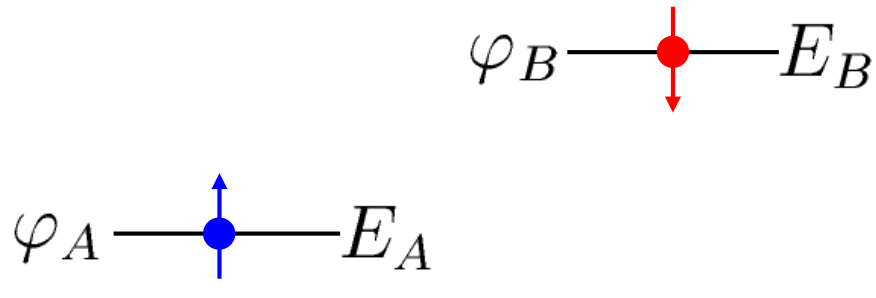

singlet

$$E = E_A + E_B$$

Exchange interactions

Kinetic exchange

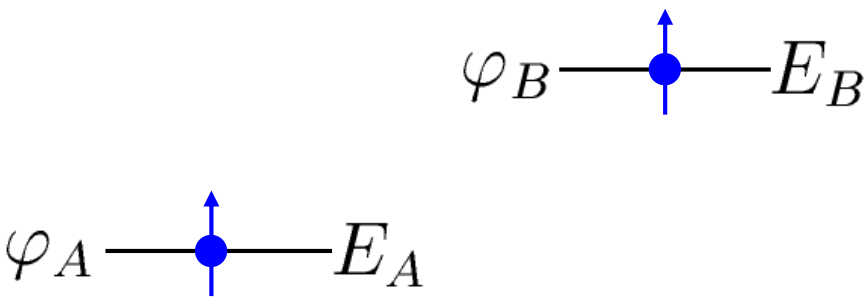

triplet

$$E = E_A + E_B$$

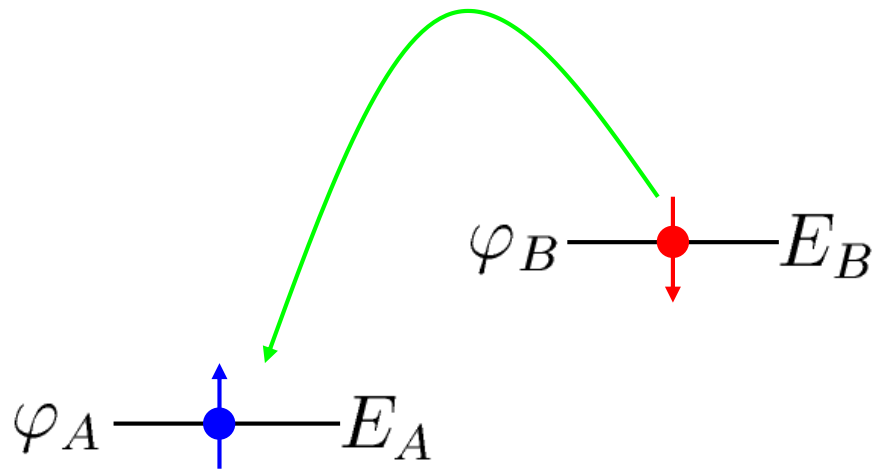

singlet

$$E = E_A + E_B$$

Exchange interactions

Kinetic exchange

$$E = 2E_A + U \gg E_A + E_B$$

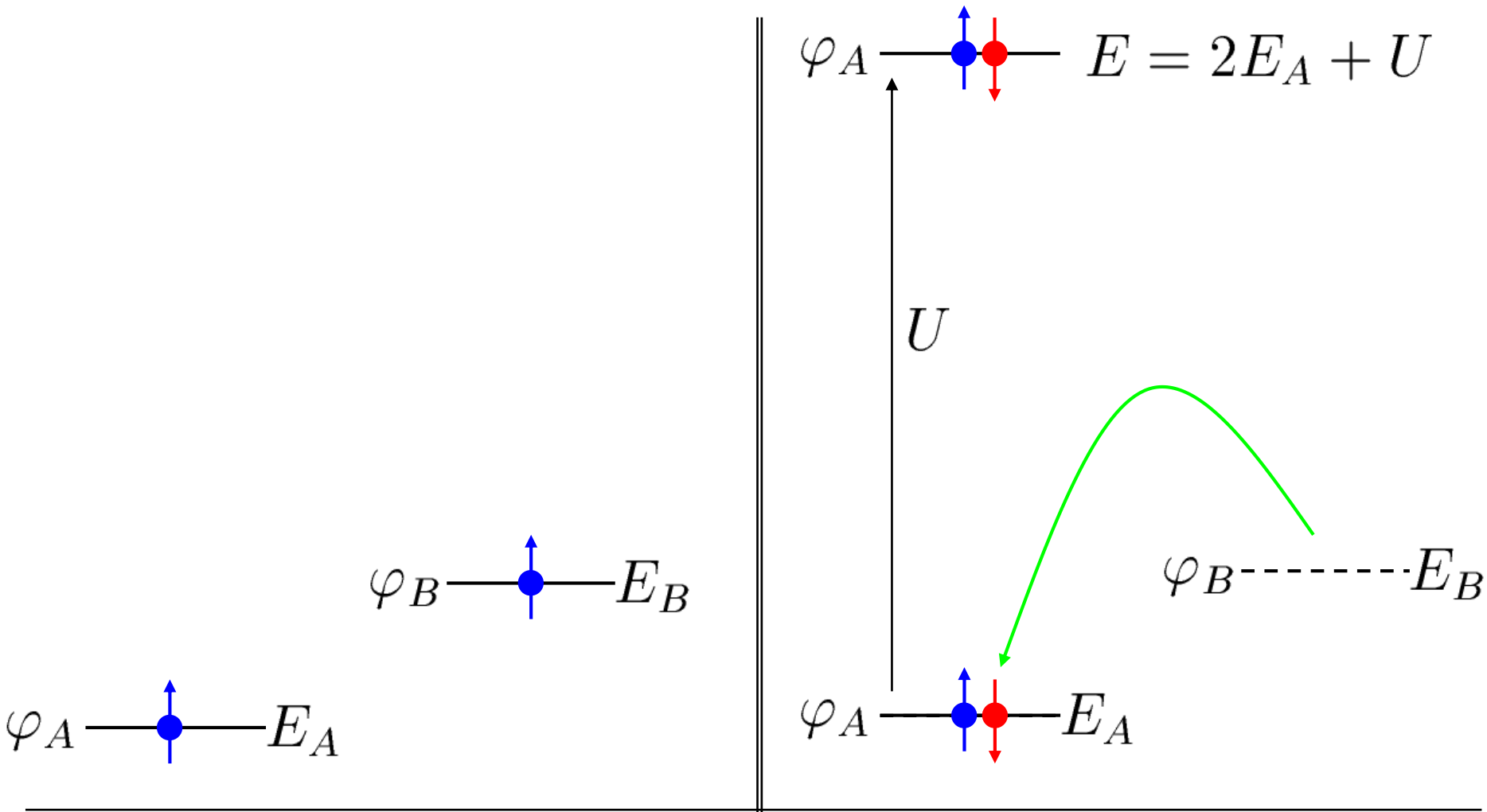

triplet

$$E = E_A + E_B$$

singlet

$$E = E_A + E_B$$

Exchange interactions

Kinetic exchange

$$E = 2E_A + U \gg E_A + E_B$$

	A	***B***	
ground state	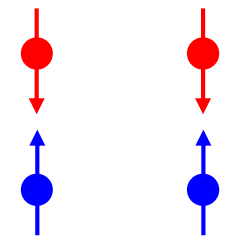		$E = E_A + E_B$
ground state	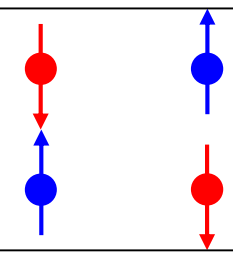		$E = E_A + E_B$
ground state			$E = 2E_A + U$
excited state			$E = 2E_B + U$

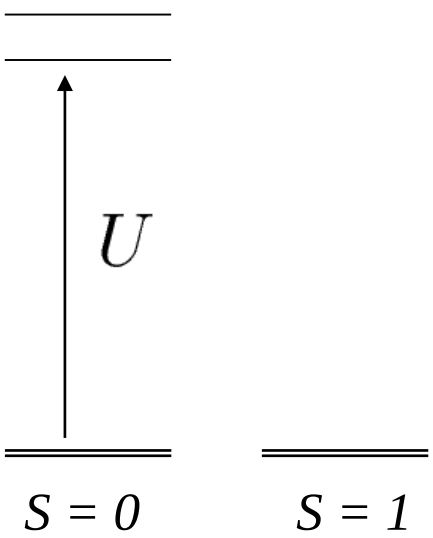

Exchange interactions

Kinetic exchange

$$\boxed{E = 2E_A + U \gg E_A + E_B}$$

$$E_n(\lambda) = E_n^{(0)} + \lambda \left\langle n^{(0)} \middle| V \middle| n^{(0)} \right\rangle + \lambda^2 \sum_{k \neq n} \frac{\left| \left\langle k^{(0)} \middle| V \middle| n^{(0)} \right\rangle \right|^2}{E_n^{(0)} - E_k^{(0)}} + O(\lambda^3)$$

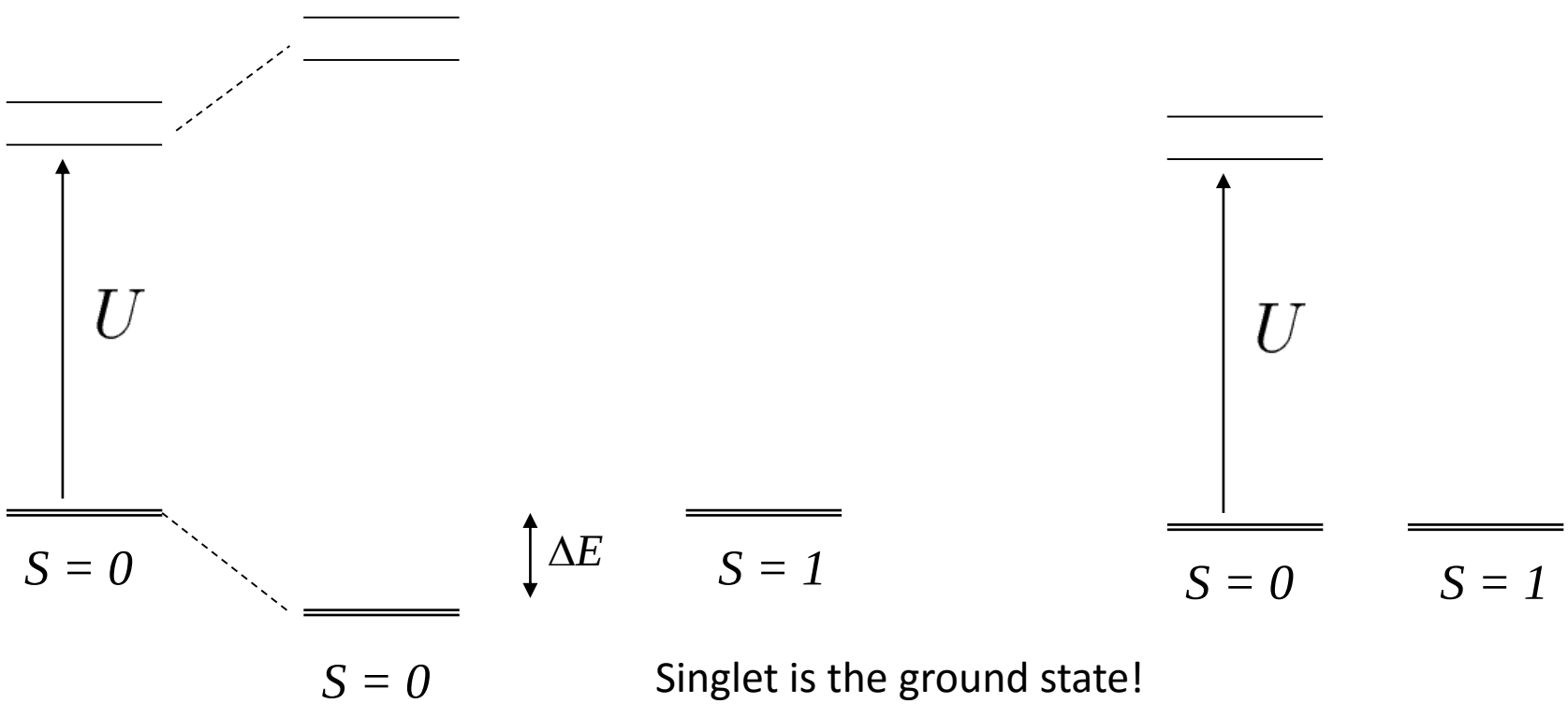

Singlet is the ground state!

Exchange interactions

Kinetic exchange

A specal case – superexchange

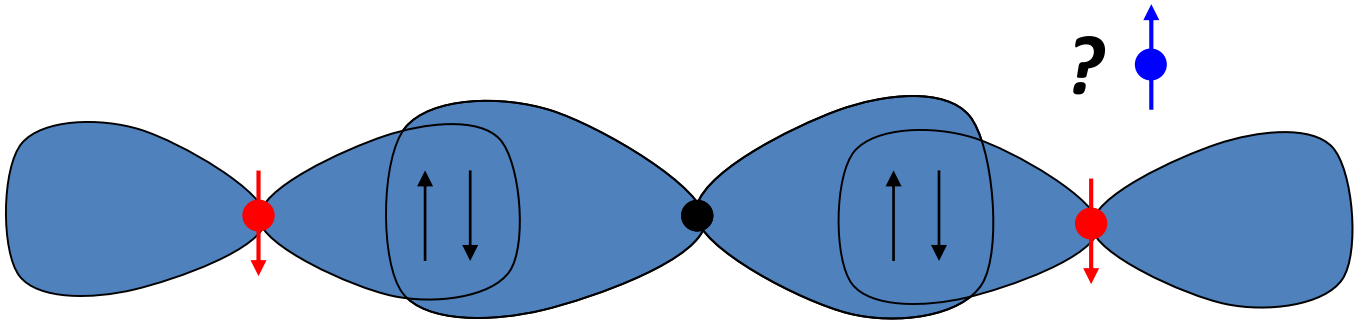

Exchange interactions

Kinetic exchange

A specal case – superexchange

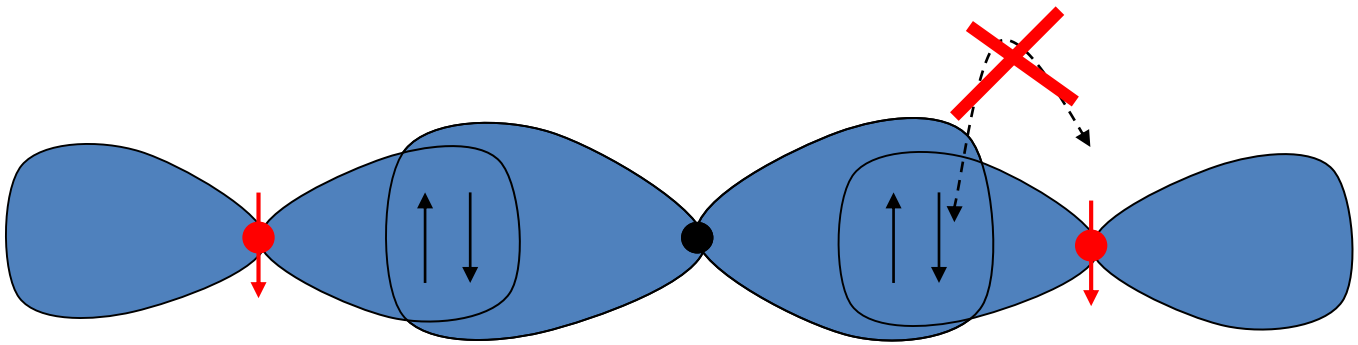

No excited states for both spins

Exchange interactions

Kinetic exchange

A specal case – superexchange

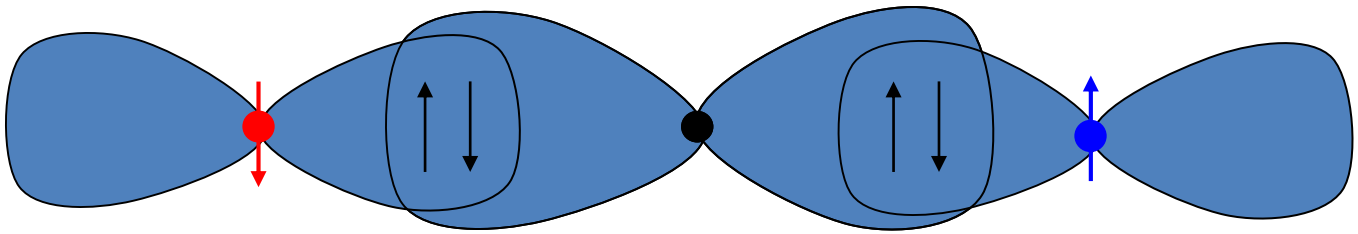

There are an excited state for BOTH spins!

$\boldsymbol{J} < 0$ (antiferromagnetic exchange)

Exchange interactions

Kinetic exchange

A specal case – superexchange

The superexchange is antiferromagnetic, even over long distances.

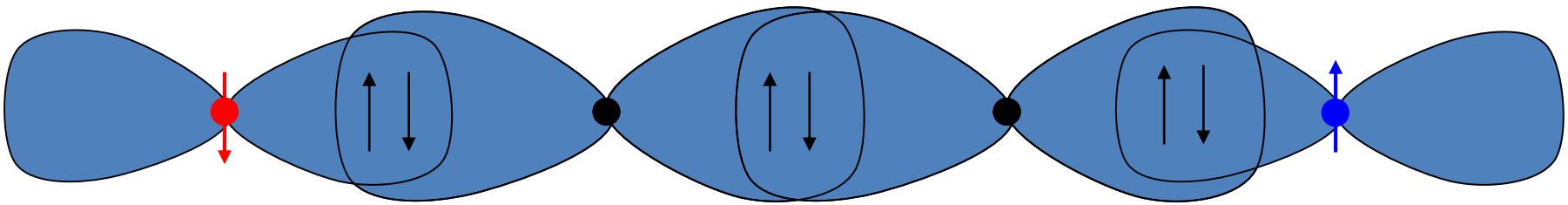

$$|J_1| > |J_2| > |J_3| > \ldots$$

There are an excited state for BOTH spins!

$\boldsymbol{J} < 0$ (antiferromagnetic exchange)

Exchange interactions

Crystal field splitting (the presence of the ligants)
⇒ quenching of the orbital momentum

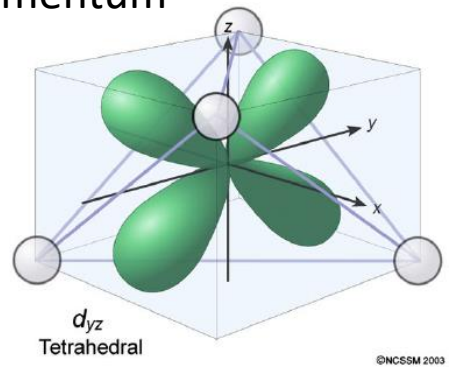

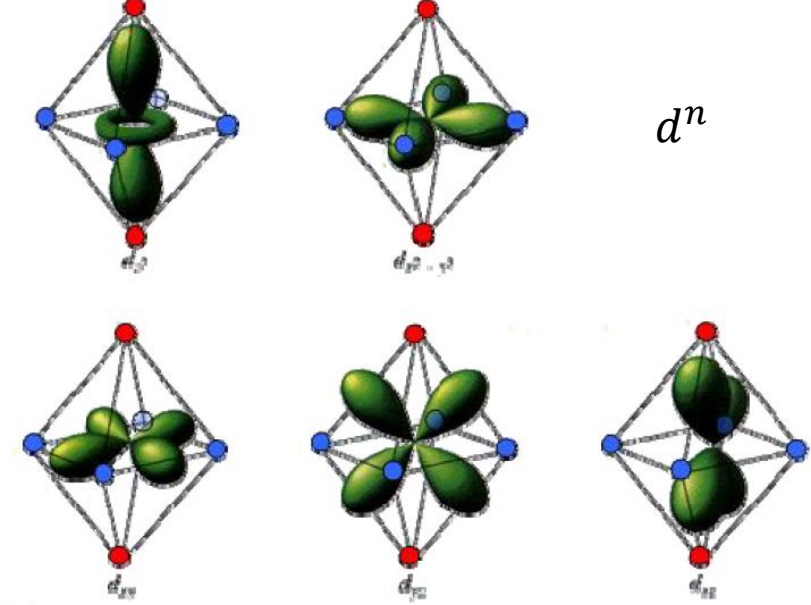

d^n

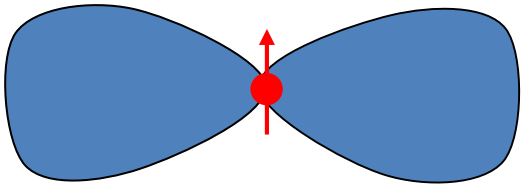

Mn^{3+} (d^4)

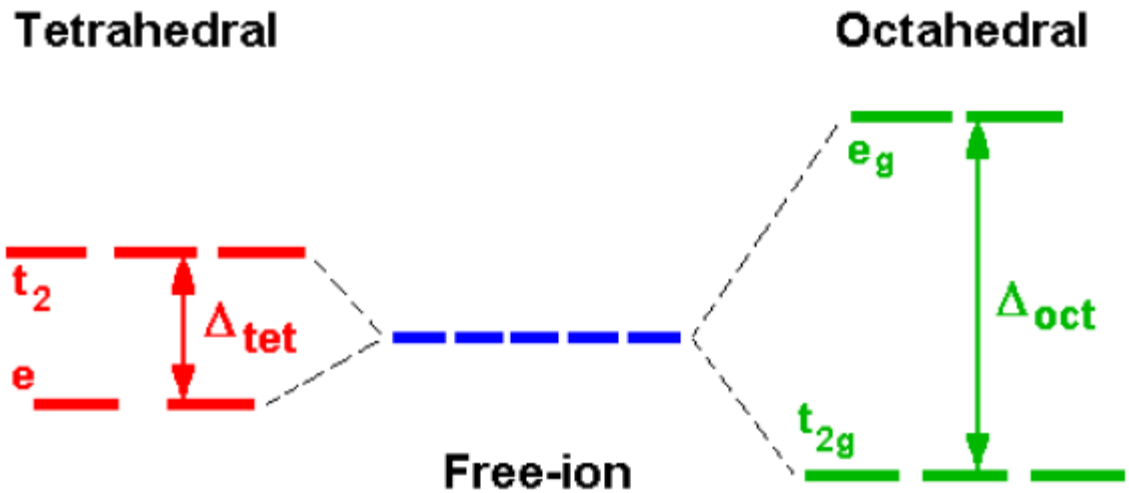

Crystal field (CF) splitting

Exchange interactions

Double exchange (in mixed vallence compounds)

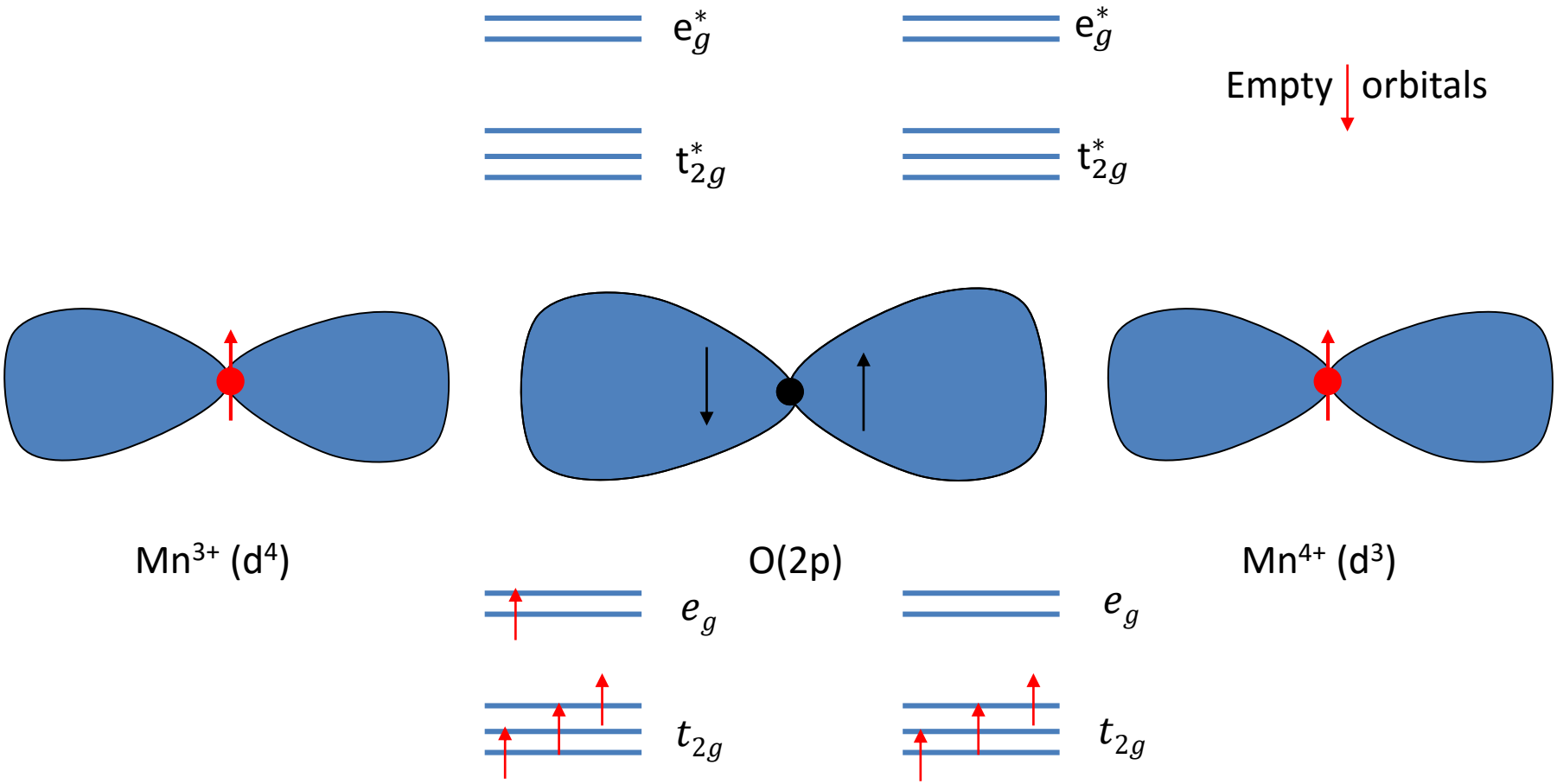

Exchange interactions

Double exchange (in mixed vallence compounds)

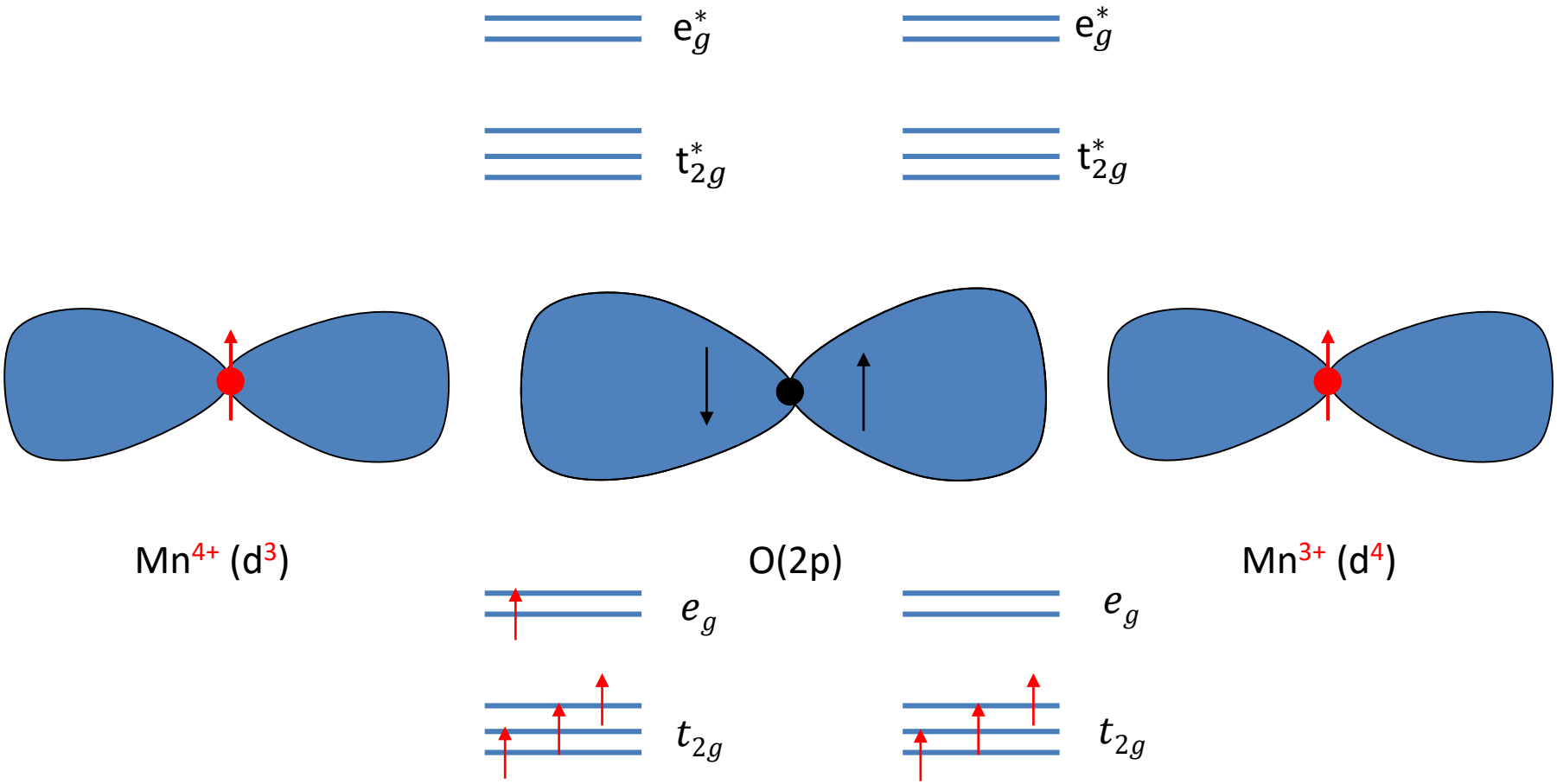

Ferromagnetism

Indirect exchange (Zener model, RKKY)

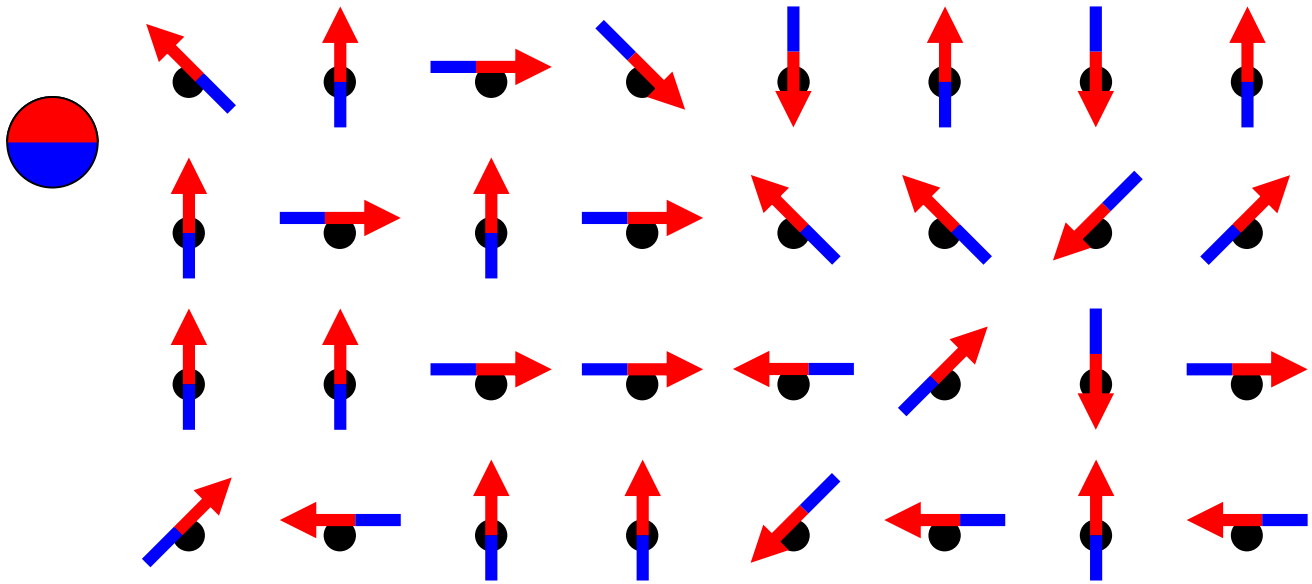

Lattice energy Carrier energy

Ferromagnetism

Indirect exchange (Zener model, RKKY)

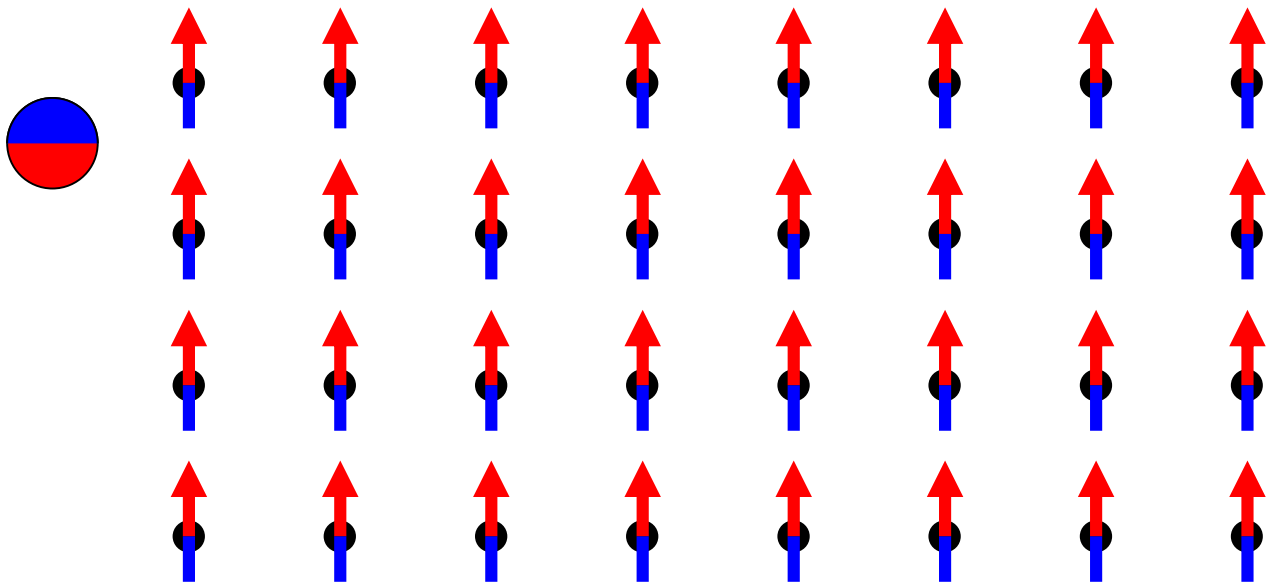

Lattice energy Carrier energy

Spin density of states

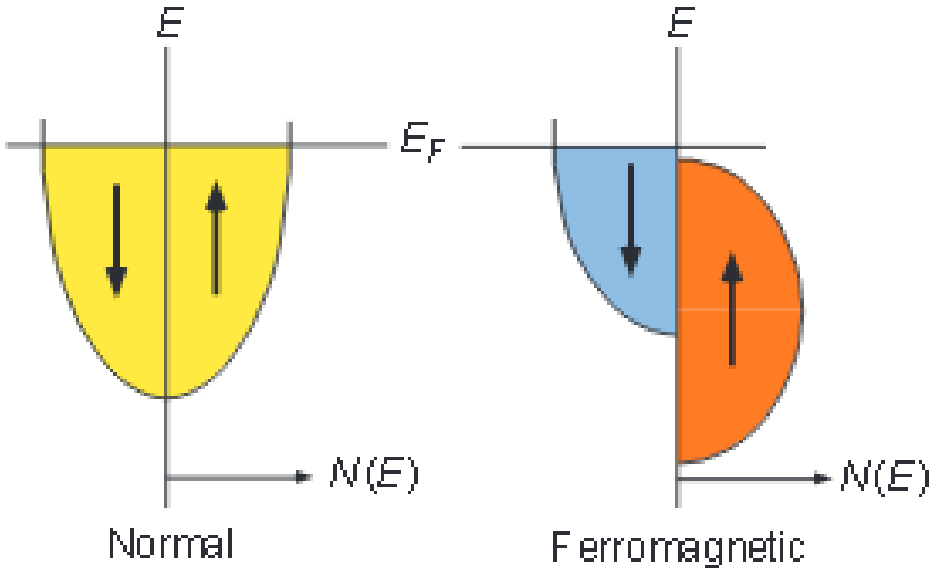

Fig. 1. A schematic representation of the density of electronic states that are available to electrons in a normal metal and in a ferromagnetic metal whose majority spin states are completely filled. E, the electron energy; E_F, the Fermi level; $N(E)$, density of states.

SCIENCE VOL **282,** 1660 (1998)

Magnetism of the matter

Example: 2 ions of spin $S = ½$, $J < 0$

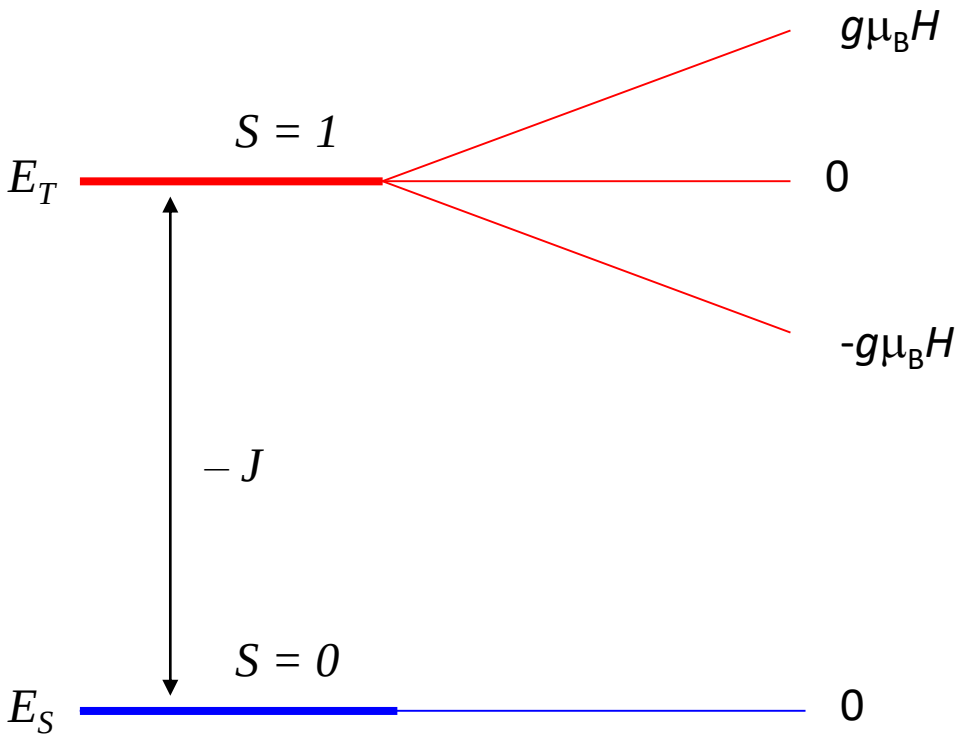

$$M(T,H) = -\frac{\partial E(T,H)}{\partial H}$$

$$\chi(T,H) = -\frac{\partial M(T,H)}{\partial H}$$

$$M = \frac{\sum_n -\left(\frac{\partial E_n}{\partial H}\right)\exp\left(-\frac{E_n}{k_B T}\right)}{\sum_n \exp\left(-\frac{E_n}{k_B T}\right)}$$

$$\chi = \frac{2N_A g^2 \mu_B}{k_B T\left(3 + \exp\left(-\frac{J}{k_B T}\right)\right)}$$

Magnetism of the matter

Example: 2 ions of spin $S = ½$, $J < 0$

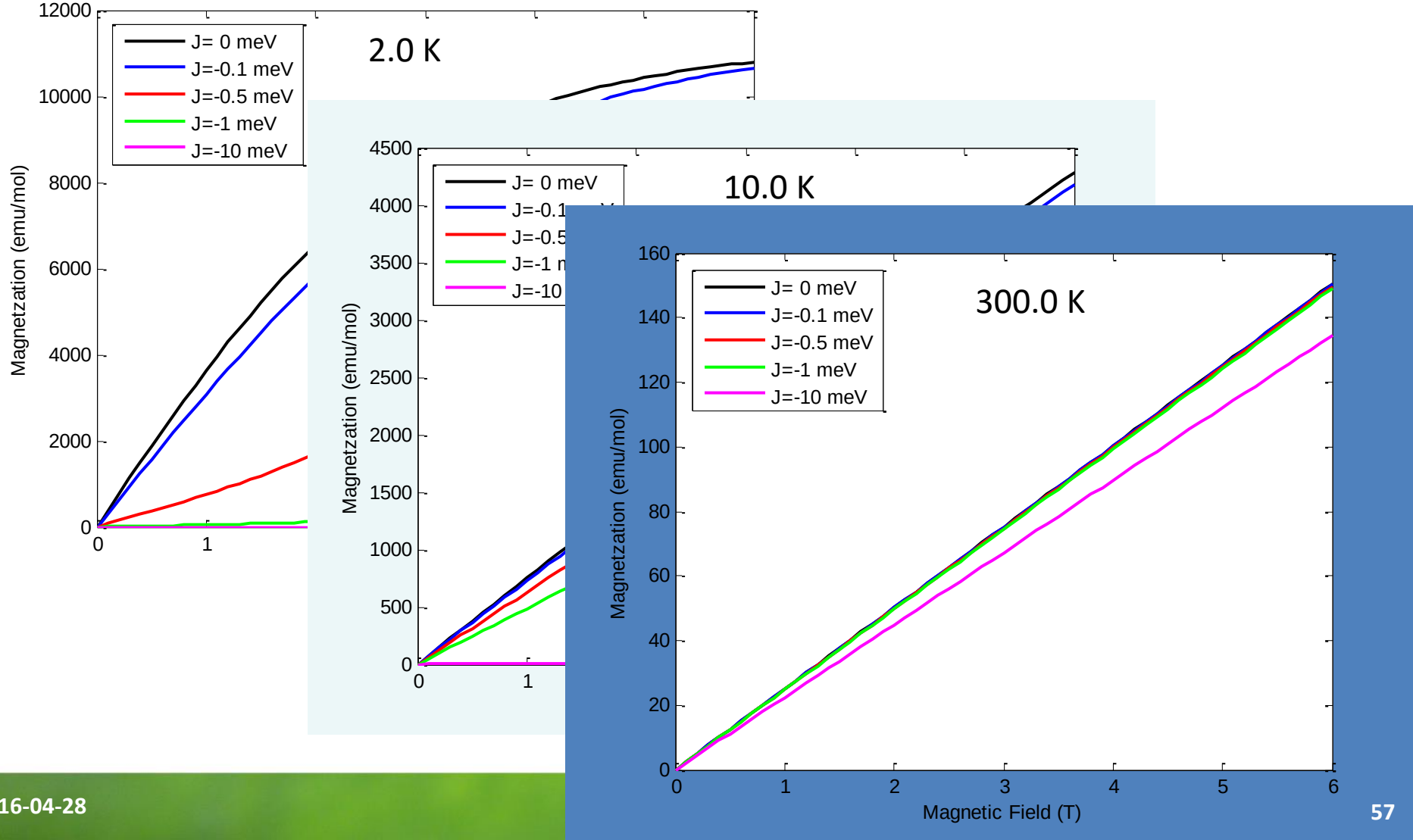

Magnetism of the matter

Example: 2 ions of spin $S = ½$, $J < 0$

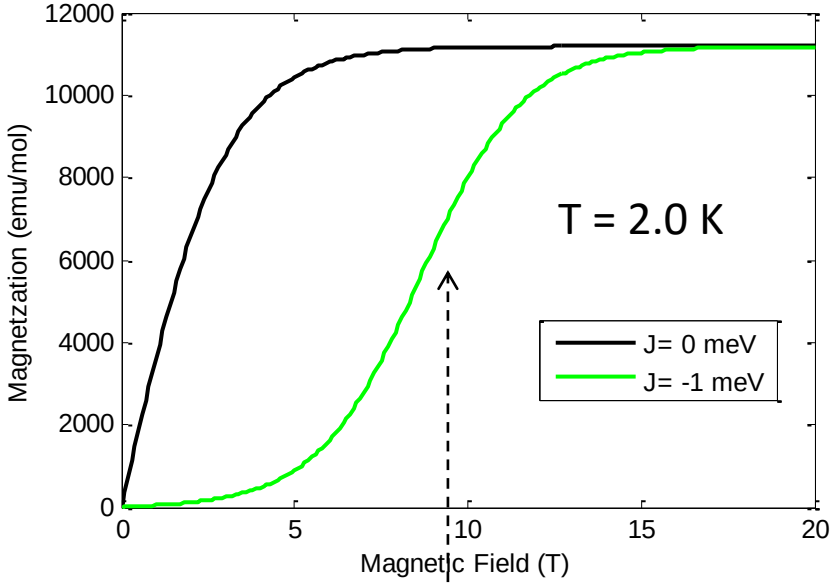

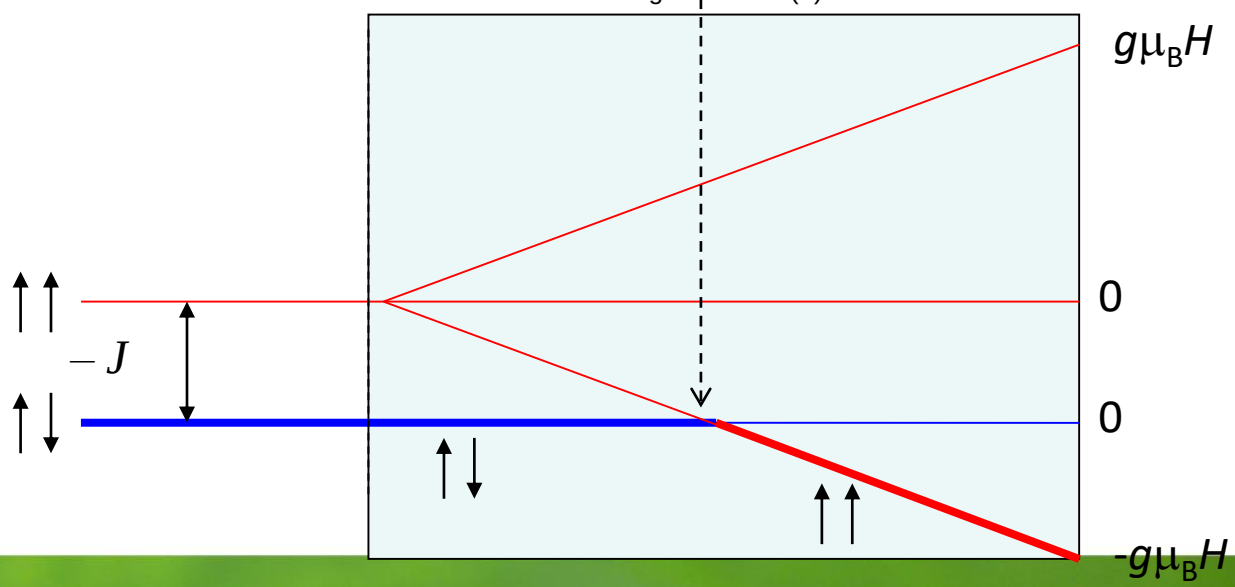

Magnetism of the matter

Example: 2 ions of spin $S = ½$, $J < 0$

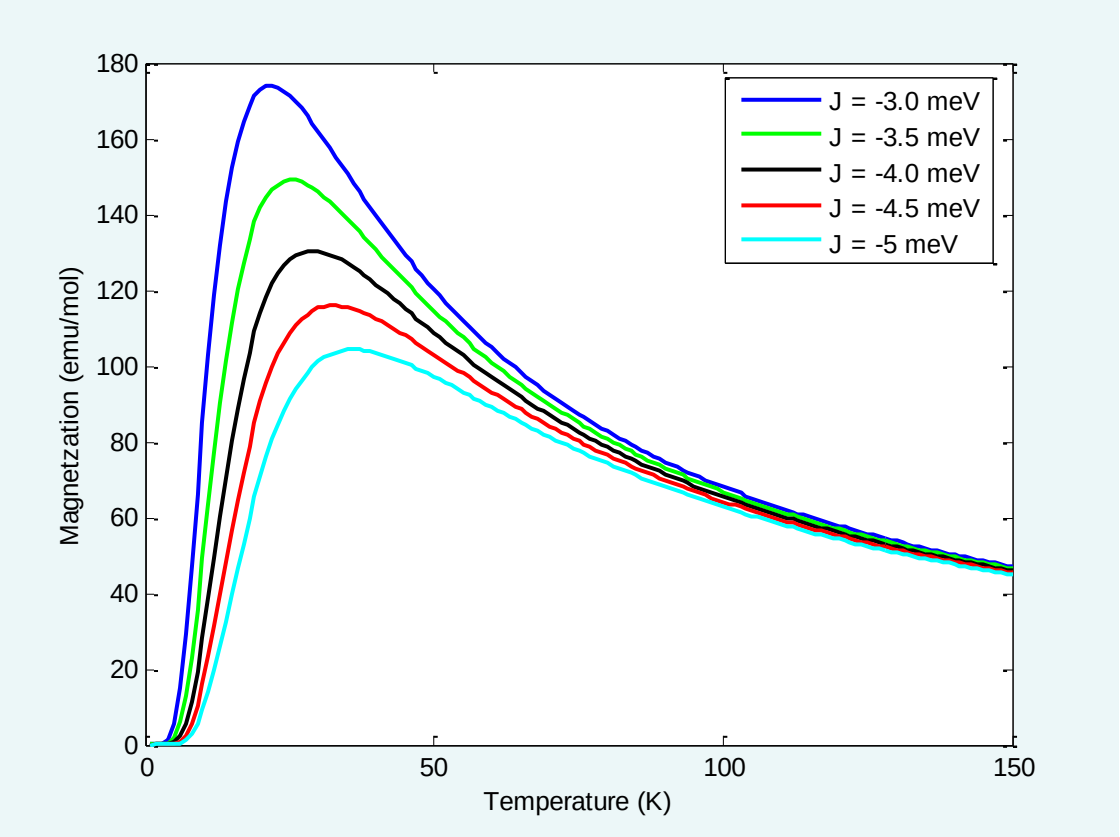

Experiment

Ewa Górecka , Adam Krówczyński, Jadwiga Szydłowska, Jacek Szczytko
students: Paweł Majewski
Department of Chemistry, University of Warsaw
Structural Research Laboratory

Samples

Isomeric bimetallic copper(II) Cu^{2+} and nickel(II) Ni^{2+} complexes

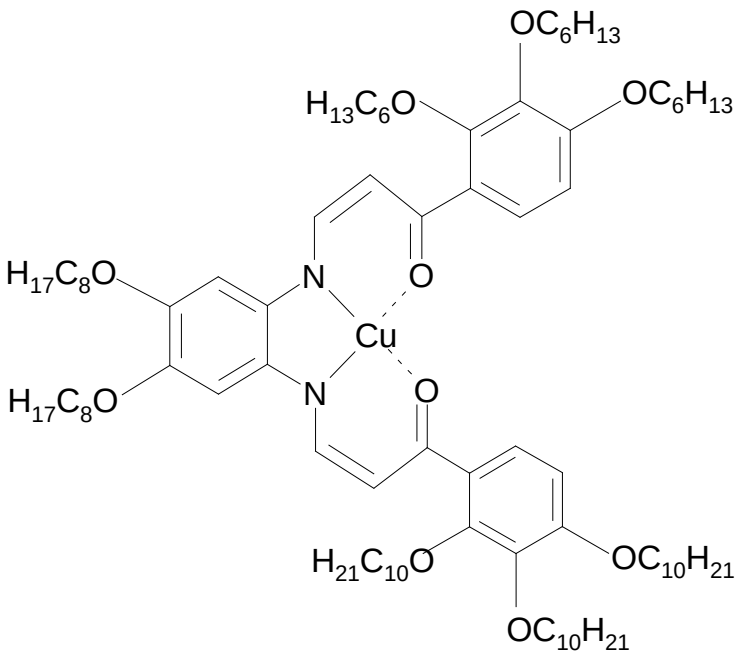

Cu^{2+}– n – Cu^{2+}

1294 1 × Cu^{2+}

coordinate bonds with lone pairs of electrons

Samples

Isomeric bimetallic copper(II) Cu^{2+} and nickel(II) Ni^{2+} complexes

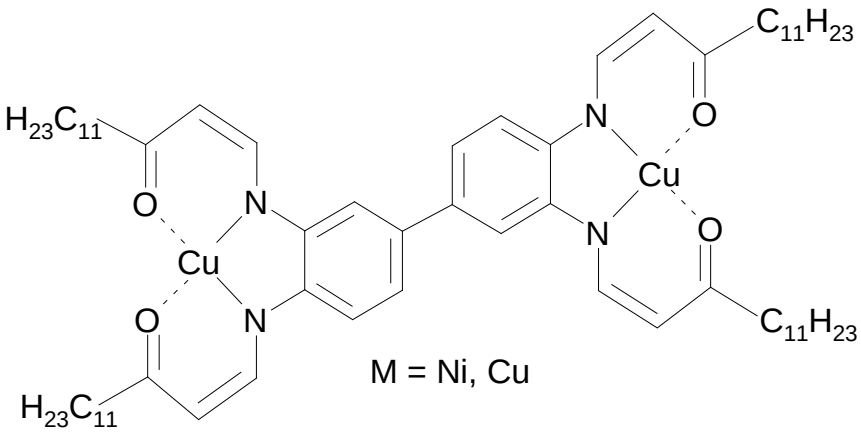

		Cu^{2+}– n – Cu^{2+}
1294	1 × Cu^{2+}	
1344	2 × Cu^{2+} biphenyl	n = 8

Samples

Isomeric bimetallic copper(II) Cu^{2+} and nickel(II) Ni^{2+} complexes

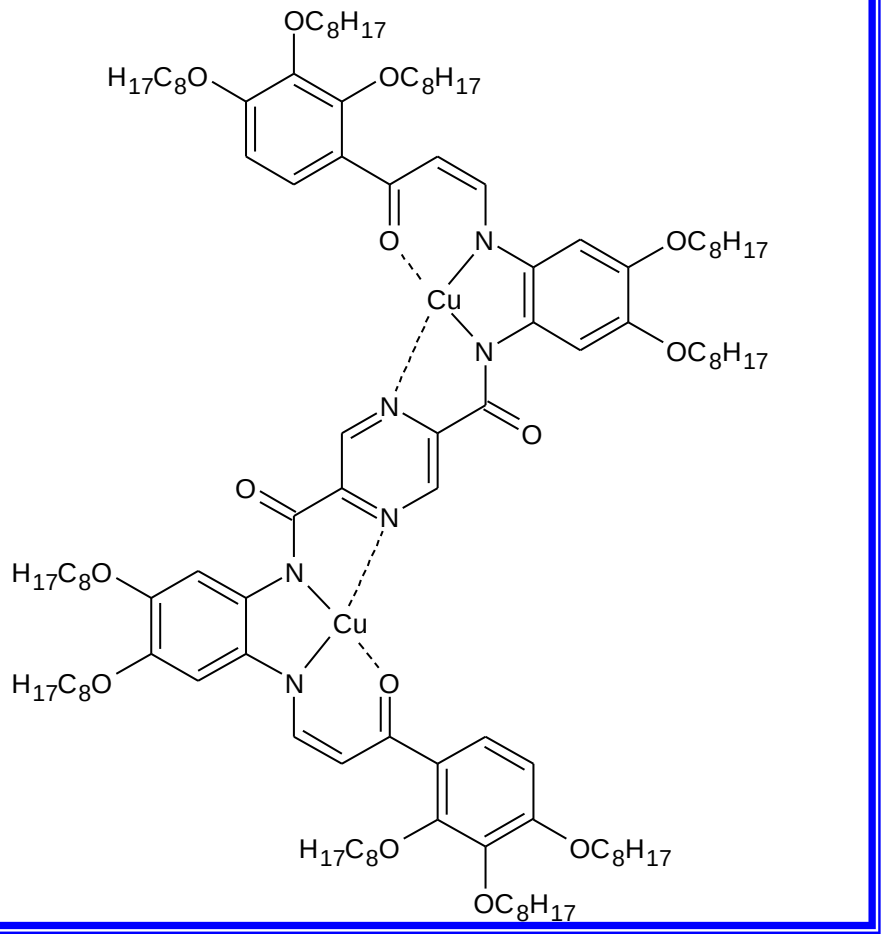

		Cu^{2+}– n – Cu^{2+}
1294	1 × Cu^{2+}	
1344	2 × Cu^{2+} biphenyl	n = 8
2955	2 × Cu^{2+} pyrazine 	N = 4

Samples

Isomeric bimetallic copper(II) Cu^{2+} and nickel(II) Ni^{2+} complexes

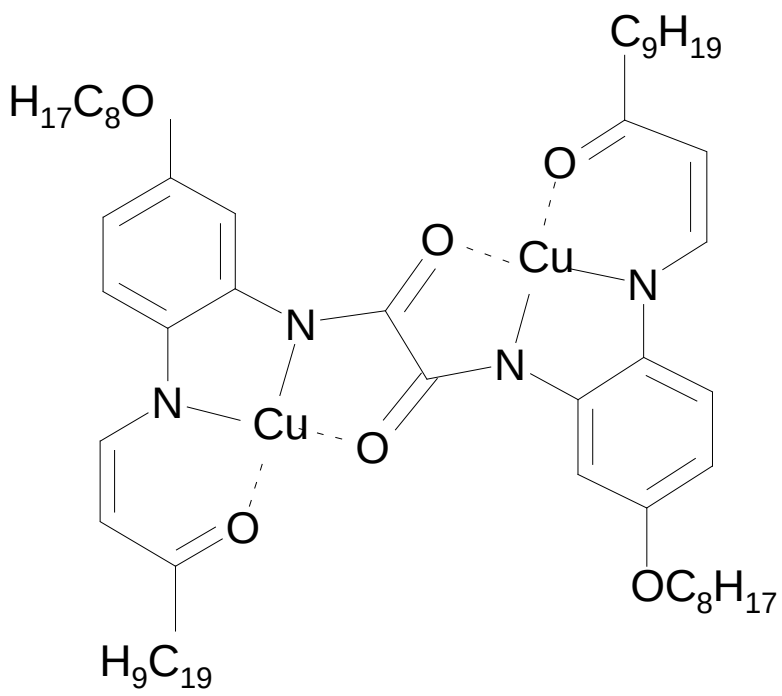

		Cu^{2+}– n – Cu^{2+}
1294	1 × Cu^{2+}	
1344	2 × Cu^{2+} biphenyl	n = 8
2955	2 × Cu^{2+} pyrazine 	n = 4
2567	2 × Cu^{2+} oxamide	n = 3

Samples

Isomeric bimetallic copper(II) Cu^{2+} and nickel(II) Ni^{2+} complexes

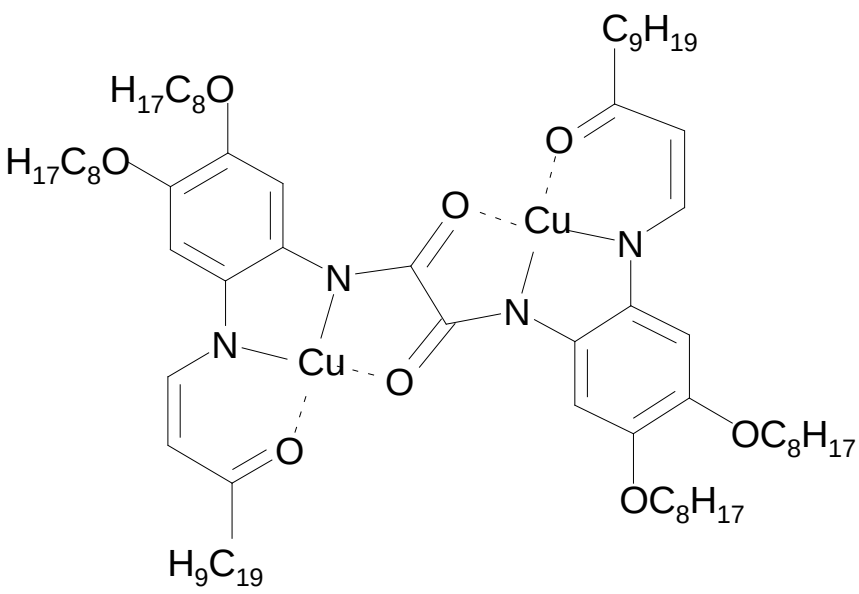

		Cu^{2+}– n – Cu^{2+}
1294	1 × Cu^{2+}	
1344	2 × Cu^{2+} biphenyl	n = 8
2955	2 × Cu^{2+} pyrazine 	n = 4
2567	2 × Cu^{2+} oxamide	n = 3
2356	2 × Cu^{2+} oxamide	n = 3

Samples

Isomeric bimetallic copper(II) Cu^{2+} and nickel(II) Ni^{2+} complexes

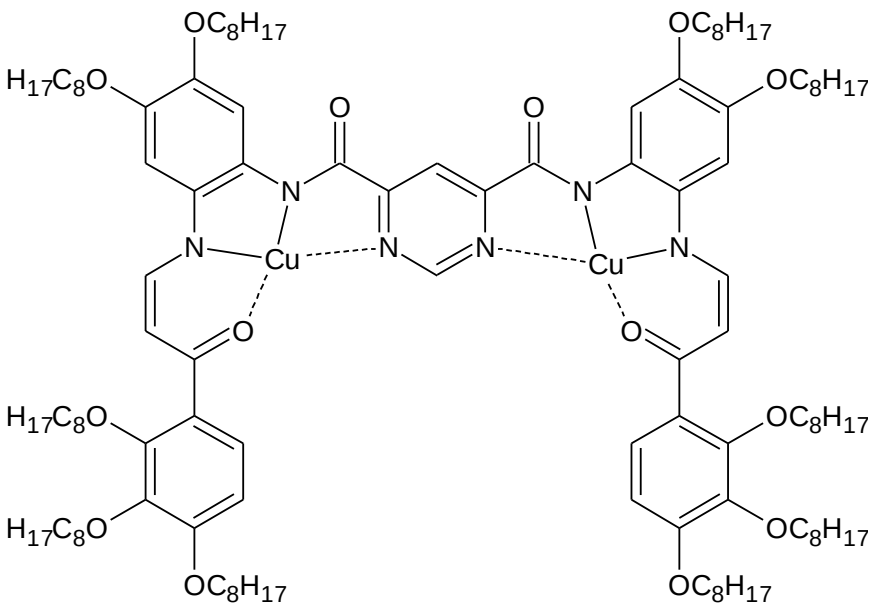

		Cu^{2+}– n – Cu^{2+}
1294	1 × Cu^{2+}	
1344	2 × Cu^{2+} biphenyl	n = 8
2955	2 × Cu^{2+} pyrazine	n = 4
2567	2 × Cu^{2+} oxamide	n = 3
2356	2 × Cu^{2+} oxamide	n = 3
2975	2 × Cu^{2+} pyrimidine	n = 3

Samples

Isomeric bimetallic copper(II) Cu^{2+} and nickel(II) Ni^{2+} complexes

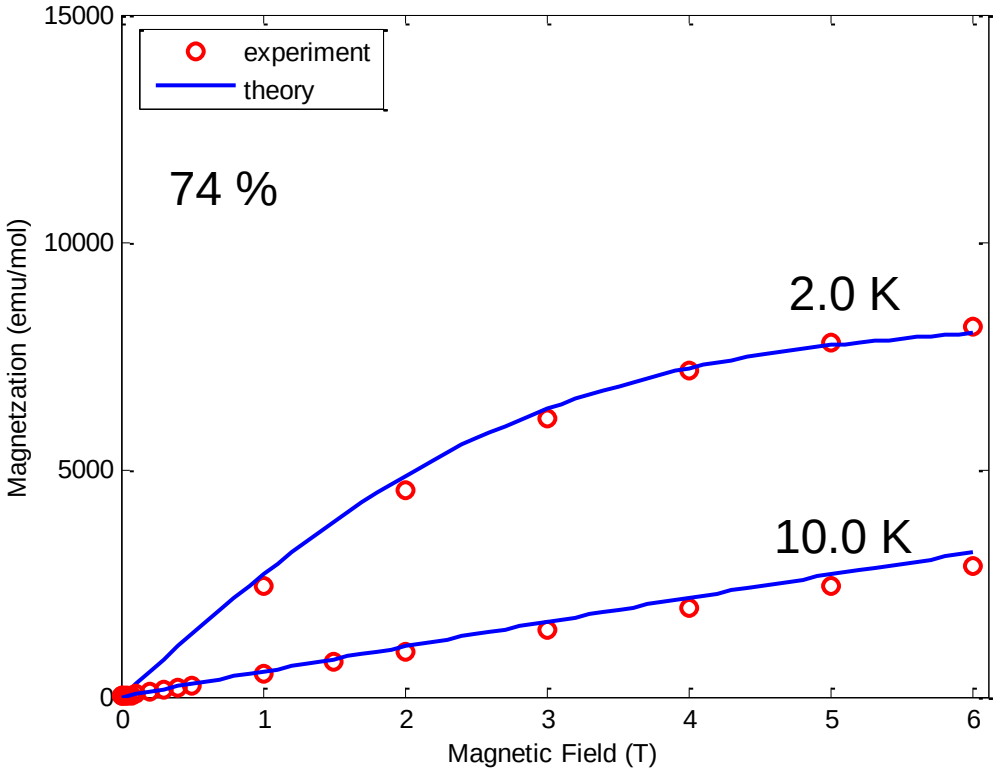

	Cu^{2+}– n – Cu^{2+}	
1294	1 × Cu^{2+}	
1344	2 × Cu^{2+} biphenyl	n = 8
2955	2 × Cu^{2+} pyrazine 	n = 4
2567	2 × Cu^{2+} oxamide	n = 3
2356	2 × Cu^{2+} oxamide	n = 3
2975	2 × Cu^{2+} pyirimidyne 	n = 3

Samples

Isomeric bimetallic copper(II) Cu^{2+} and nickel(II) Ni^{2+} complexes

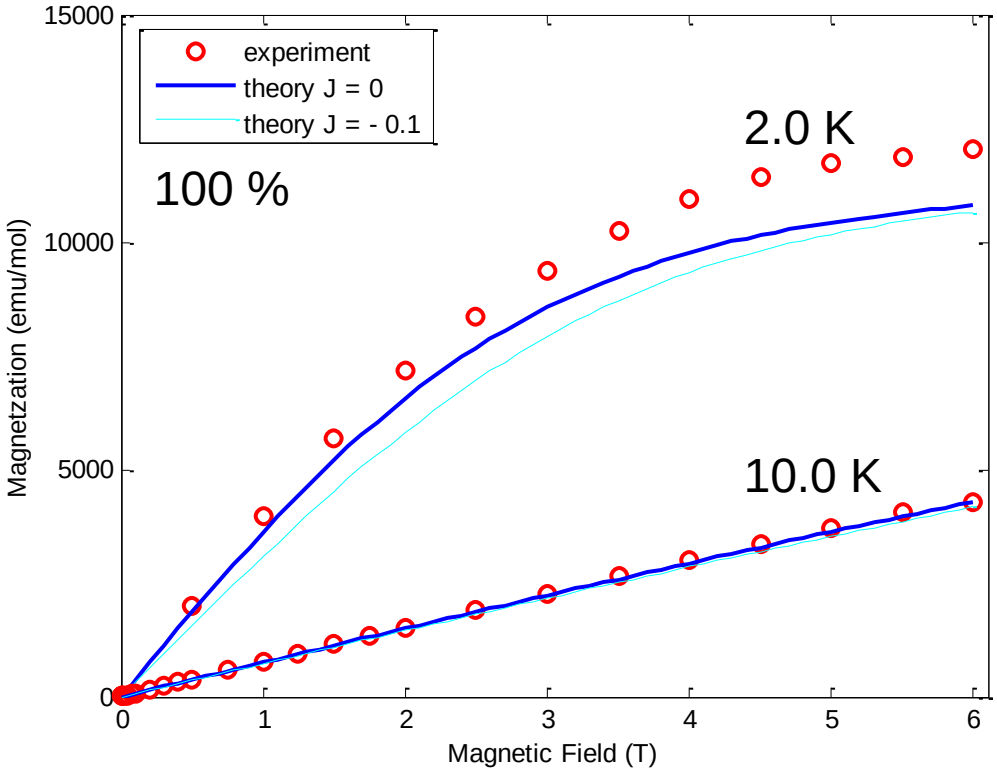

		Cu^{2+}– n – Cu^{2+}
1294	1 × Cu^{2+}	
1344	2 × Cu^{2+} biphenyl	n = 8
2955	2 × Cu^{2+} pyrazine 	n = 4
2567	2 × Cu^{2+} oxamide	n = 3
2356	2 × Cu^{2+} oxamide	n = 3
2975	2 × Cu^{2+} pyirimidyne 	n = 3

Samples

Isomeric bimetallic copper(II) Cu^{2+} and nickel(II) Ni^{2+} complexes

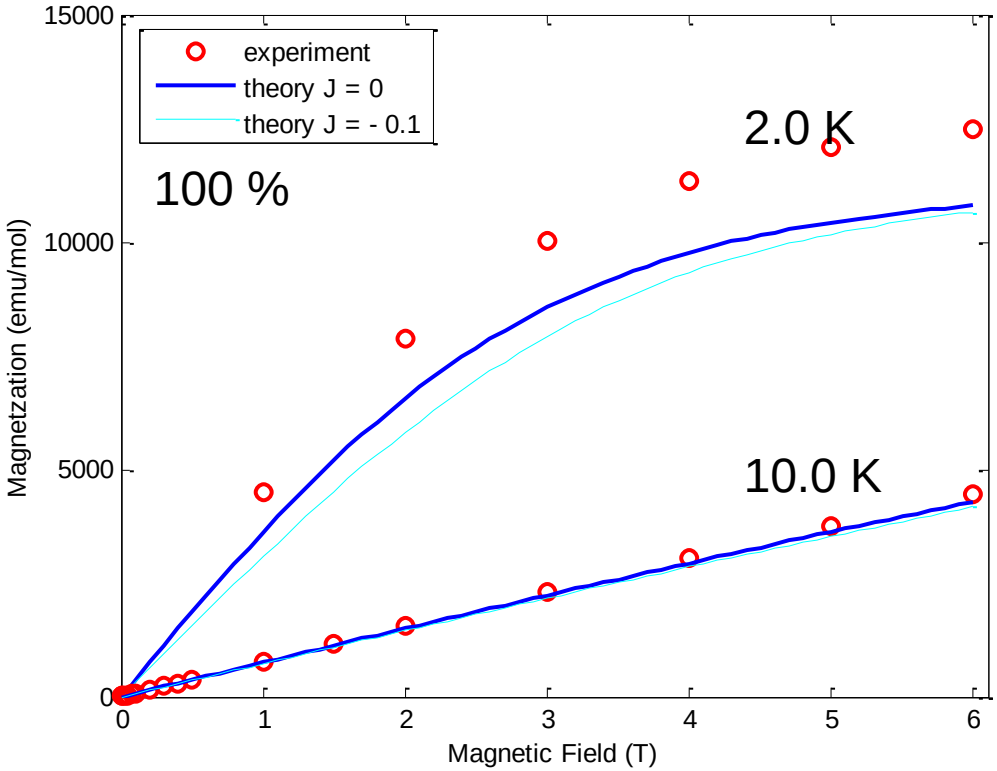

		Cu^{2+}– n – Cu^{2+}
1294	1 × Cu^{2+}	
1344	2 × Cu^{2+} biphenyl	n = 8
2955	2 × Cu^{2+} pyrazine 	n = 4
2567	2 × Cu^{2+} oxamide	n = 3
2356	2 × Cu^{2+} oxamide	n = 3
2975	2 × Cu^{2+} pyirimidyne 	n = 3

Samples

Isomeric bimetallic copper(II) Cu^{2+} and nickel(II) Ni^{2+} complexes

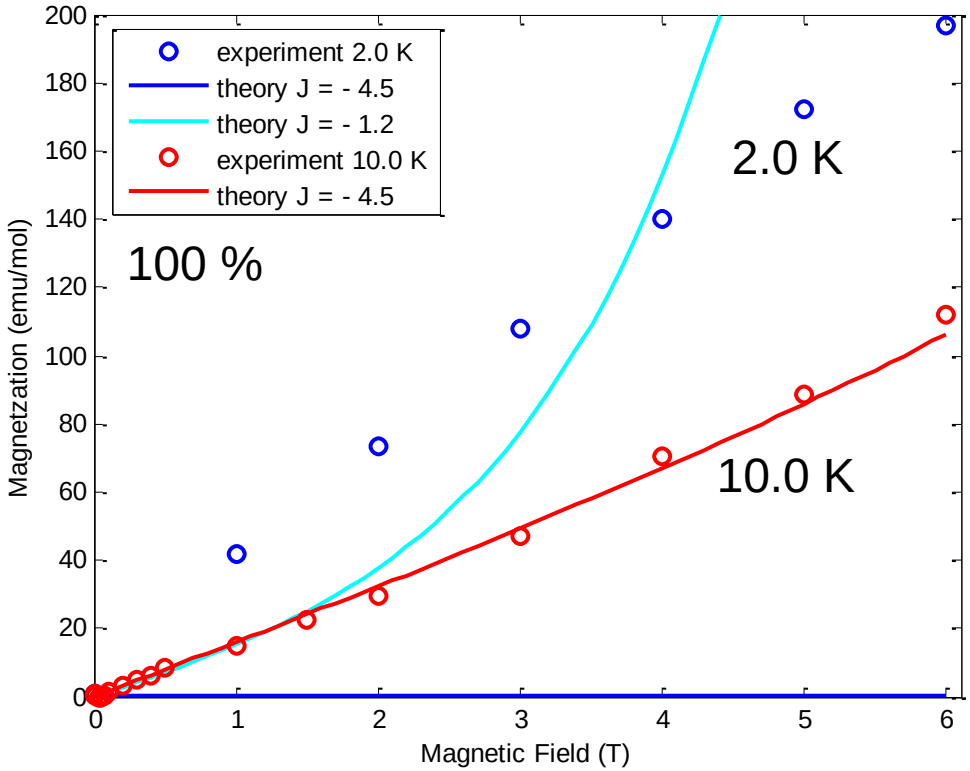

		Cu^{2+}– n – Cu^{2+}
1294	1 × Cu^{2+}	
1344	2 × Cu^{2+} biphenyl	n = 8
2955	2 × Cu^{2+} pyrazine 	n = 4
2567	2 × Cu^{2+} oxamide	n = 3
2356	2 × Cu^{2+} oxamide	n = 3
2975	2 × Cu^{2+} pyirimidyne 	n = 3

Samples

Isomeric bimetallic copper(II) Cu^{2+} and nickel(II) Ni^{2+} complexes

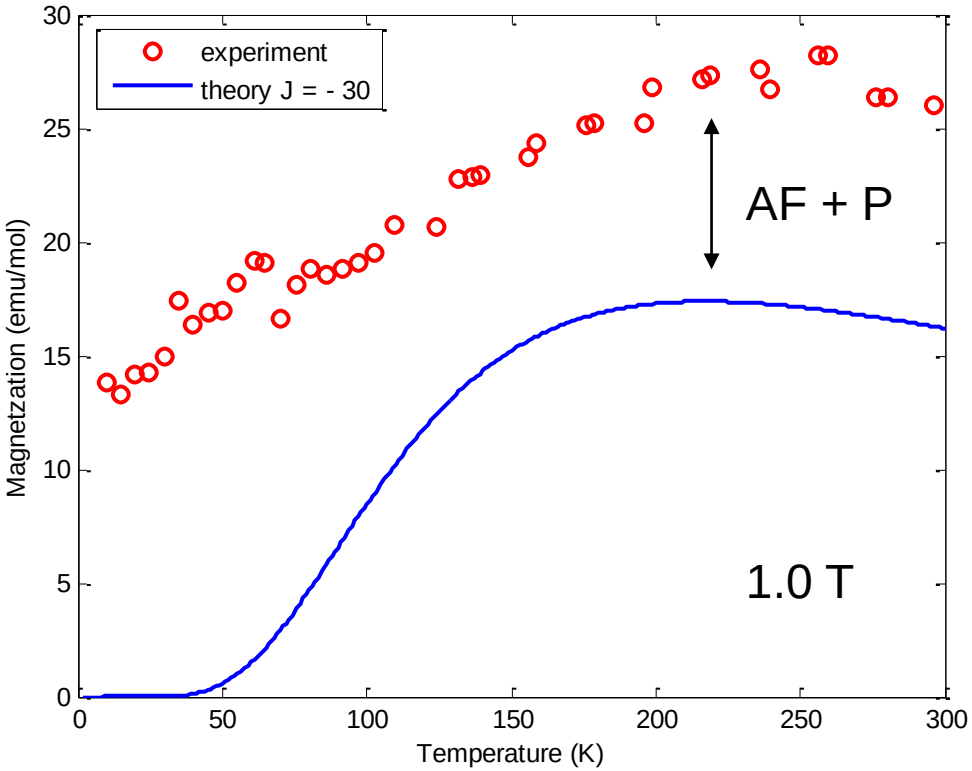

		Cu^{2+}– n – Cu^{2+}
1294	1 × Cu^{2+}	
1344	2 × Cu^{2+} bifenyl	n = 8
2955	2 × Cu^{2+} pirazyna 	n = 4
2567	2 × Cu^{2+} oksamid	n = 3
2356	2 × Cu^{2+} oksamid	n = 3
2975	2 × Cu^{2+} pirymidyna 	n = 3

Samples

Isomeric bimetallic copper(II) Cu^{2+} and nickel(II) Ni^{2+} complexes

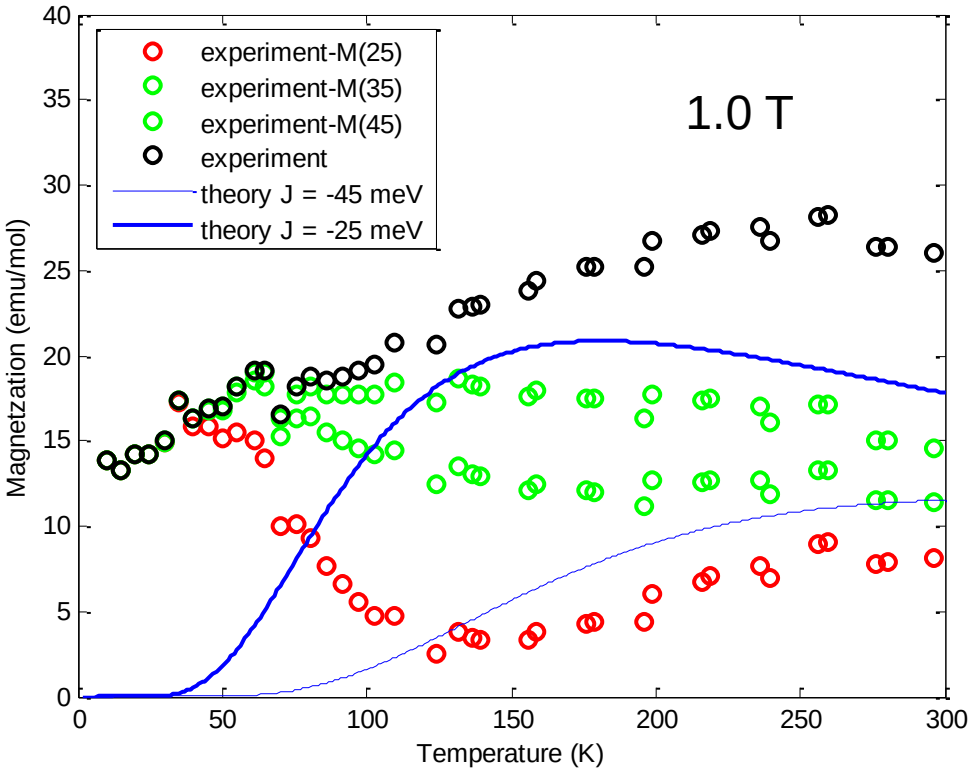

		Cu^{2+}– n – Cu^{2+}
1294	1 × Cu^{2+}	
1344	2 × Cu^{2+} bifenyl	n = 8
2955	2 × Cu^{2+} pirazyna 	n = 4
2567	2 × Cu^{2+} oksamid	n = 3
2356	2 × Cu^{2+} oksamid	n = 3
2975	2 × Cu^{2+} pirymidyna 	n = 3

Samples

Isomeric bimetallic copper(II) Cu^{2+} and nickel(II) Ni^{2+} complexes

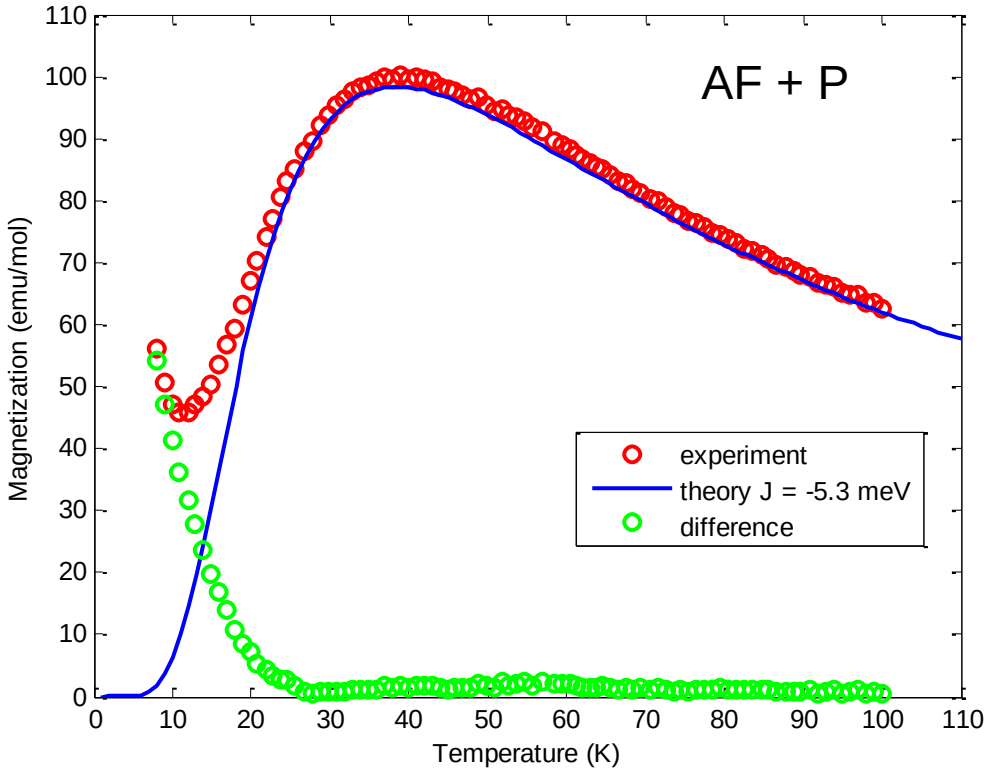

		Cu^{2+}– n – Cu^{2+}
1294	1 × Cu^{2+}	
1344	2 × Cu^{2+} bifenyl	n = 8
2955	2 × Cu^{2+} pirazyna 	n = 4
2567	2 × Cu^{2+} oksamid	n = 3
2356	2 × Cu^{2+} oksamid	n = 3
2975	2 × Cu^{2+} pirymidyna 	n = 3

Samples

Isomeric bimetallic copper(II) Cu^{2+} and nickel(II) Ni^{2+} complexes

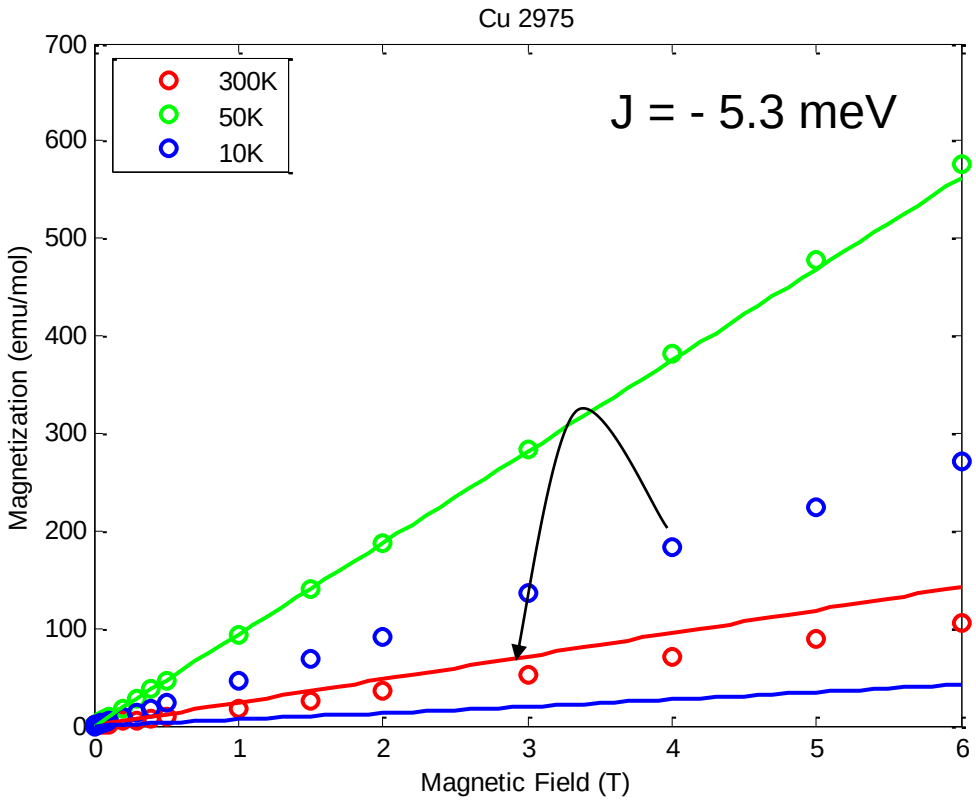

		Cu^{2+}– n – Cu^{2+}
1294	1 × Cu^{2+}	
1344	2 × Cu^{2+} bifenyl	n = 8
2955	2 × Cu^{2+} pirazyna 	n = 4
2567	2 × Cu^{2+} oksamid	n = 3
2356	2 × Cu^{2+} oksamid	n = 3
2975	2 × Cu^{2+} pirymidyna 	n = 3

Results

2567

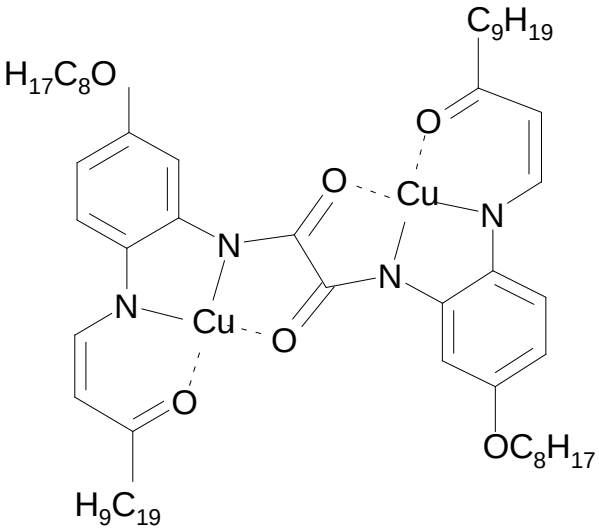

Cu^{2+}– 3 – Cu^{2+}

2975

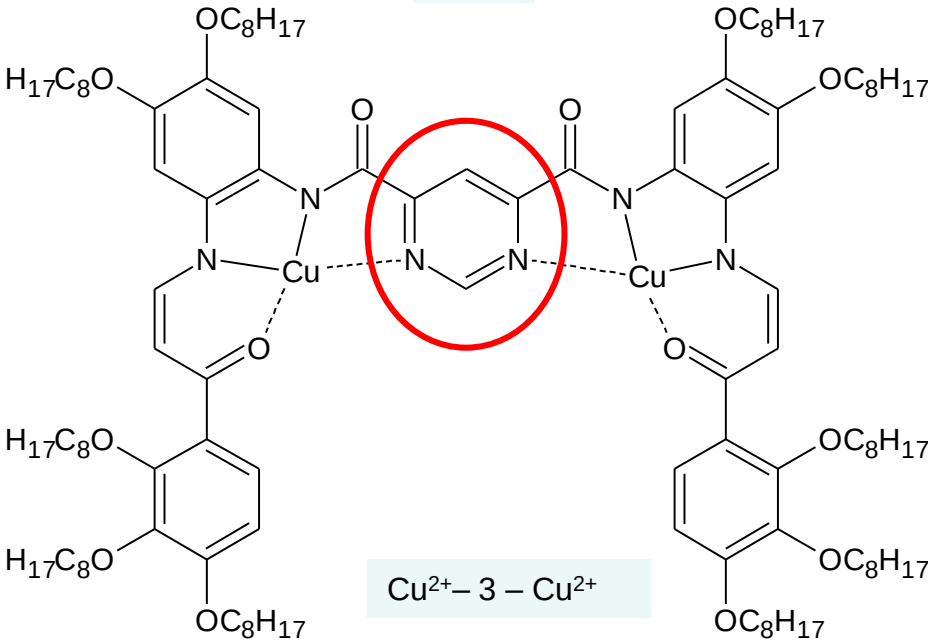

Cu^{2+}– 3 – Cu^{2+}

30

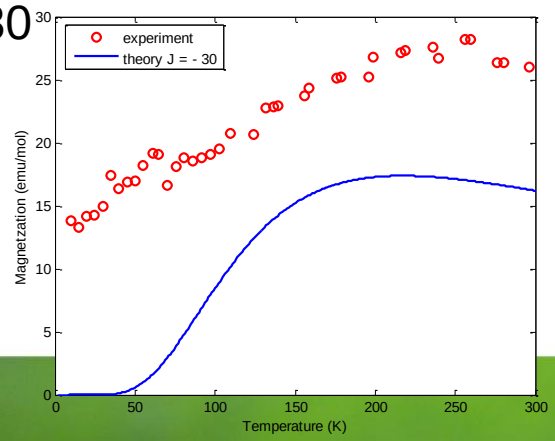

100

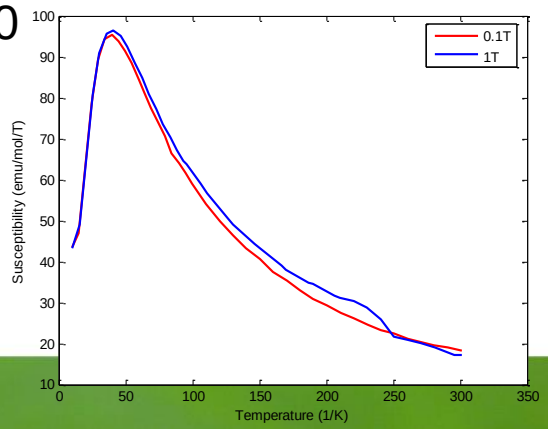

Hypothesis

2567

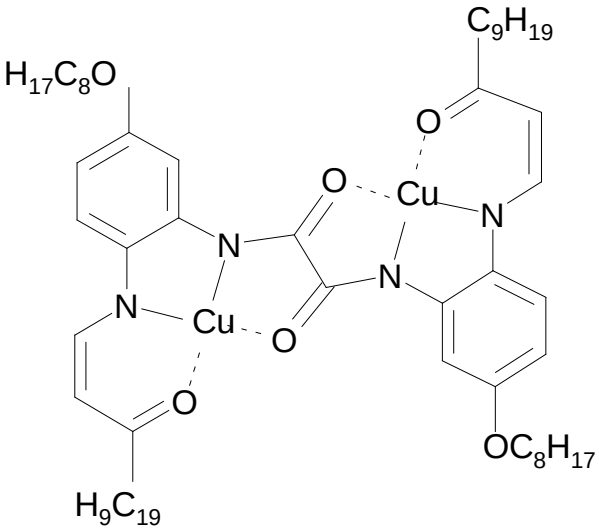

Cu^{2+}– 3 – Cu^{2+}

2975

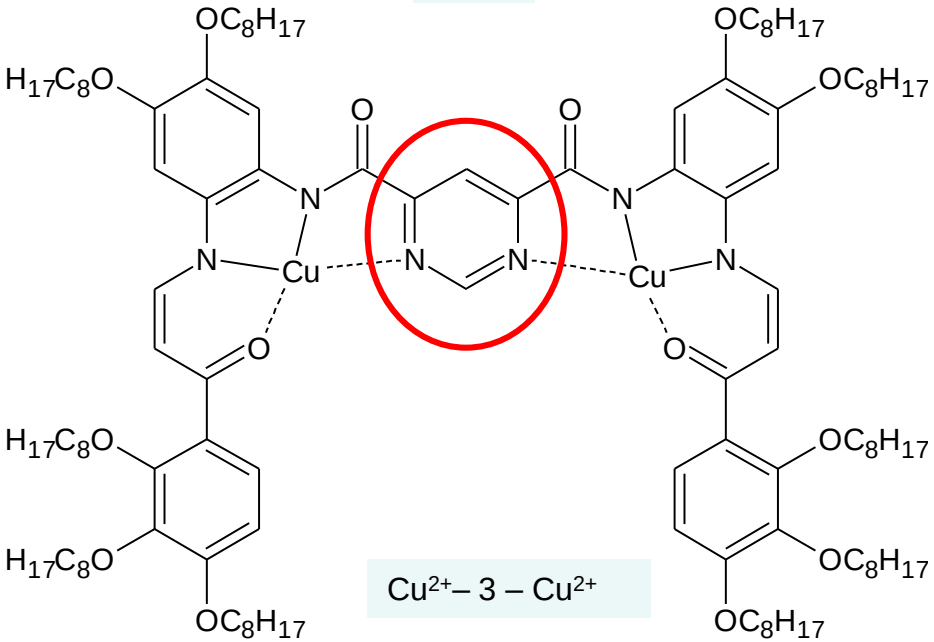

Cu^{2+}– 3 – Cu^{2+}

$$H = -2\,J\,S_1 S_2$$

$$J = J_3^{AF} \; <0$$

$$J = \overset{<0}{J_3^{AF}} + \overset{>0}{J^{F}}$$

superexchange

indirect exchange

Samples

Isomeric bimetallic copper(II) Cu^{2+} and nickel(II) Ni^{2+} complexes

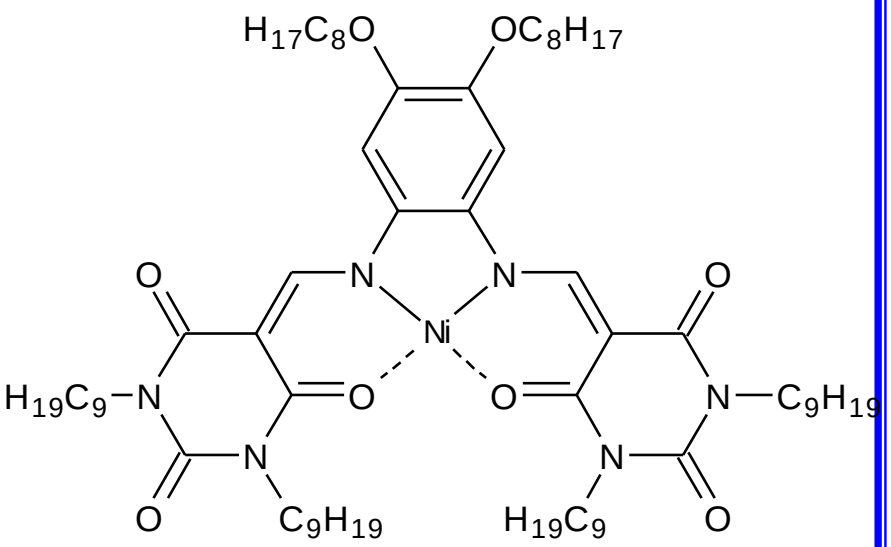

2763 agata

	Ni^{2+}– n – Ni^{2+}
2763	1 × Ni^{2+}

Samples

Isomeric bimetallic copper(II) Cu^{2+} and nickel(II) Ni^{2+} complexes

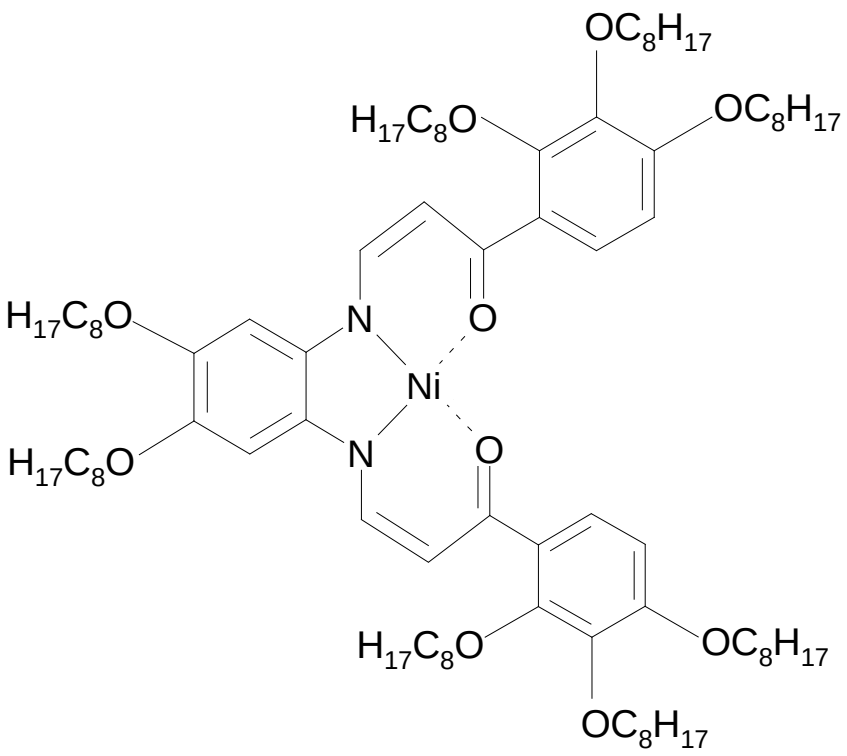

	Ni^{2+}– n – Ni^{2+}
2763	1 × Ni^{2+}
1421	1 × Ni^{2+}

Samples

Isomeric bimetallic copper(II) Cu^{2+} and nickel(II) Ni^{2+} complexes

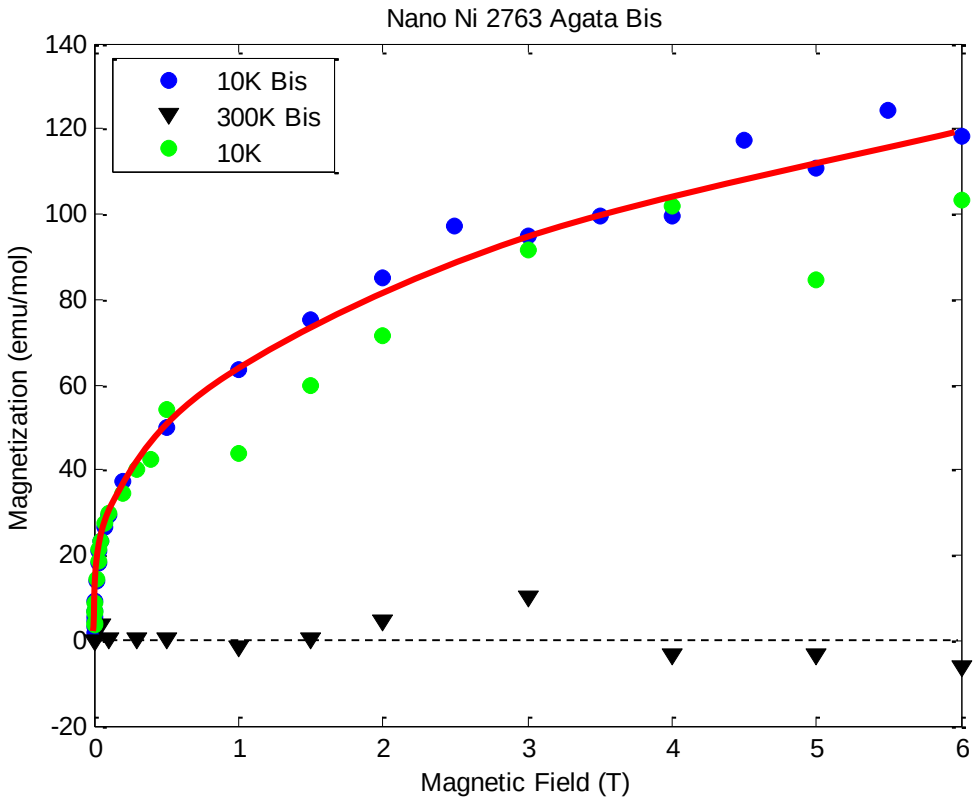

	Ni^{2+}– n – Ni^{2+}
2763	1 × Ni^{2+}
1421	1 × Ni^{2+}

Samples

Isomeric bimetallic copper(II) Cu^{2+} and nickel(II) Ni^{2+} complexes

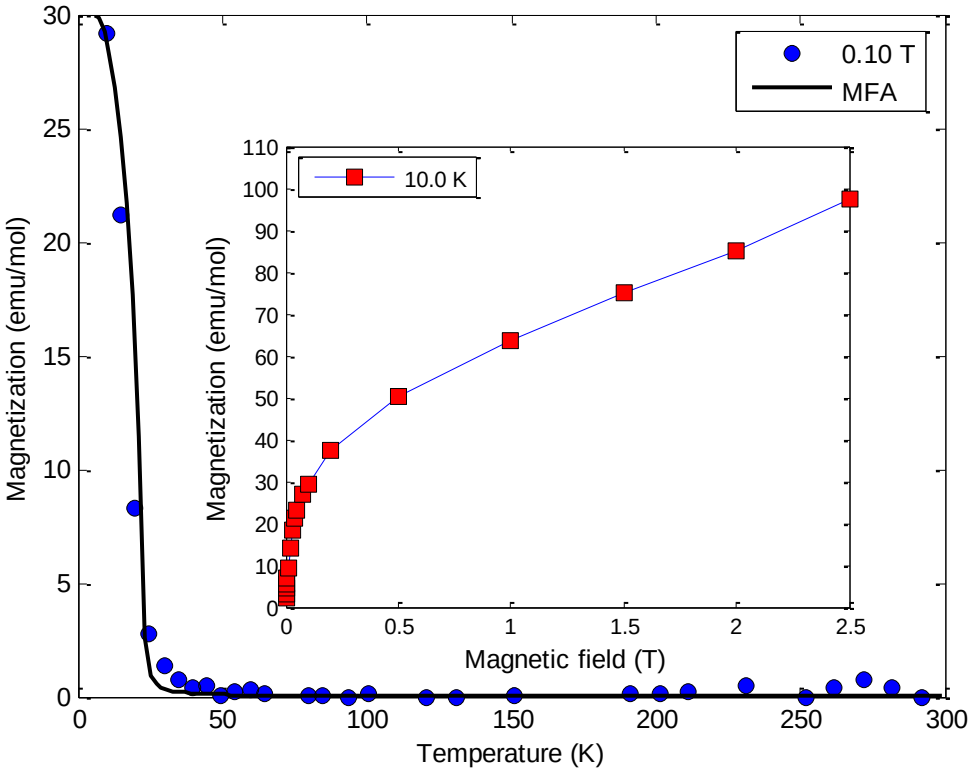

	Ni^{2+}– n – Ni^{2+}
2763	1 × Ni^{2+}
1421	1 × Ni^{2+}

Samples

Isomeric bimetallic copper(II) Cu^{2+} and nickel(II) Ni^{2+} complexes

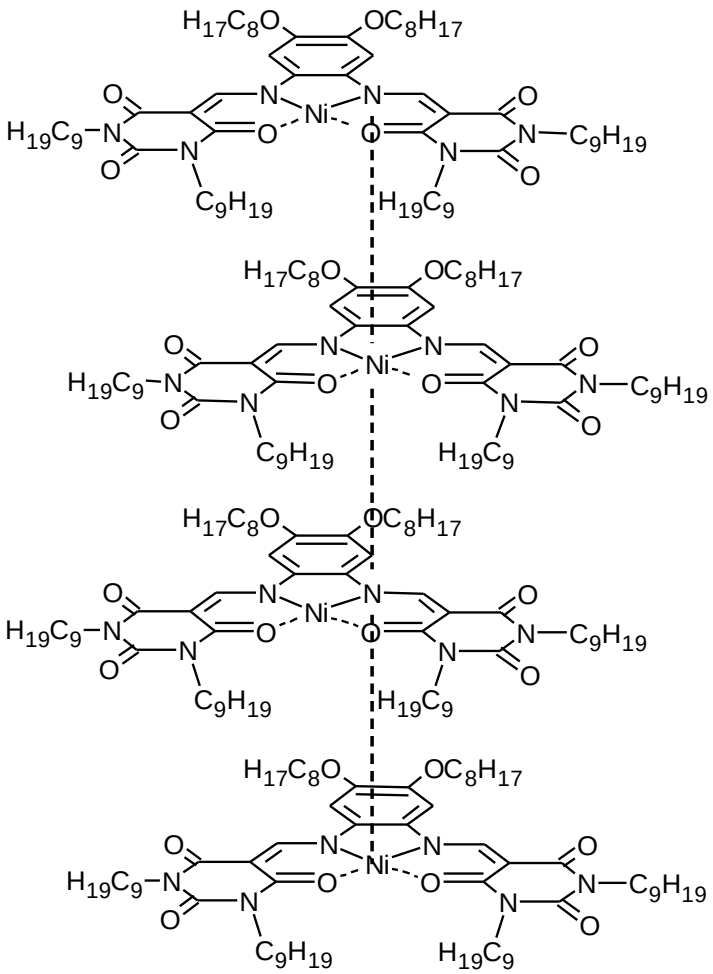

	Ni^{2+}– n – Ni^{2+}
2763	1 × Ni^{2+}
1421	1 × Ni^{2+}

Szydłowska, Szczytko et al.CHEMPHYSCHEM **11** ,1735-1741 (2010)

Samples

Isomeric bimetallic copper(II) Cu^{2+} and nickel(II) Ni^{2+} complexes

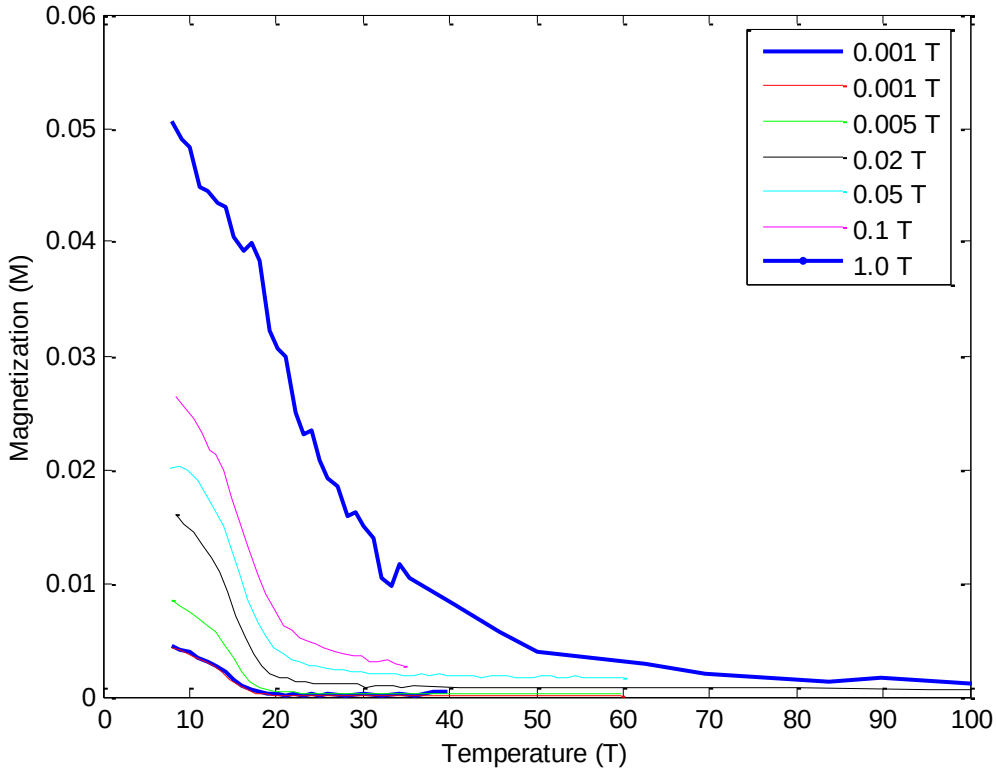

	Ni^{2+}– n – Ni^{2+}
2763	1 × Ni^{2+}
1421	1 × Ni^{2+}

Samples

Isomeric bimetallic copper(II) Cu^{2+} and nickel(II) Ni^{2+} complexes

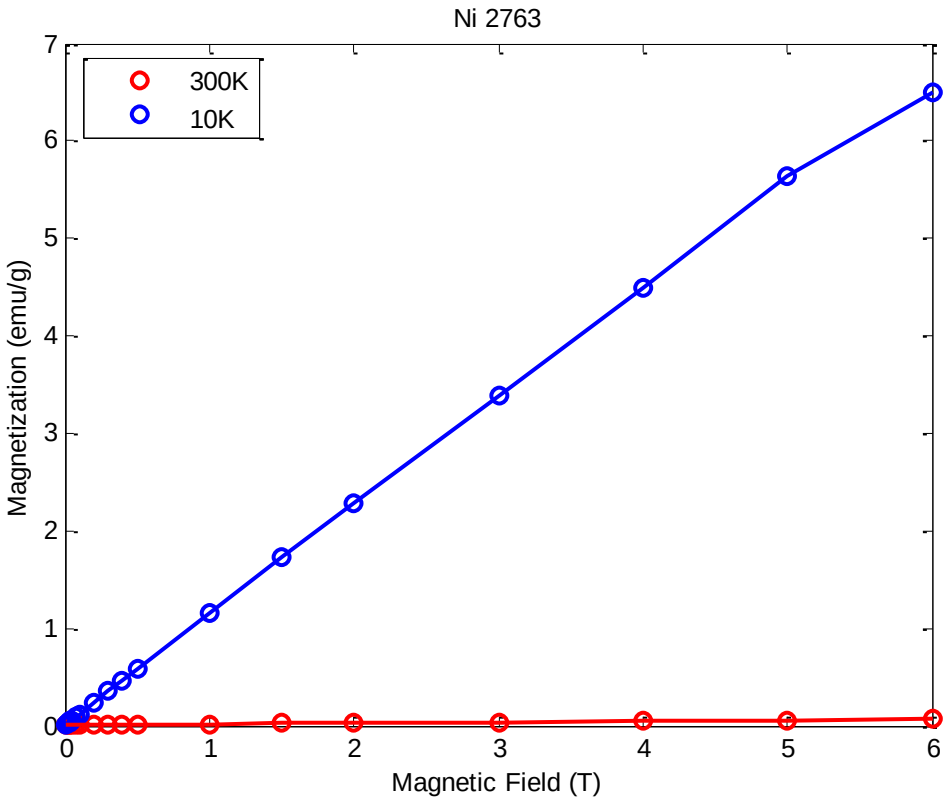

	Ni^{2+}– n – Ni^{2+}
2763	1 × Ni^{2+}
1421	1 × Ni^{2+}

Samples

Isomeric bimetallic copper(II) Cu^{2+} and nickel(II) Ni^{2+} complexes

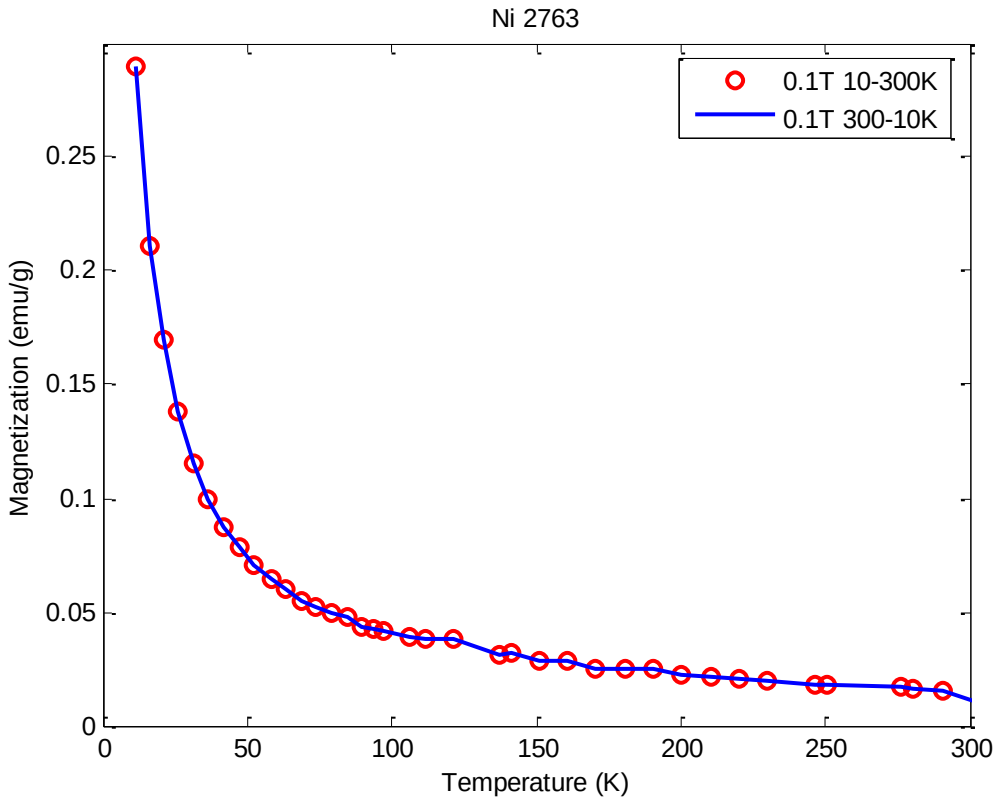

	Ni^{2+}– n – Ni^{2+}
2763	1 × Ni^{2+}
1421	1 × Ni^{2+}

Samples

Isomeric bimetallic copper(II) Cu^{2+} and nickel(II) Ni^{2+} complexes

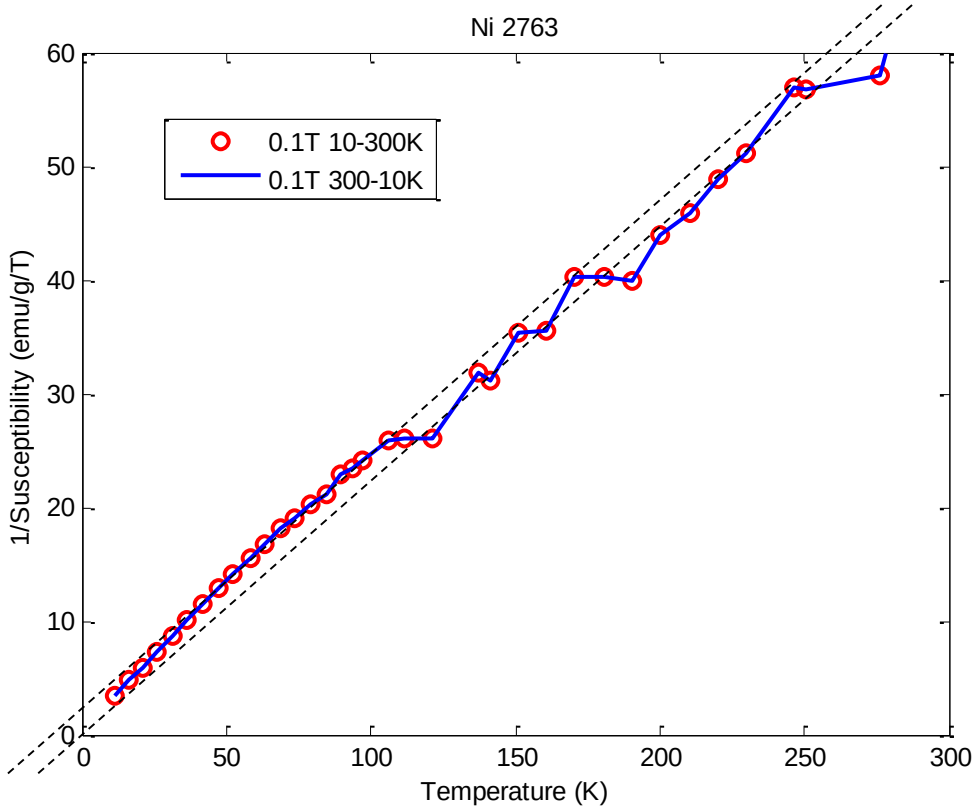

	Ni^{2+}– n – Ni^{2+}
2763	1 × Ni^{2+}
1421	1 × Ni^{2+}

Spintronic devices

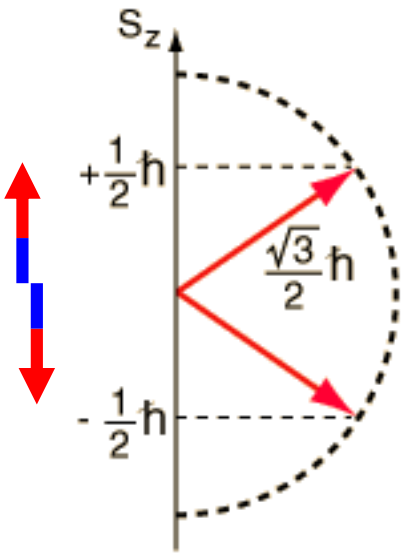

Spintronic devices

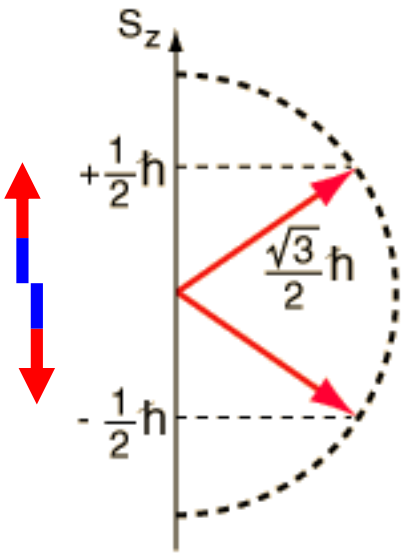

Stern-Gerlach experiment (1922 r.)

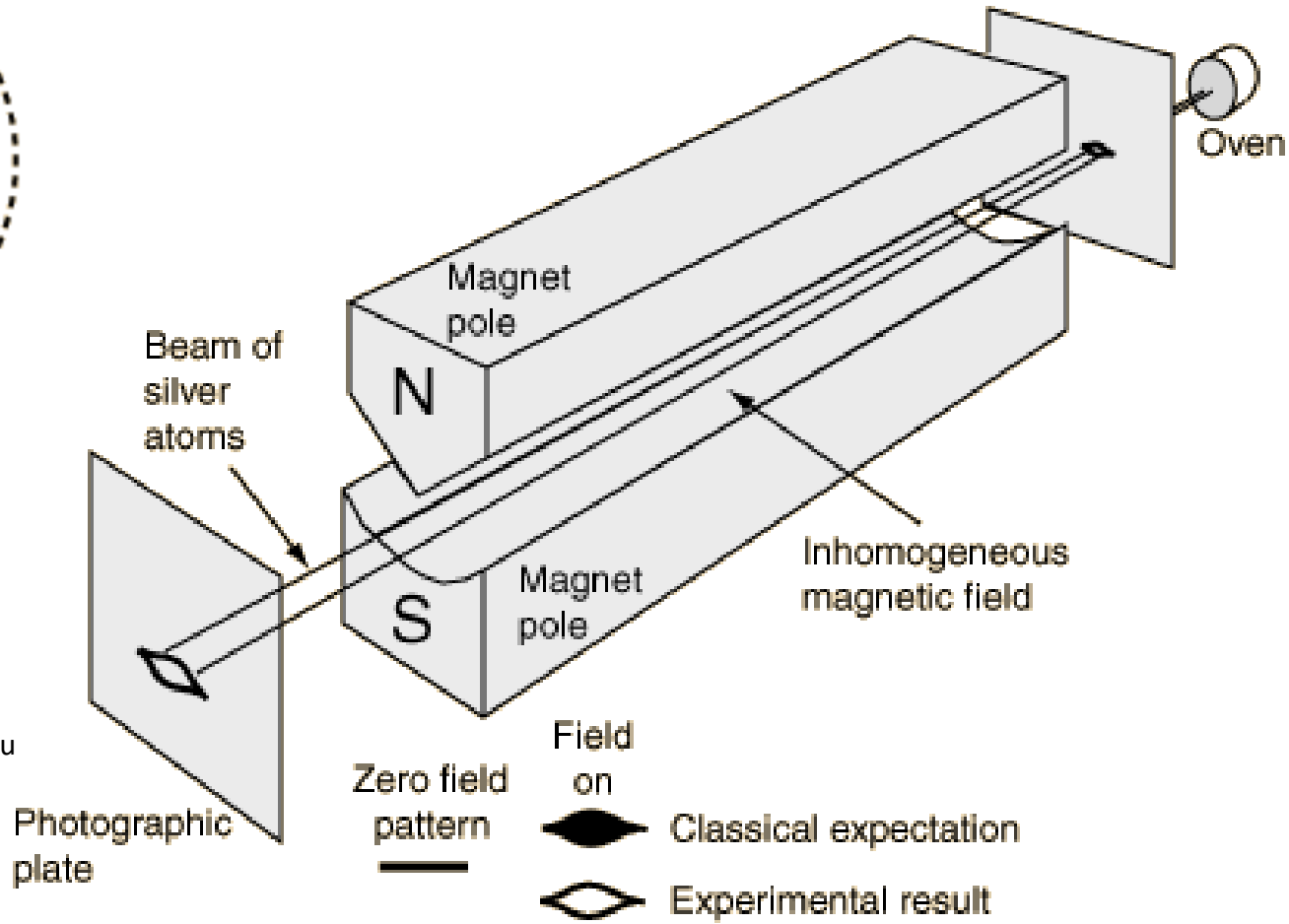

http://hyperphysics.phy-astr.gsu.edu

Spintronic devices

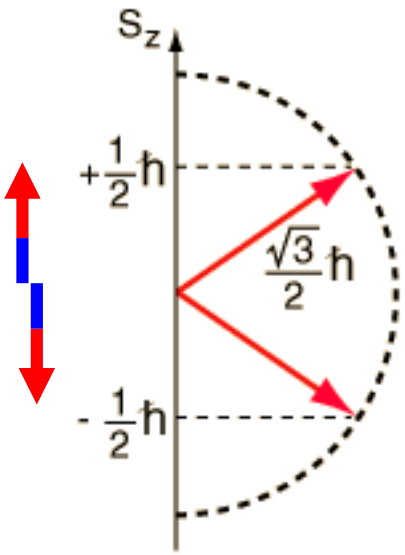

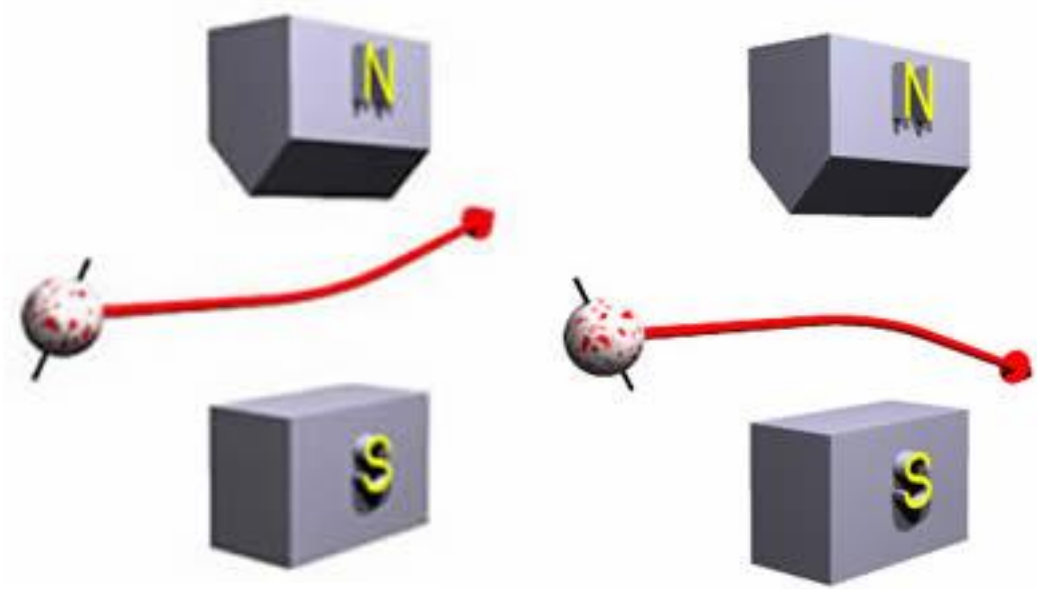

http://www.upscale.utoronto.ca/GeneralInterest/Harrison/SternGerlach/SternGerlach.html

Spintronic devices

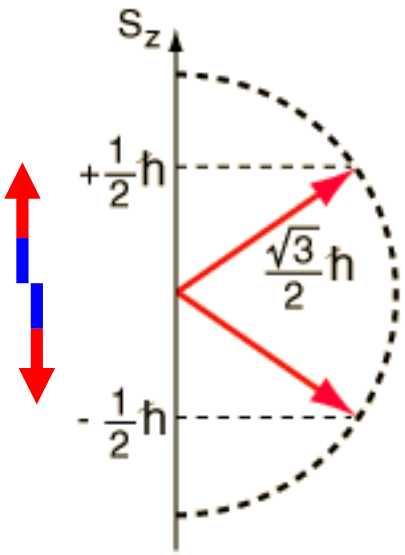

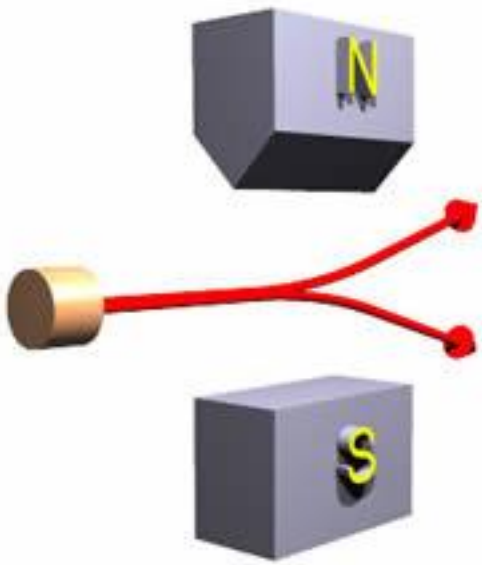

http://www.upscale.utoronto.ca/GeneralInterest/Harrison/SternGerlach/SternGerlach.html

Spintronic devices

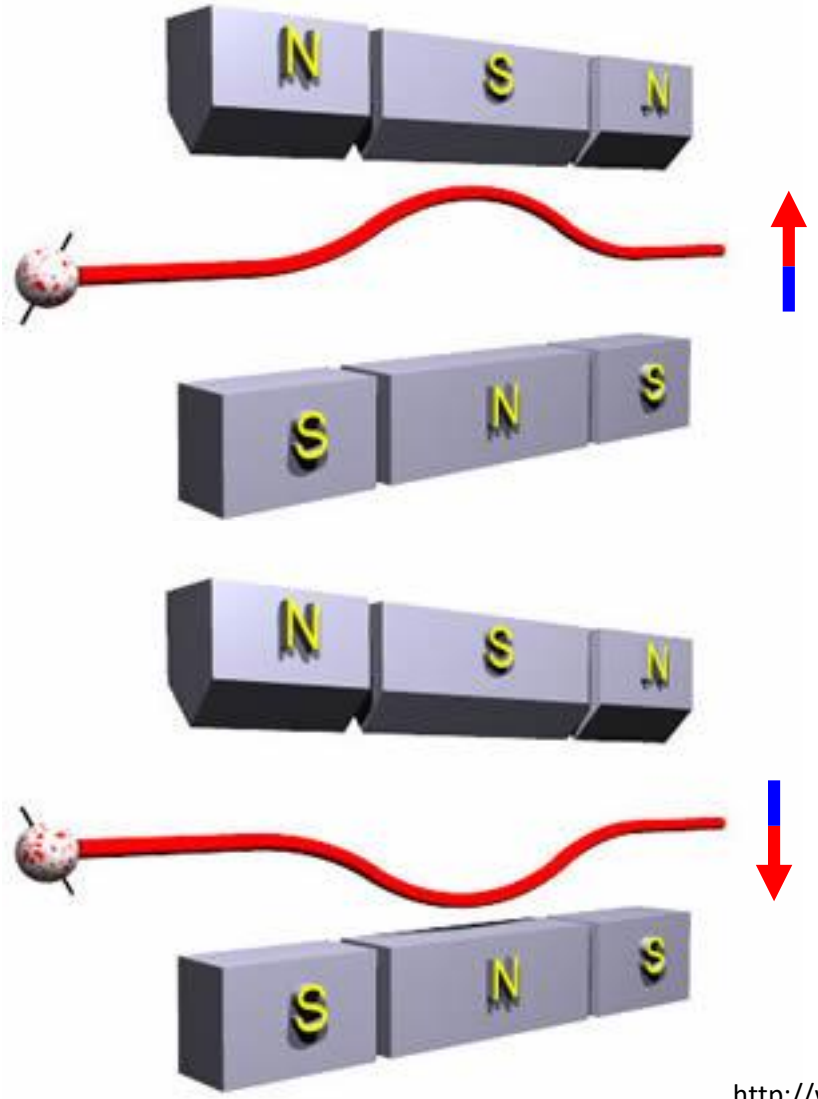

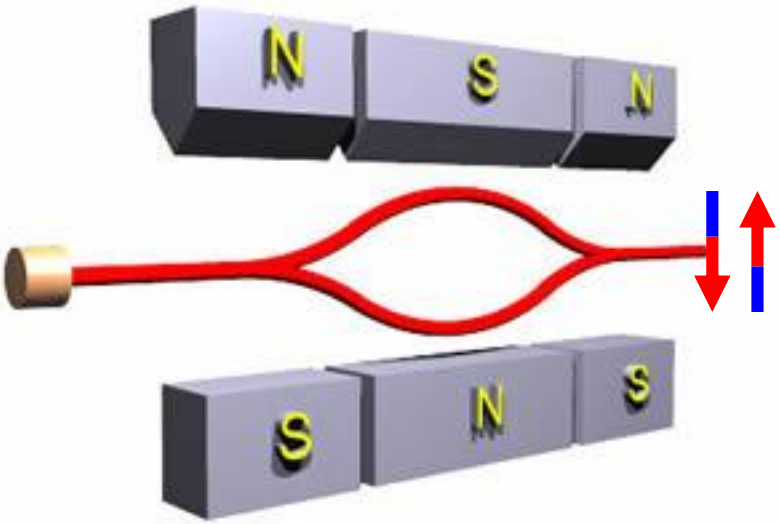

http://www.upscale.utoronto.ca/GeneralInterest/Harrison/SternGerlach/SternGerlach.html

Spintronic devices

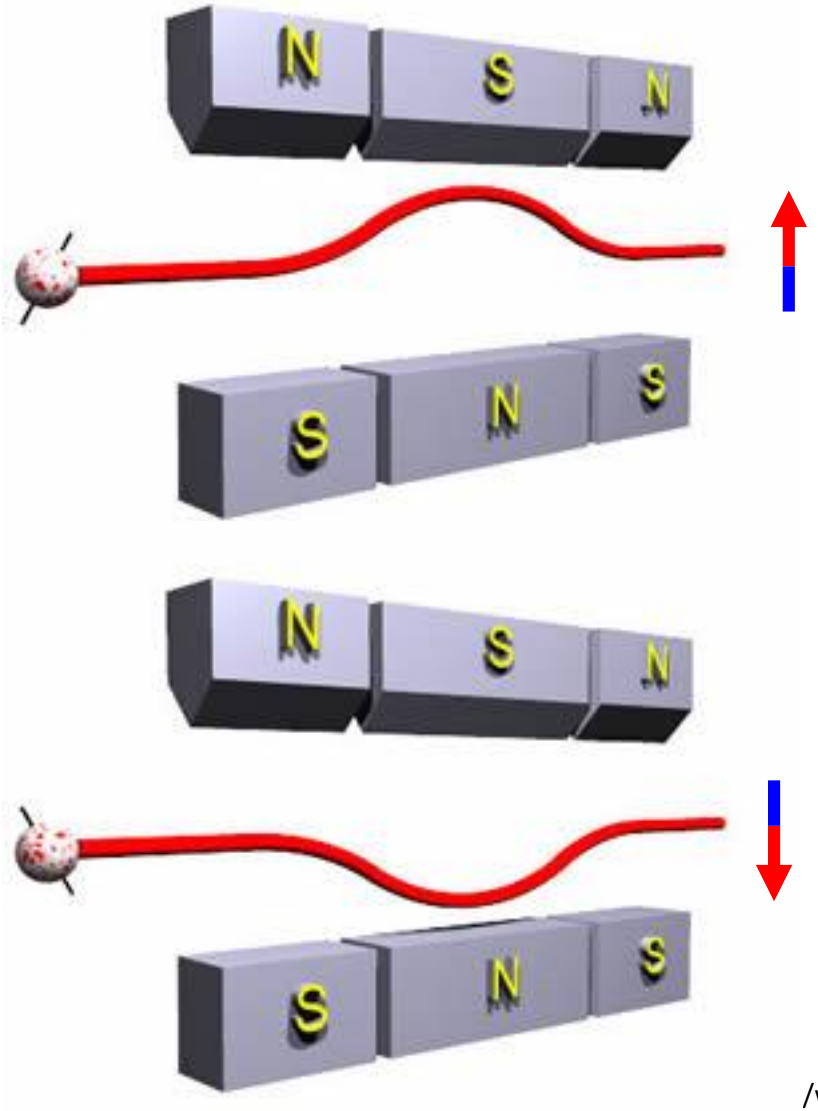

Spin filter!

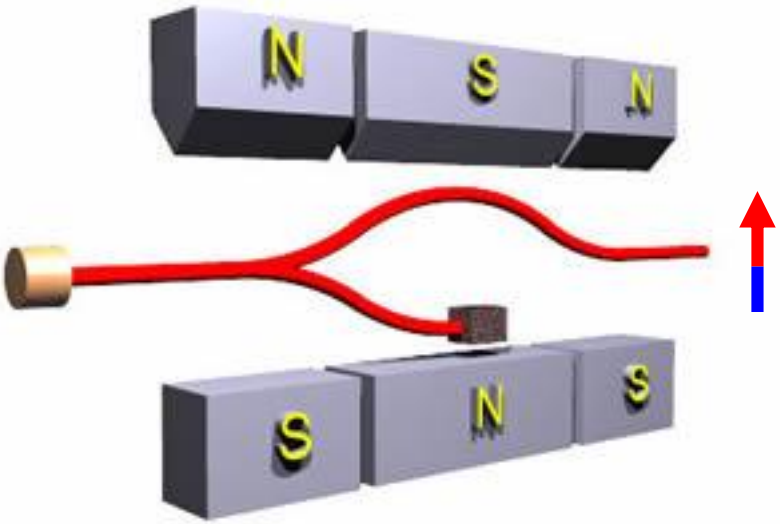

/www.upscale.utoronto.ca/GeneralInterest/Harrison/SternGerlach/SternGerlach.html

Spin-filter

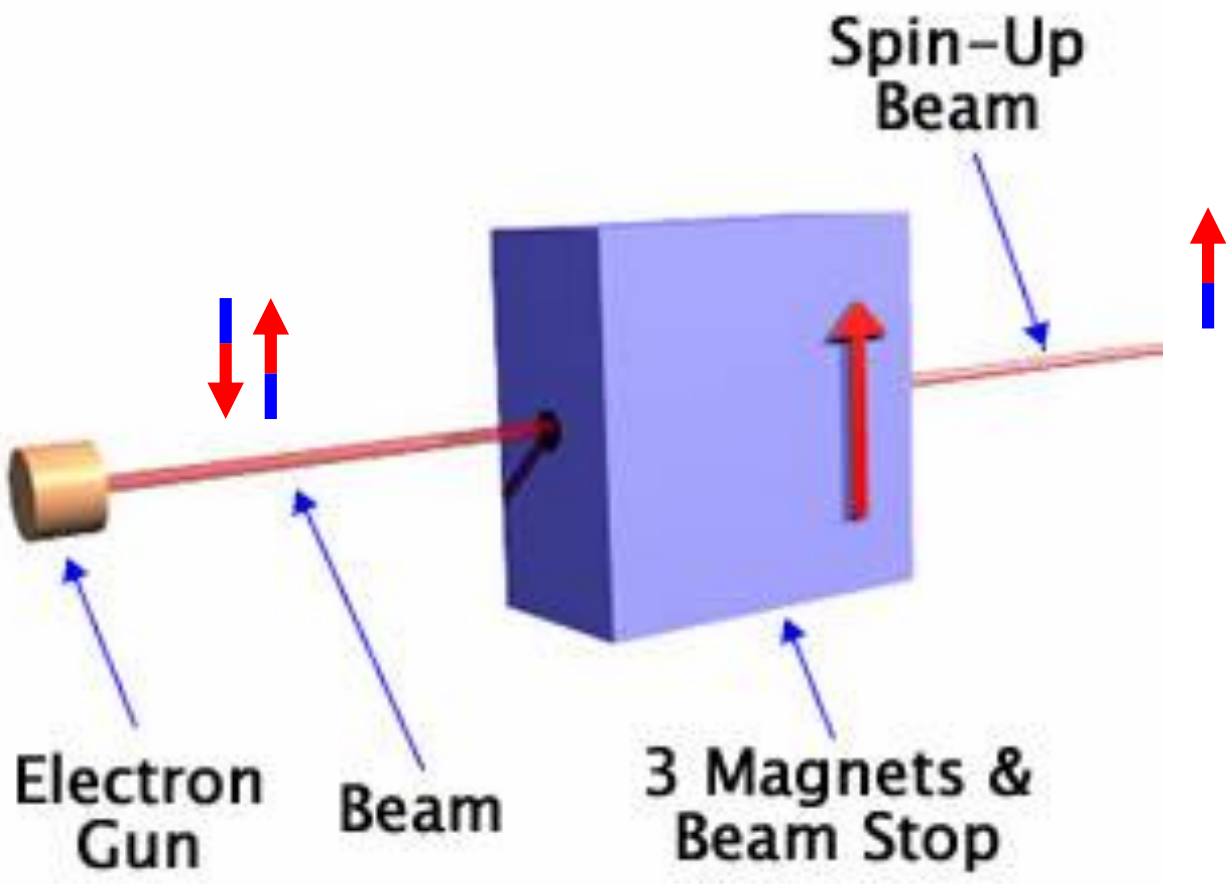

http://www.upscale.utoronto.ca/GeneralInterest/Harrison/SternGerlach/SternGerlach.html

Spin-filter

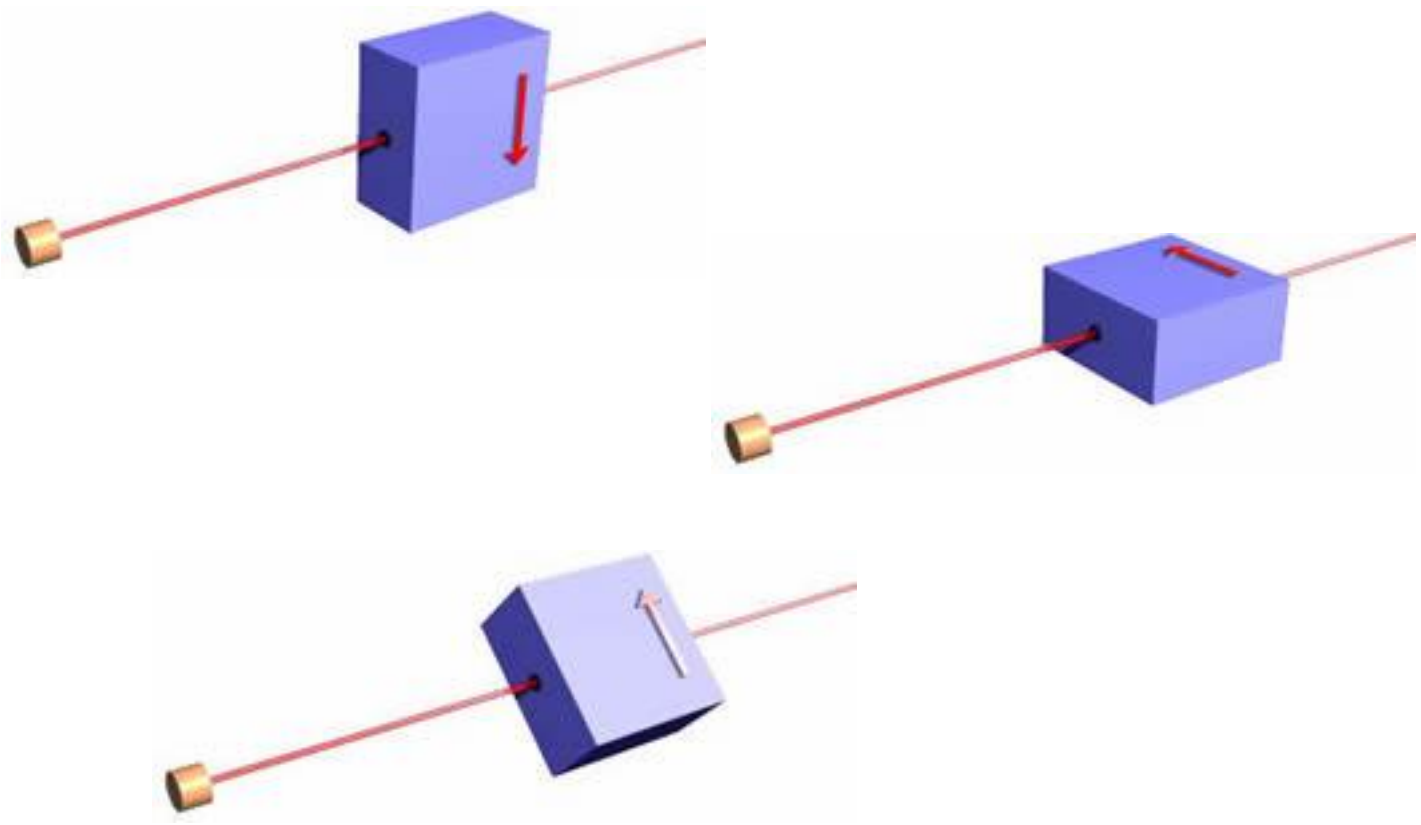

http://www.upscale.utoronto.ca/GeneralInterest/Harrison/SternGerlach/SternGerlach.html

Spin-filter

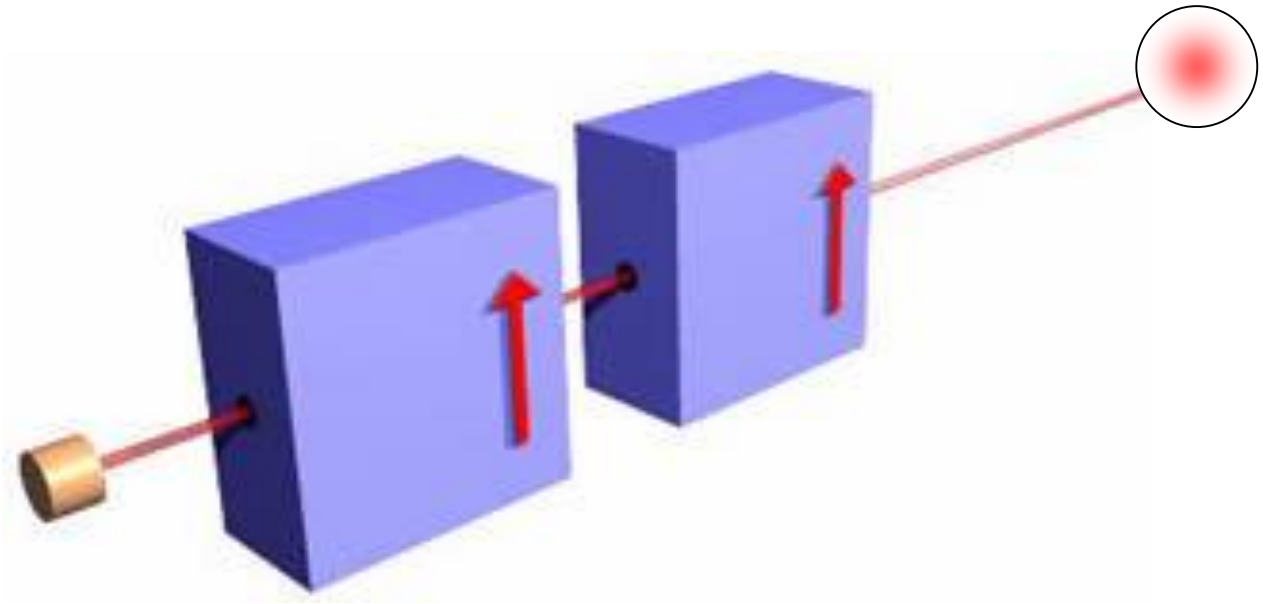

http://www.upscale.utoronto.ca/GeneralInterest/Harrison/SternGerlach/SternGerlach.html

Spin-filter

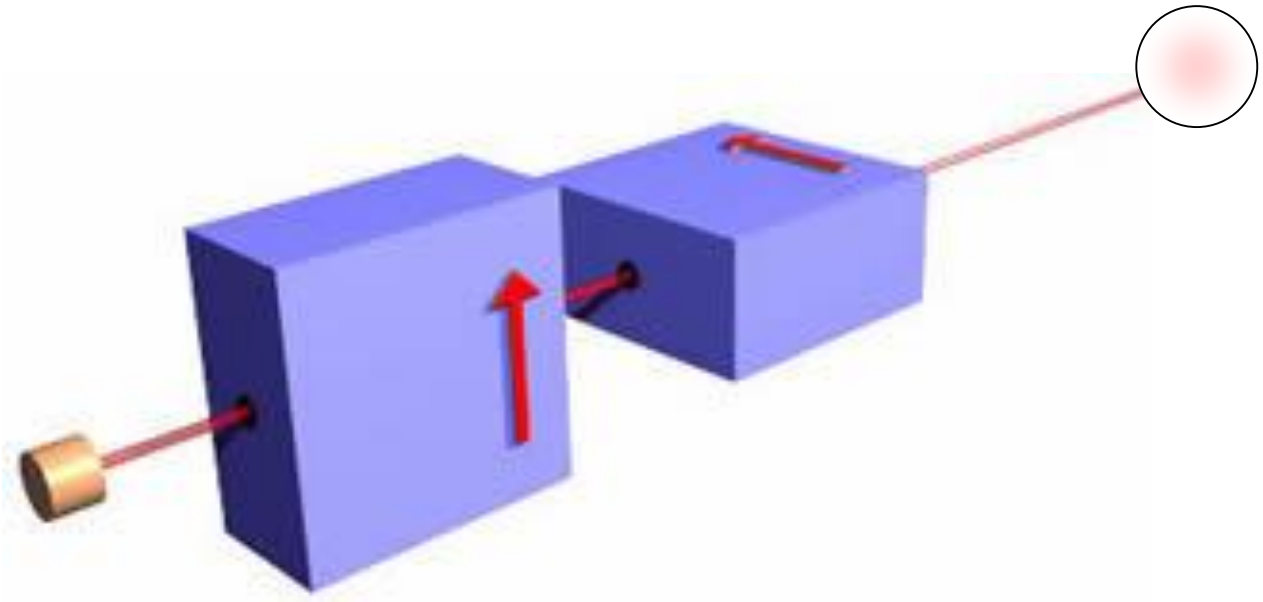

http://www.upscale.utoronto.ca/GeneralInterest/Harrison/SternGerlach/SternGerlach.html

Spin-filter

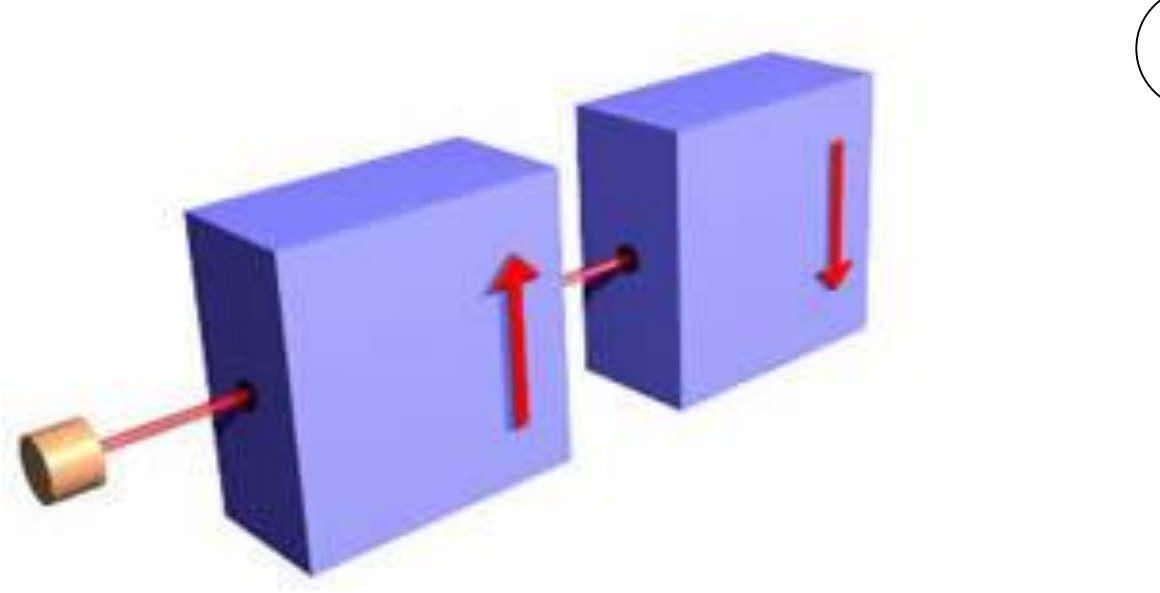

http://www.upscale.utoronto.ca/GeneralInterest/Harrison/SternGerlach/SternGerlach.html

Spin-filter

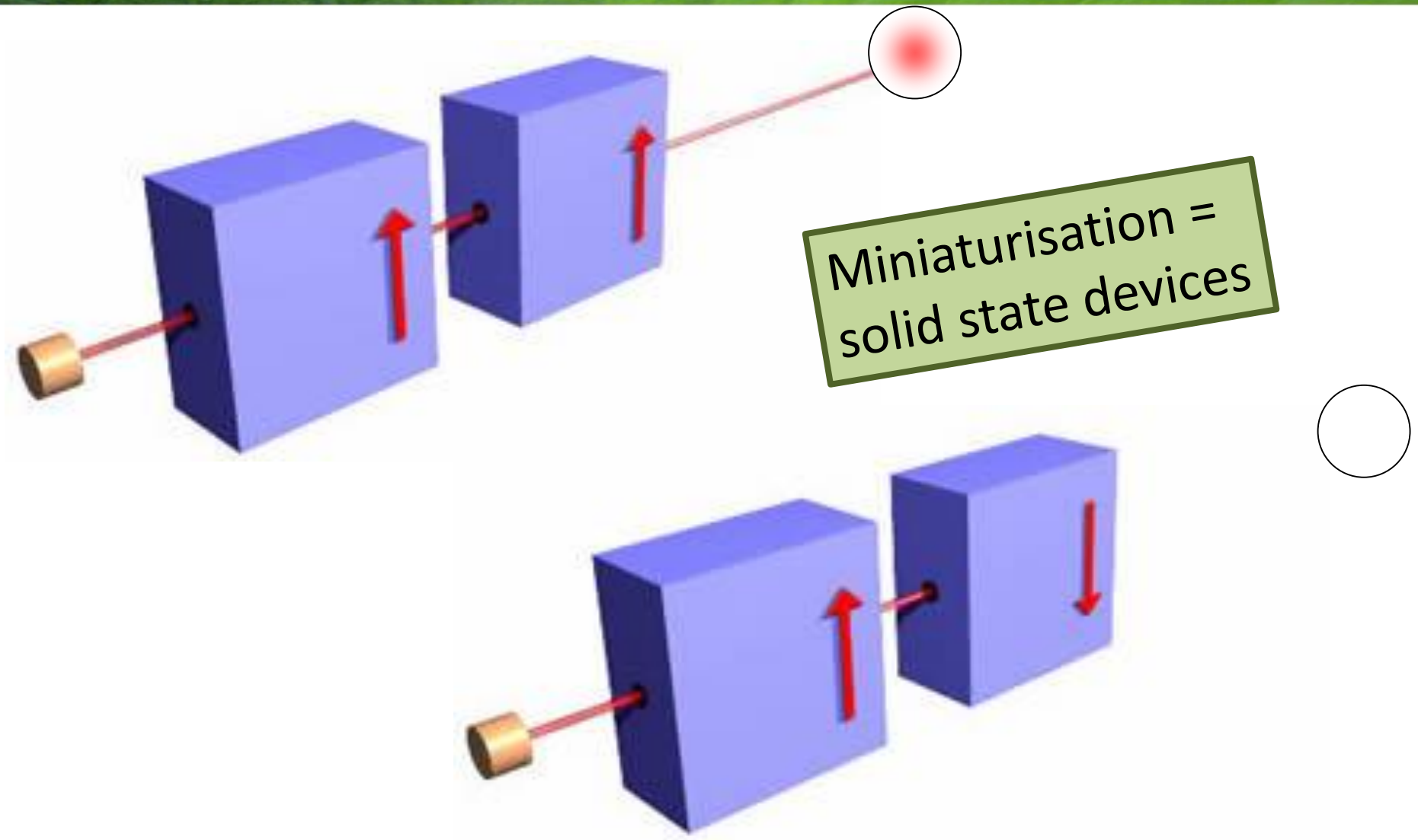

http://www.upscale.utoronto.ca/GeneralInterest/Harrison/SternGerlach/SternGerlach.html

Giant Magnetoresistance

The Nobel Prize in Physics 2007
Albert Fert, Peter Grünberg

The Nobel Prize in Physics 2007

Photo: U. Montan
Albert Fert

Photo: U. Montan
Peter Grünberg

The Nobel Prize in Physics 2007 was awarded jointly to Albert Fert and Peter Grünberg *"for the discovery of Giant Magnetoresistance"*

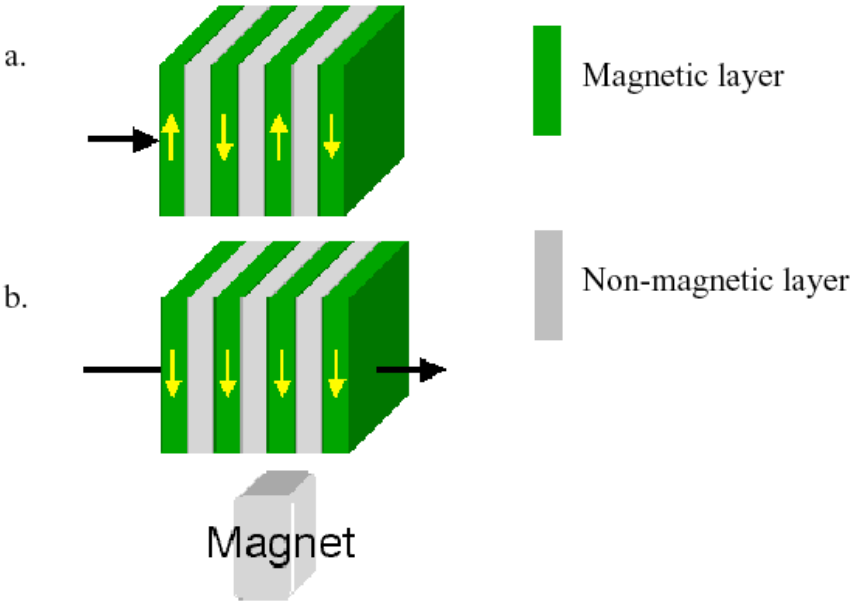

Ferromagnetism

Indirect exchange (Zener model, RKKY)

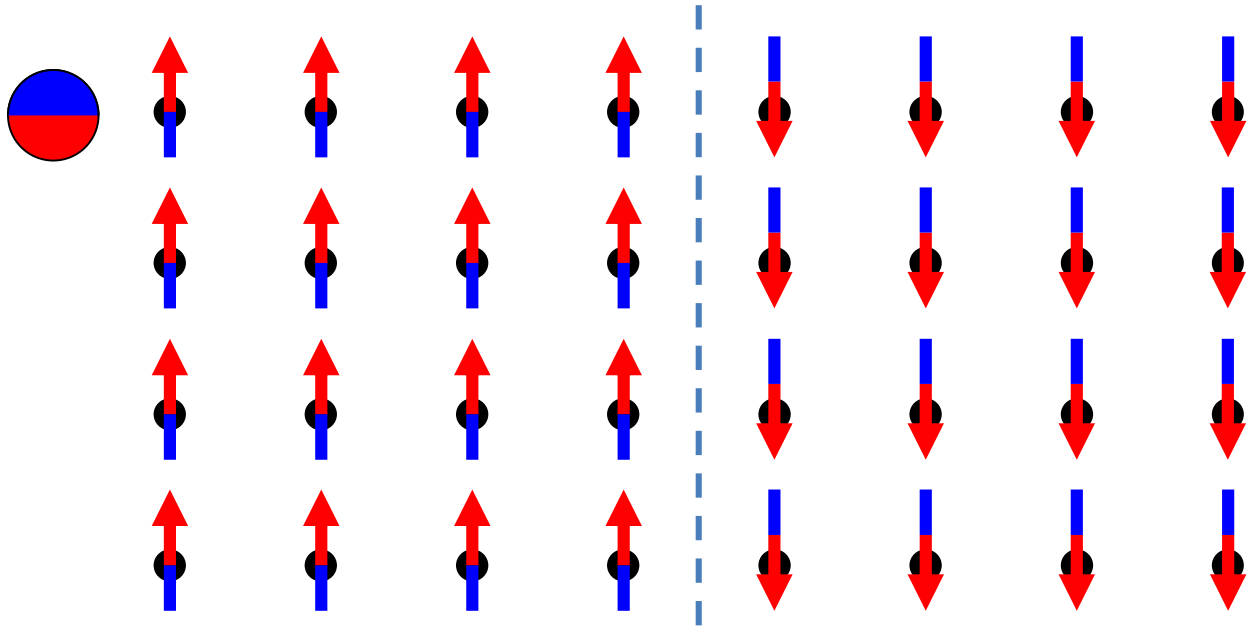

(in)organic spintronics

Magnetoelectronics

Gary A. Prinz

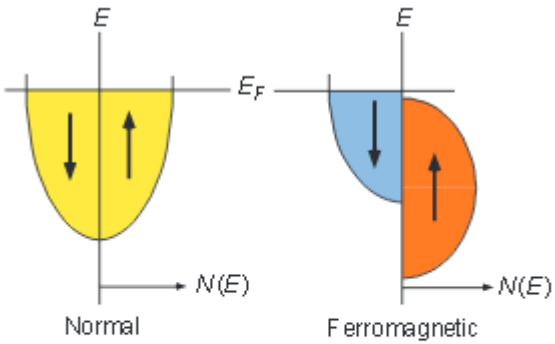

Fig. 1. A schematic representation of the density of electronic states that are available to electrons in a normal metal and in a ferromagnetic metal whose majority spin states are completely filled. E, the electron energy; E_F, the Fermi level; $N(E)$, density of states.

Spin bottleneck magnetoresistance

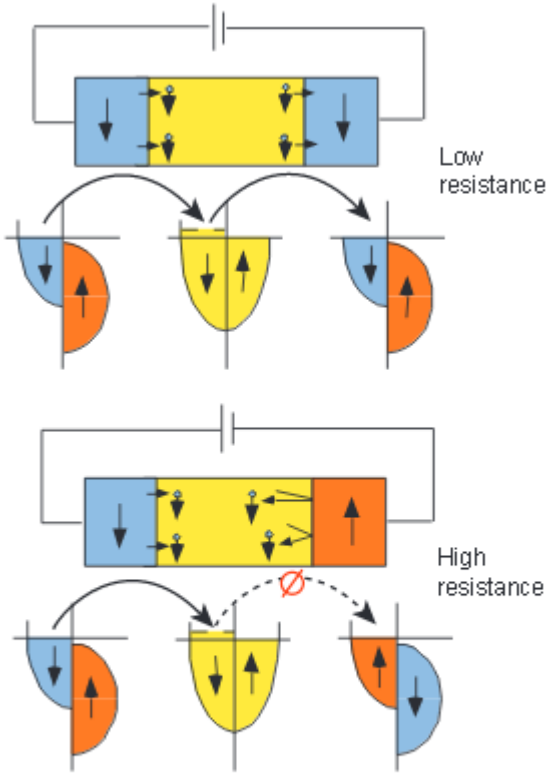

Fig. 2. Schematic representations of spin-polarized transport from a ferromagnetic metal, through a normal metal, and into a second ferromagnetic metal for aligned and antialigned magnetic moments. ∅, disallowed channel.

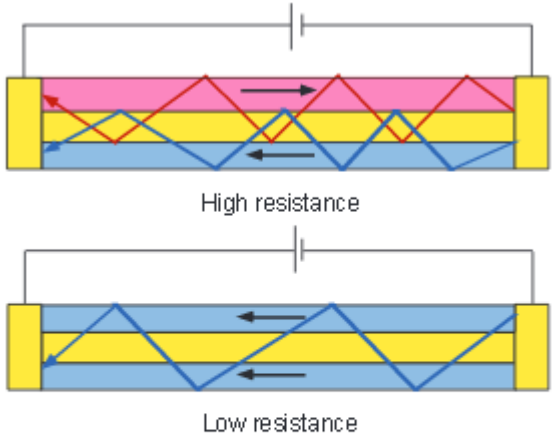

Fig. 3. Schematic representations of transport that is parallel to the plane of a layered magnetic metal sandwich structure for aligned (low resistance) and antialigned (high resistance) orientations.

SCIENCE VOL **282,** 1660 (1998)

(in)organic spintronics

Magnetoelectronics

Gary A. Prinz

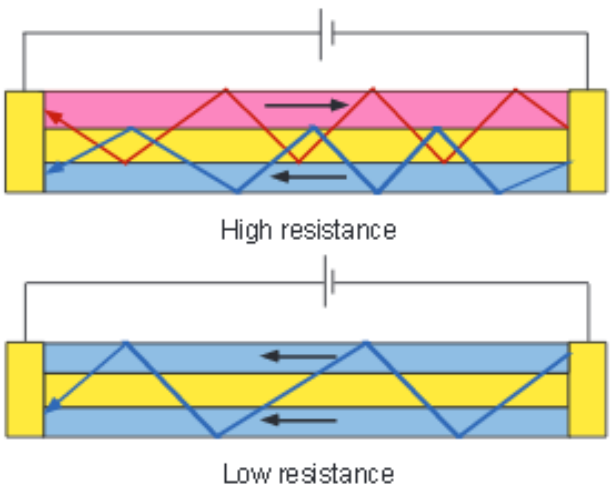

Fig. 3. Schematic representations of transport that is parallel to the plane of a layered magnetic metal sandwich structure for aligned (low resistance) and antialigned (high resistance) orientations.

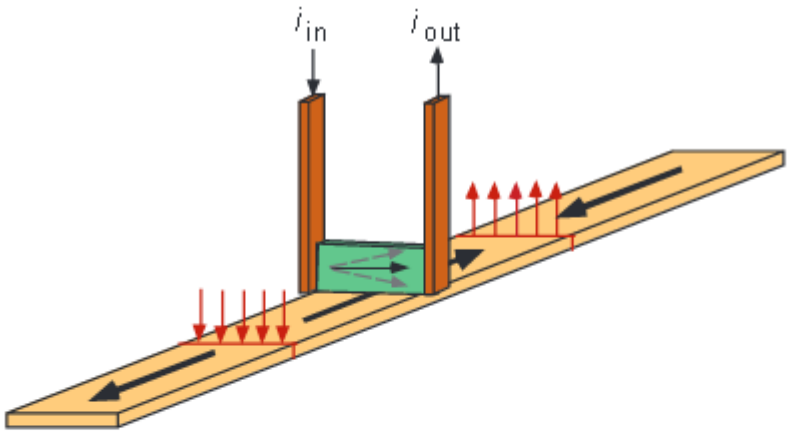

Fig. 4. A schematic representation of a GMR read head (green) that passes over recording media containing magnetized regions. The magnetization direction of the soft layer in the head responds to the fields that emanate from the media by rotating either up or down. The resulting change in the resistance is sensed by the current *i* passing through the GMR element.

SCIENCE VOL **282,** 1660 (1998)

(in)organic spintronics

Magnetoelectronics

Gary A. Prinz

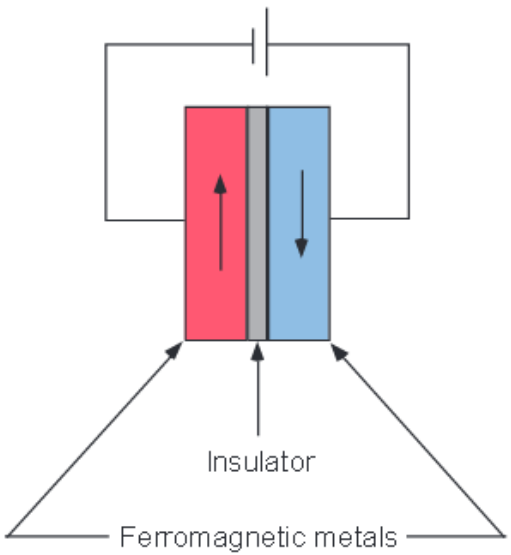

Fig. 6. A magnetic tunnel junction formed by a thin insulating barrier separating two ferromagnetic metal films. Current passing through the junction encounters higher resistance when the magnetic moments are antialigned and lower resistance when they are aligned.

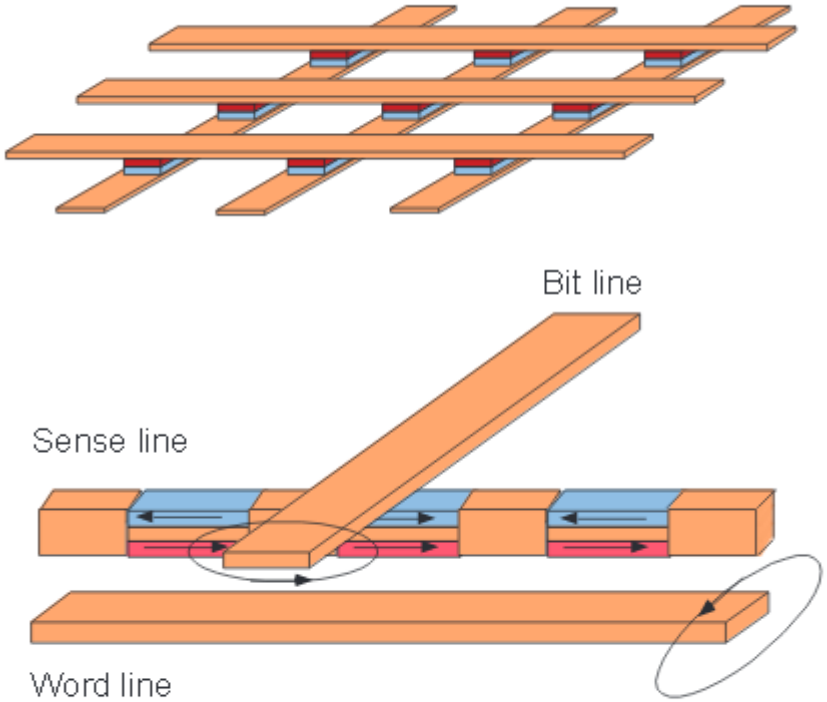

Fig. 5. A schematic representation of RAM that is constructed of GMR elements connected in series. The elements are manipulated for writing or reading by applying magnetic fields that are generated by currents passing through lines above and below the elements.

SCIENCE VOL **282,** 1660 (1998)

(in)organic spintronics – spin valve

The spin-valve transistor

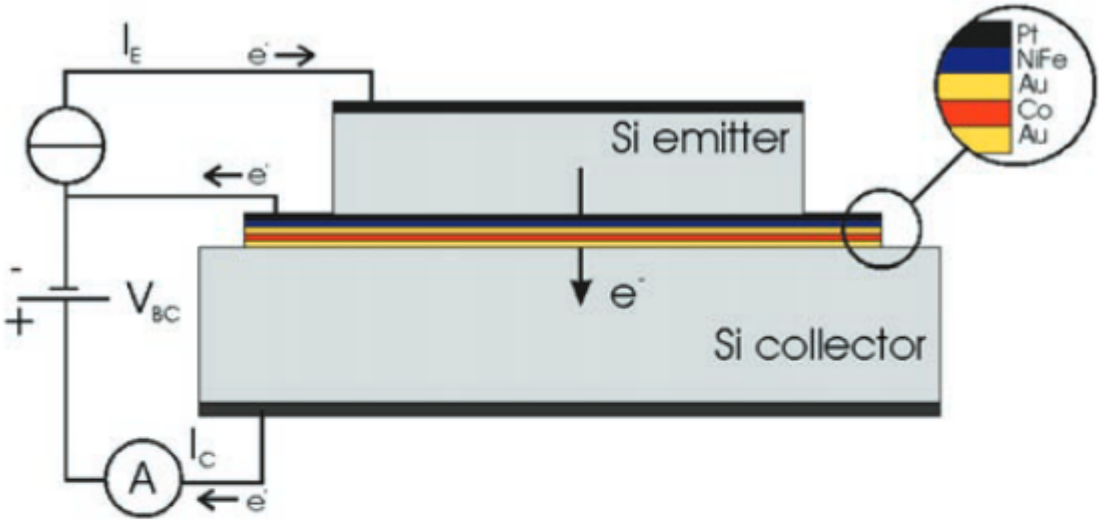

Figure 1. Schematic diagram of the cross-section of a spin-valve transistor showing the emitter, base and collector. The emitter is forward biased and the collector is reverse biased. I_E is the emitter current and I_C is the collector current. The base layer contains a spin valve (NiFe/Au/Co) in addition to a Si–Pt emitter diode and a Si–Au collector diode.

J. Phys. D: Appl. Phys. 33 (2000) 2911–2920

Diluted Magnetic Semiconductors

NATURE | VOL 408 | 21/28 DECEMBER 2000 | www.nature.com

Electric-field control of ferromagnetism

H. Ohno, D. Chiba, F. Matsukura, T. Omiya, E. Abe, T. Dietl*, Y. Ohno & K. Ohtani

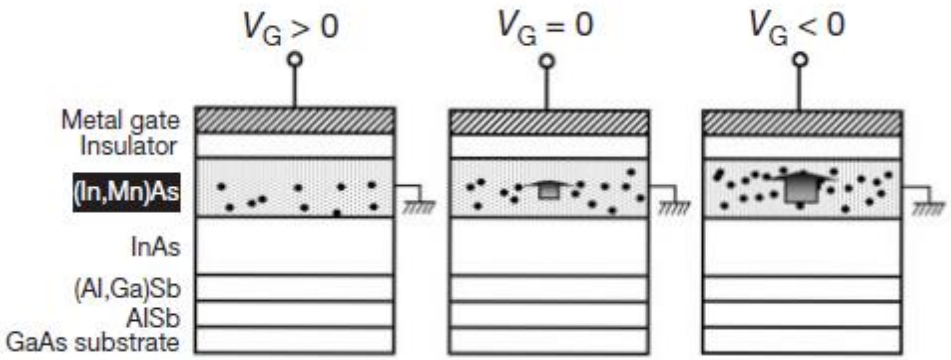

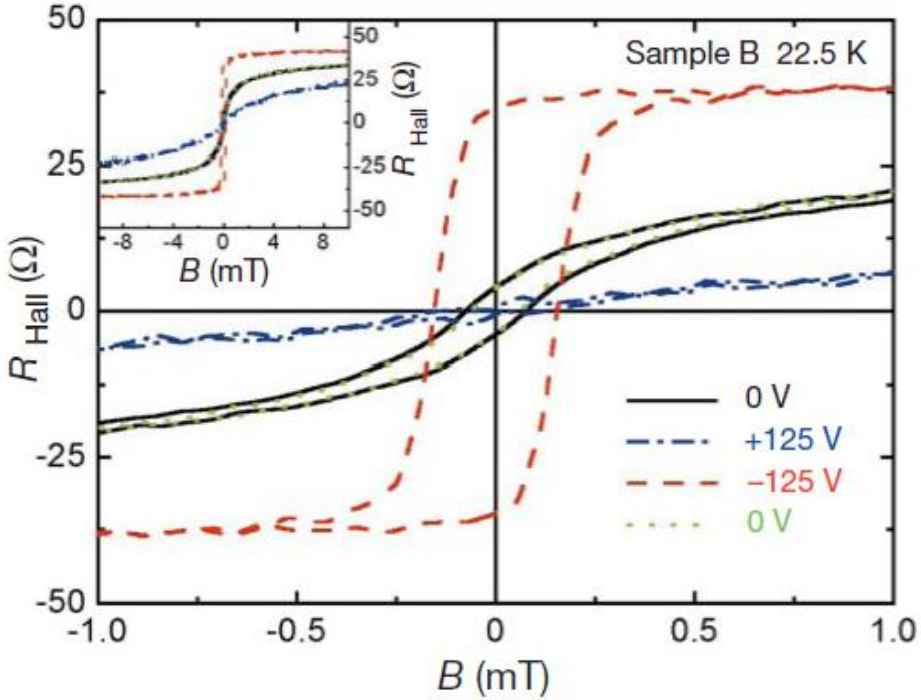

(in)organics spintronics – spin valve

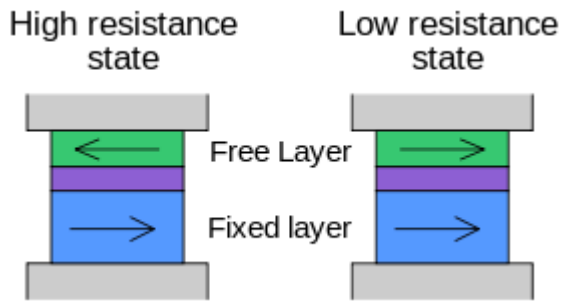

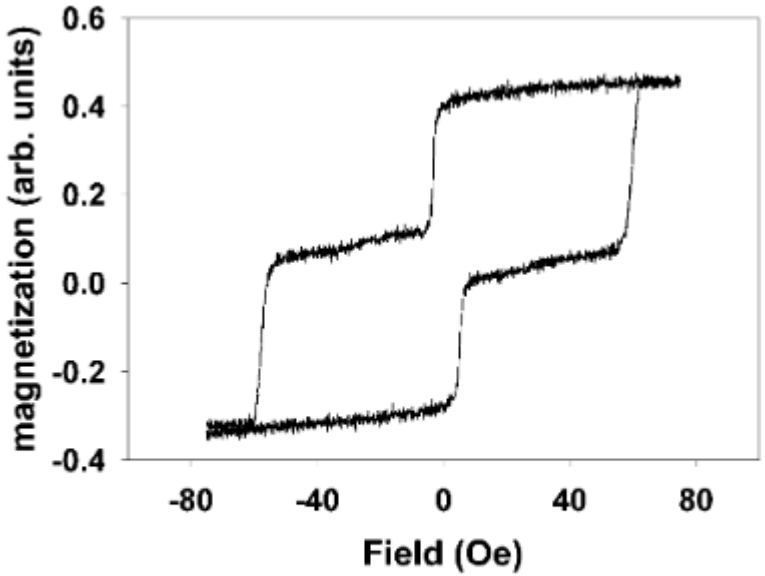

Figure 3. Magnetization as a function of the magnetic field of the spin valve (NiFe (3 nm)/Au (3.5 nm)/Co (3 nm)) grown on Si/Pt (2 nm). The curve shows well defined switching of the Co and permalloy layers at the respective coercive fields.

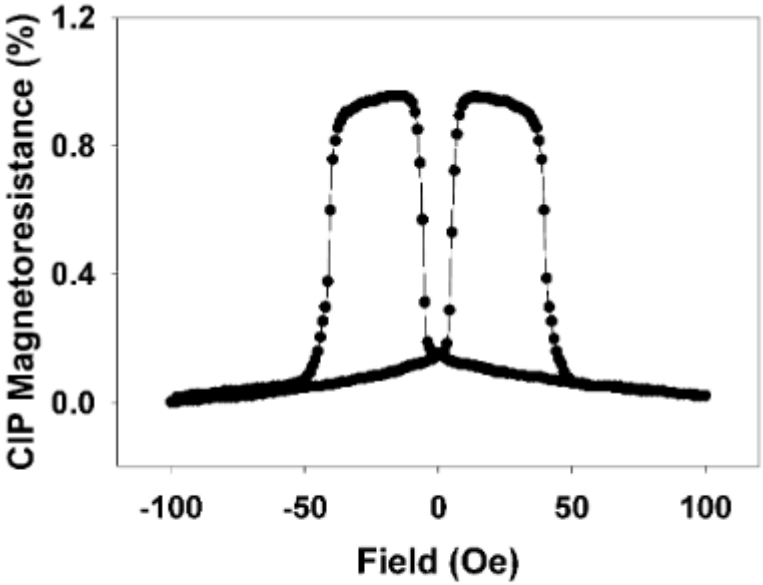

Figure 4. The magnetoresistance against the magnetic field of the spin valve (NiFe (3 nm)/Au (3.5 nm/Co (3 nm)/Au (2 nm)) grown on Si/Pt (2 nm) showing a magnetoresistance of about 1%.

Spintronics

Magnetic tunnel junction (MTJ)

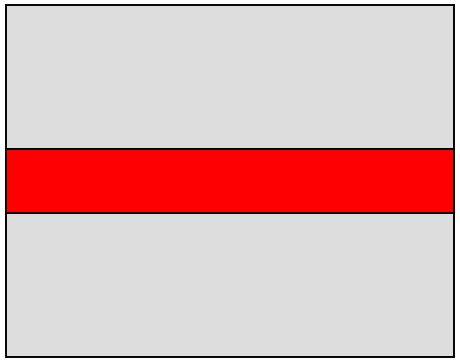

Ferromag. (soft)

Insulator (barrier)

Ferromag. (hard)

Ferromag.
  Co, Py, FeCo, etc.
Barrier
  Al2O3, MgO, etc.

$$TMR(\%)=(R_{AP}-R_P)/R_P*100$$

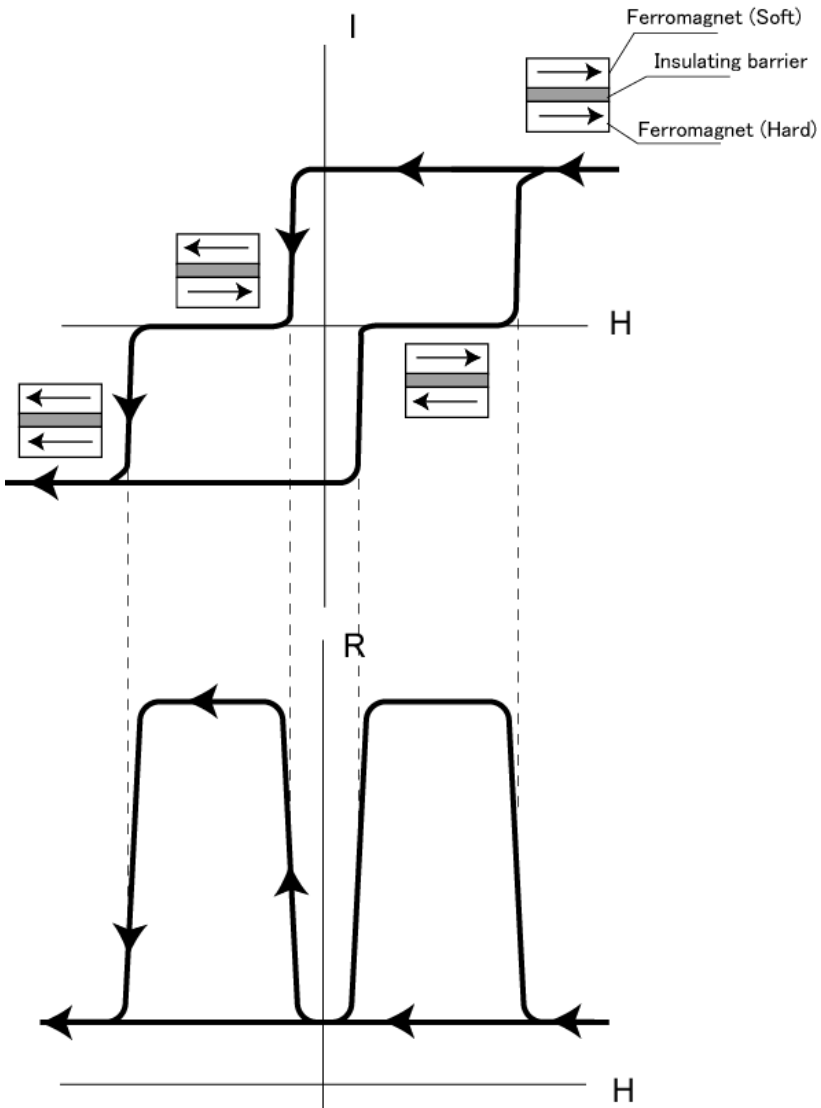

Takahiro Moriyama http://www.ece.udel.edu/~appelbau/spintronics/

Giant Magnetoresistance

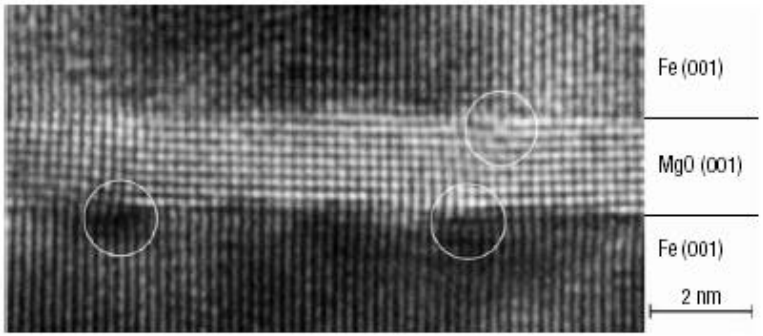

MgO

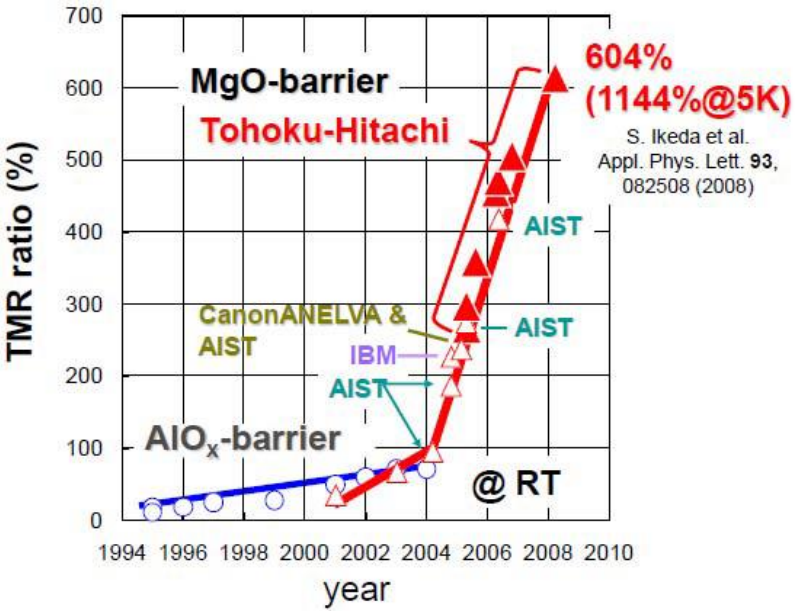

Spin-dependent tunneling conductance of Fe|MgO|Fe sandwiches
W. H. Butler, X.-G. Zhang, T. C. Schulthess, and J. M. MacLaren
Phys. Rev. B 63, 054416 (2001)

Organic Spintronics – spin valve

Molecular spin valves

Alq_3 hydroxy-quinoline aluminium

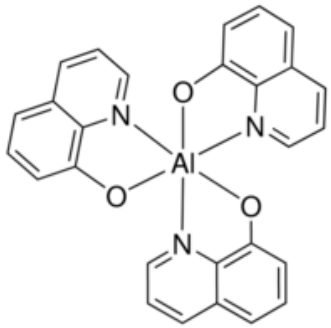

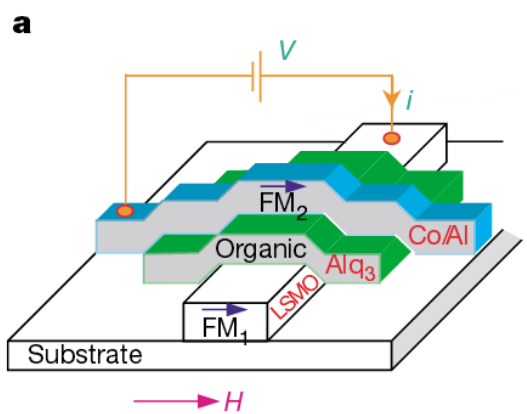

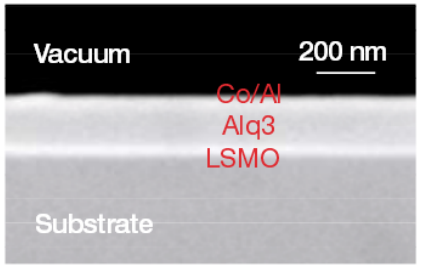

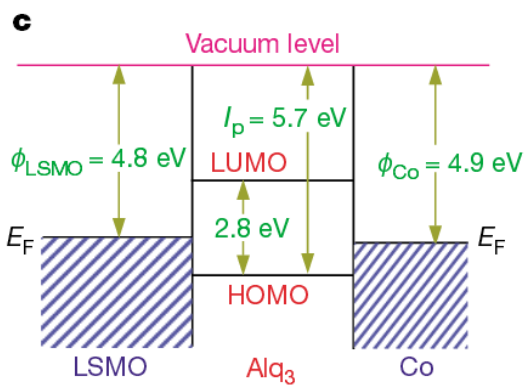

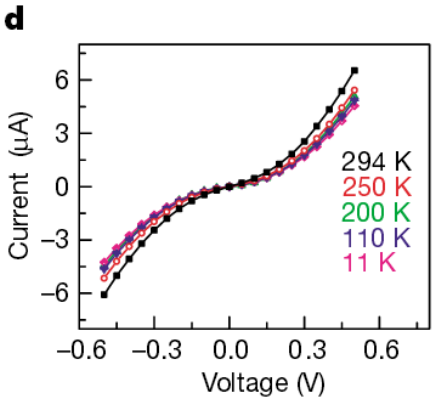

letters to nature

Giant magnetoresistance in organic spin-valves

Z. H. Xiong, Di Wu, Z. Valy Vardeny & Jing Shi

Department of Physics, University of Utah, Salt Lake City, Utah 84112, USA

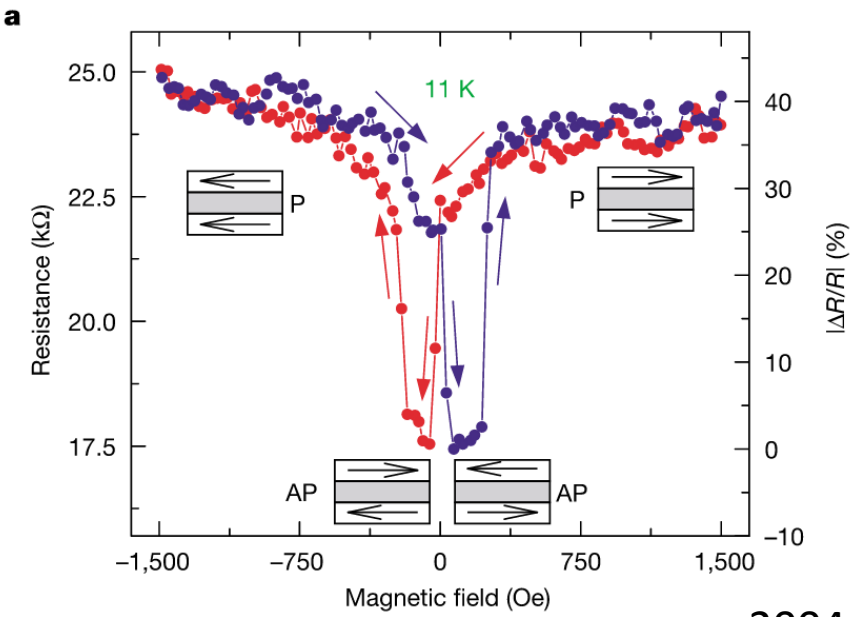

2004

Organic Spintronics

S. Sanvito, Nature Physics 6, 562 (2010)

MOLECULAR SPINTRONICS

The rise of spinterface science

Little is known about the mechanisms that govern the injection of spins into organic molecules. A new study suggests that the metal/organic interface is key, paving the way for a new field in which interfaces are specifically designed for spin applications. This is this field of 'spinterface' science.

Stefano Sanvito

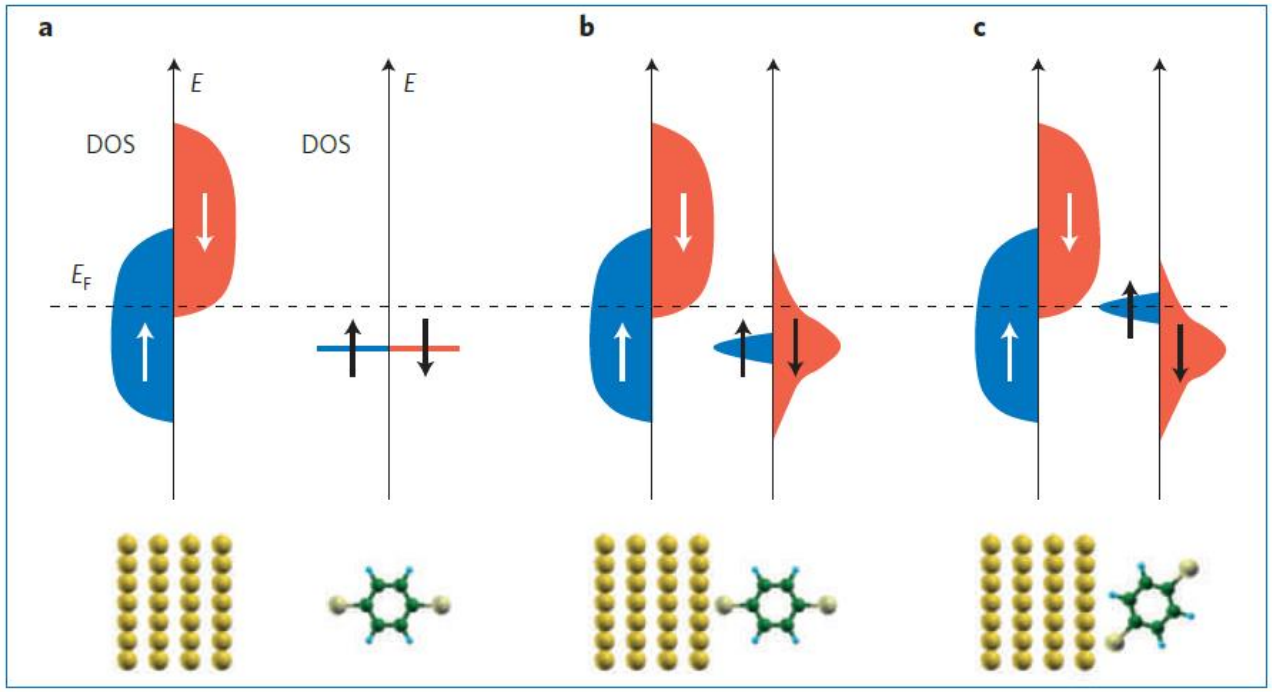

Figure 1 | Schematic of the spin-filtering mechanism at an organic/inorganic hybrid interface. **a**, When the magnetic metal (left) and the molecule (right) are well separated, the overall DOS is simply the superposition of the individual DOS of the two spin components (blue represents the spin-up DOS and red the spin-down DOS) — that is, a broad spin-polarized DOS for the metal and a series of discrete energy levels for the molecule (here only the HOMO is represented). In this case, the DOS of the metal alone determines the spin-polarization of the tunnelling current. **b**,**c**, When the molecule is brought into contact with the metal the DOS gets modified into two ways: the energy levels broaden (**b**) (the broadening is exaggerated in the figure) and their position shifts in energy (**c**). In both cases new peaks in the DOS might appear at the E_F of the electrodes, arising from new hybrid interfacial states. It is this new DOS that determines the spin-polarization of the injected current, which can be dramatically different, and even reversed, compared with the polarization of the electrodes (as in **b**).

Organic Spintronics

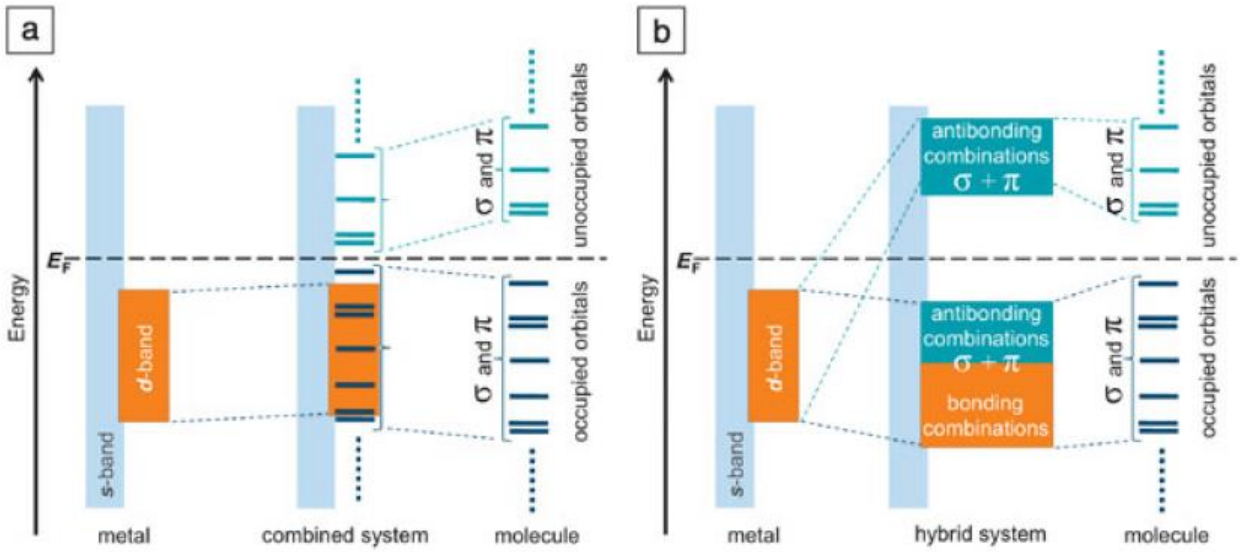

Figure 1. A general scheme illustrating the energy level alignment due to the interaction between an organic molecule and a metallic surface. (a) Physisorption creates a weak molecule-metal interaction causing renormalization of the highest occupied molecular orbital (HOMO)-lowest unoccupied molecular orbital (LUMO) gap in the molecule due to polarization effects.[18,19] (b) Chemisorption creates a strong molecule-metal interaction where the atomic-type orbitals that initially form the molecular orbitals hybridize with the metallic bands, leading to bonding and anti-bonding hybrid bands with mixed molecular-metallic character. Note: E_F, Fermi energy level.

Nicolae Atodiresei and Karthik V. Raman ■ MRS BULLETIN • VOLUME 39 • JULY 2014 • www.mrs.org/bulletin

Organic Spintronics

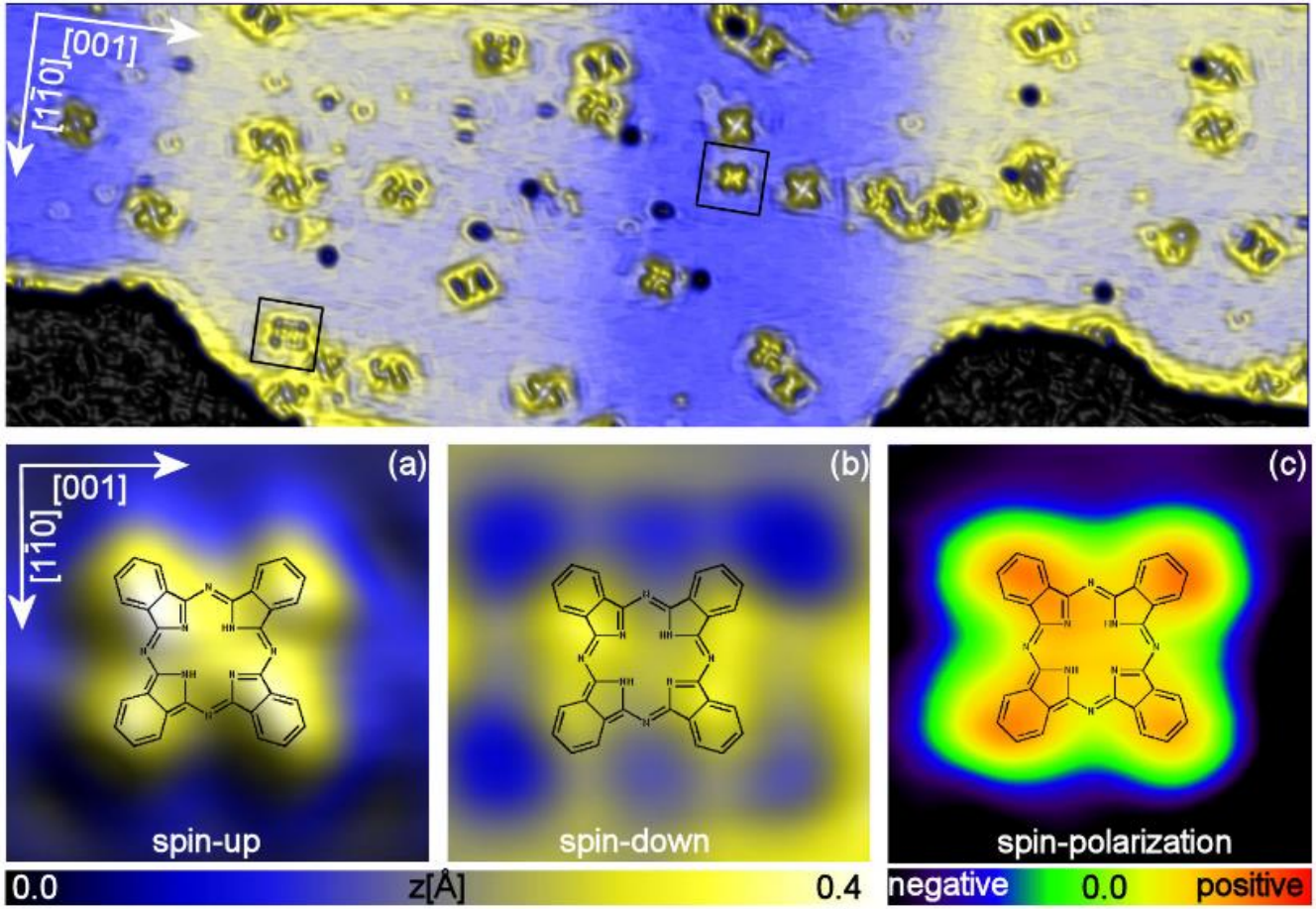

FIG. 3 (color online). Overview SP-STM image of a multi-domain (blue/yellow) 2 ML Fe stripe on W(110) with intact and few metalized H_2Pc present in three distinct orientations. Experimental (22 Å × 22 Å) SP-STM images for H_2Pc adsorbed on 2 ML Fe/W(110) at $U = +0.05$ V for both spin channels [i.e., up (↑) and down (↓)] and local spin polarization. H_2Pc molecules show a high, locally varying spin polarization ranging from attenuation to inversion with respect to the ferromagnetic Fe film.

Nicolae Atodiresei et al. Phys. Rev. Lett. 105, 066601 (2010)

Organic Spintronics

APPLIED PHYSICS LETTERS **106**, 082408 (2015)

Is spin transport through molecules really occurring in organic spin valves? A combined magnetoresistance and inelastic electron tunnelling spectroscopy study

Marta Galbiati,[1] Sergio Tatay,[1] Sophie Delprat,[1] Hung Le Khanh,[1] Bernard Servet,[2] Cyrile Deranlot,[1] Sophie Collin,[1] Pierre Seneor,[1,a)] Richard Mattana,[1,b)] and Frédéric Petroff[1]
[1]*Unité Mixte de Physique CNRS/Thales, 1 Av. A. Fresnel, 91767 Palaiseau, France and Université Paris-Sud, 91405 Orsay, France*
[2]*Thales Research & Technology, 1 Av. A. Fresnel, 91767 Palaiseau, France*

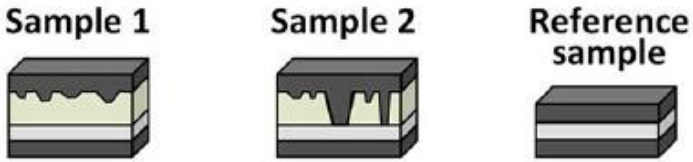

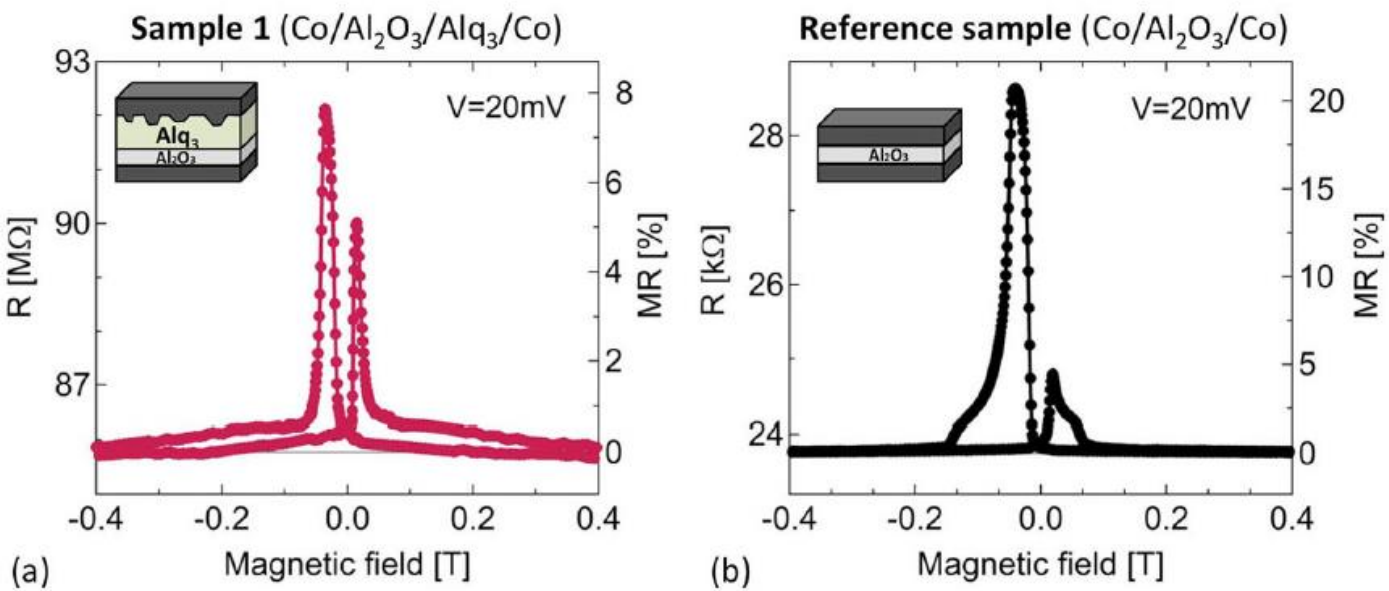

Organic Spintronics

ADVANCED MATERIALS

DOI: 10.1002/adma.200700559

Bistable Spin-Crossover Nanoparticles Showing Magnetic Thermal Hysteresis near Room Temperature**

By *Eugenio Coronado,* José Ramón Galán-Mascarós,* María Monrabal-Capilla, Javier García-Martínez*, and *Pablo Pardo-Ibáñez*

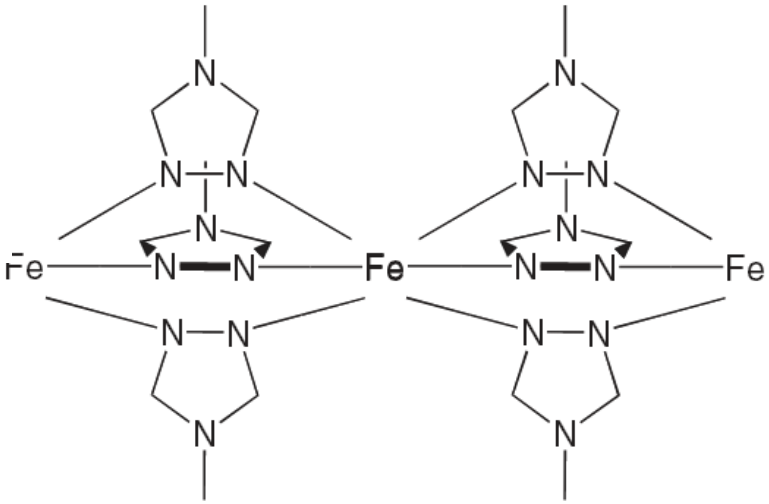

Scheme 1. Polymeric structure of the $[Fe(trz)_3]X_2$[15] family.

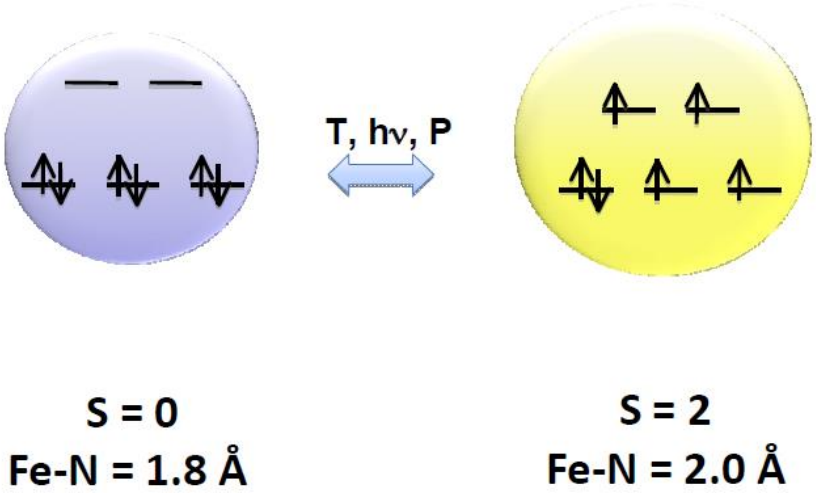

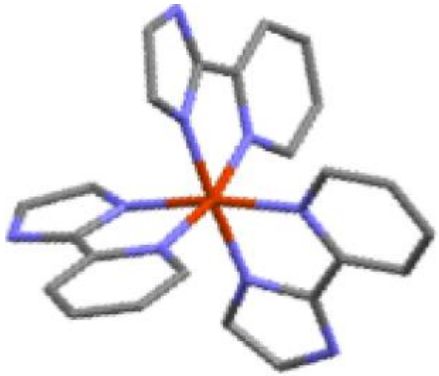

VNIVERSITAT DE VALÈNCIA

Organic Spintronics

Crystal field splitting (the presence of the ligants)
⇒ quenching of the orbital momentum

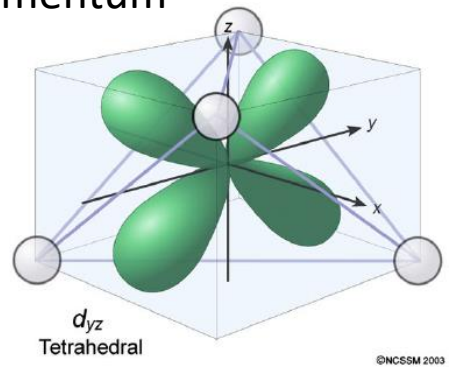

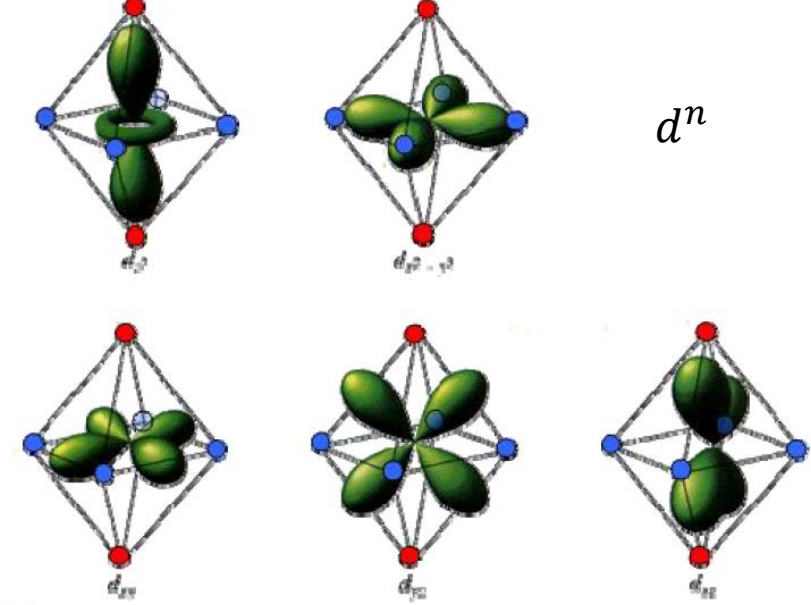

d^n

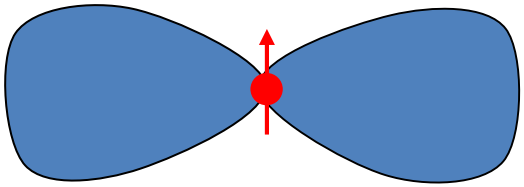

Fe^{2+} (d^6)

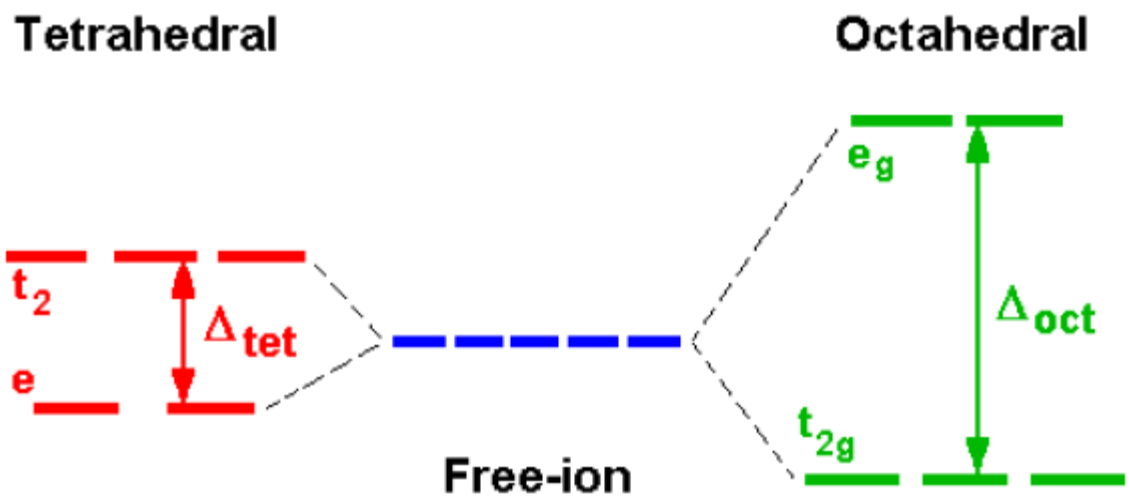

Crystal field (CF) splitting

Organic Spintronics

ADVANCED MATERIALS

DOI: 10.1002/adma.200700559

Bistable Spin-Crossover Nanoparticles Showing Magnetic Thermal Hysteresis near Room Temperature**

By *Eugenio Coronado,* José Ramón Galán-Mascarós,* María Monrabal-Capilla, Javier García-Martínez*, and *Pablo Pardo-Ibáñez*

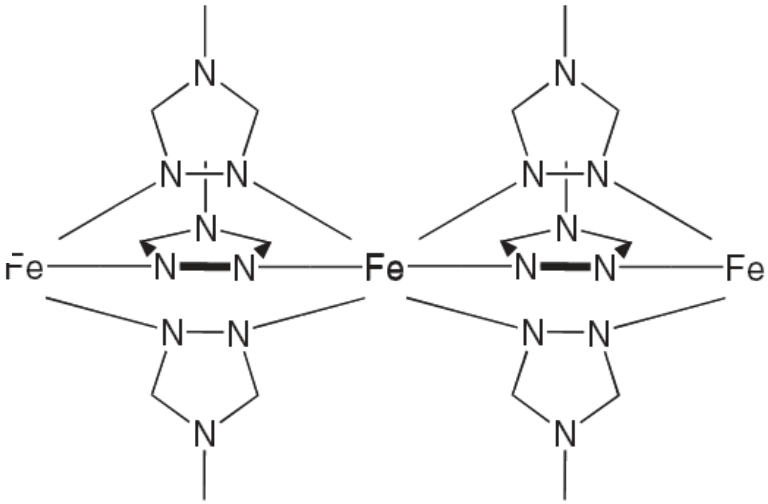

Scheme 1. Polymeric structure of the $[Fe(trz)_3]X_2$[15] family.

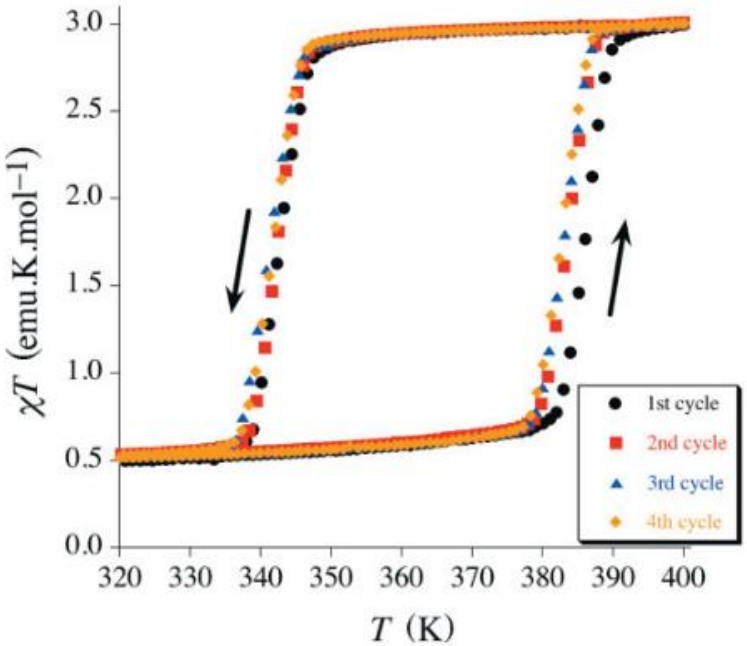

Figure 3. Magnetic thermal hysteresis for as-prepared $[Fe(Htrz)_2(trz)](BF_4)$ nanoparticles (magnetic moment represented per mole of Fe).

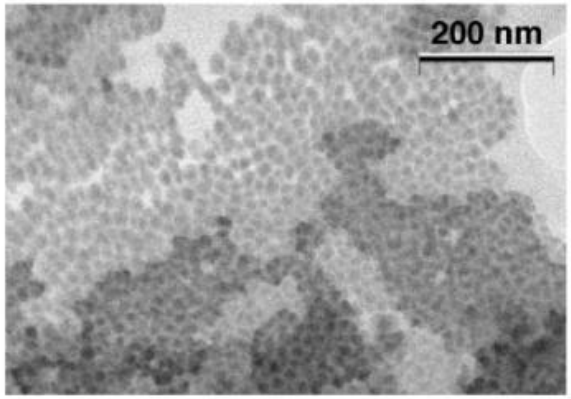

Figure 2. TEM image of as-prepared $[Fe(Htrz)_2(trz)](BF_4)$ nanoparticles.

Organic Spintronics

ADVANCED MATERIALS

DOI: 10.1002/adma.200700559

Bistable Spin-Crossover Nanoparticles Showing Magnetic Thermal Hysteresis near Room Temperature**

By *Eugenio Coronado,* José Ramón Galán-Mascarós,* María Monrabal-Capilla, Javier García-Martínez*, and *Pablo Pardo-Ibáñez*

Figure 1. Bistability of a suspension of the title nanoparticles in octane: in the low-spin state (left) and in the high-spin state (right).

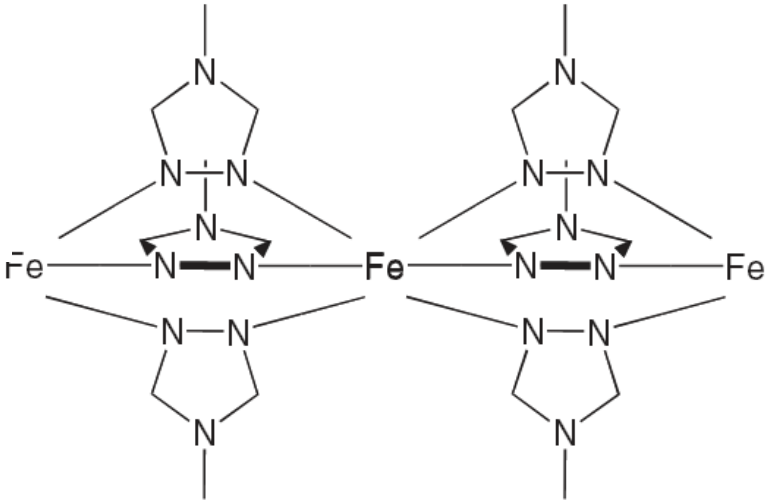

Scheme 1. Polymeric structure of the $[Fe(trz)_3]X_2$[15] family.

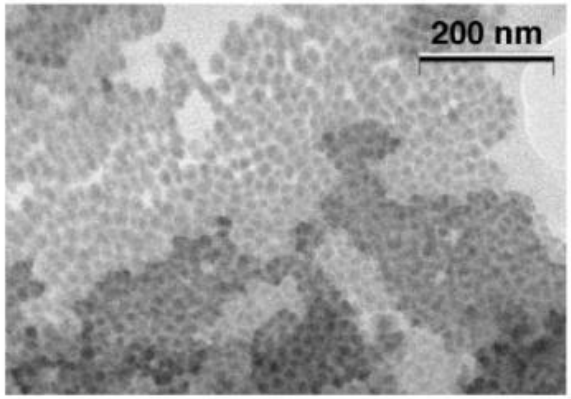

Figure 2. TEM image of as-prepared $[Fe(Htrz)_2(trz)](BF_4)$ nanoparticles.

Organic Spintronics

Materials Views
www.MaterialsViews.com

ADVANCED MATERIALS
www.advmat.de

Room-Temperature Electrical Addressing of a Bistable Spin-Crossover Molecular System

Ferry Prins, María Monrabal-Capilla, Edgar A. Osorio, Eugenio Coronado, and Herre S. J. van der Zant**

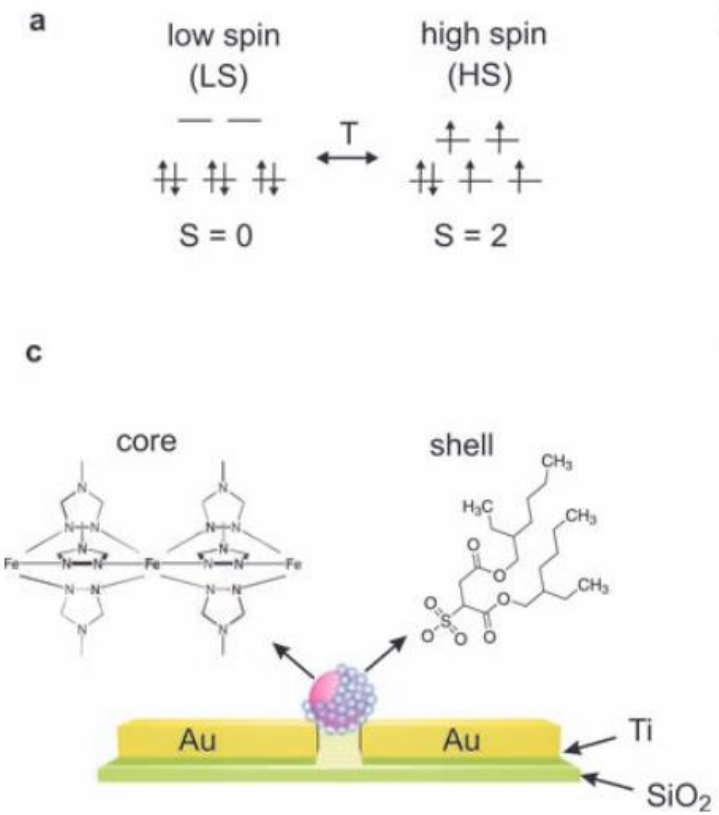

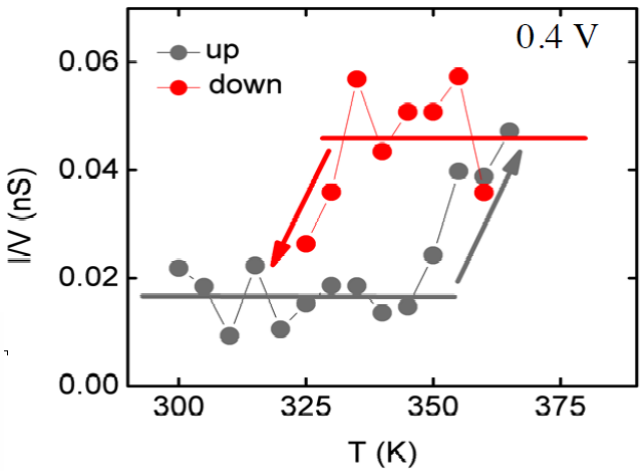

Spin-dependent conductivity

Organic Spintronics

Rare-earth complexes

Na[Dy(5,7Clq)$_4$](DMF)

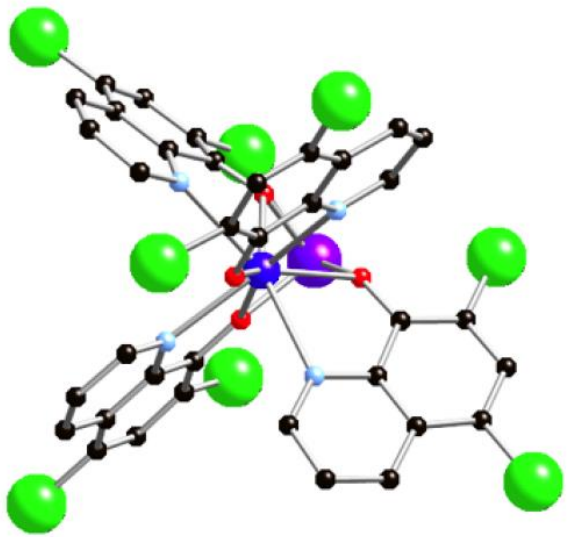

HoW_{10}

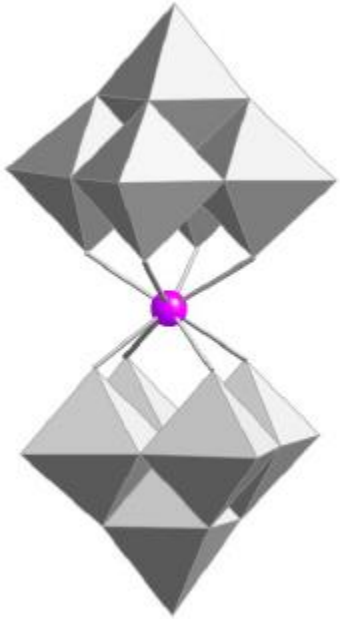

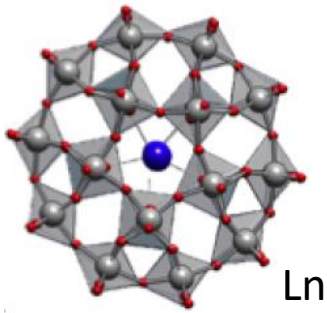

LnW_{30}

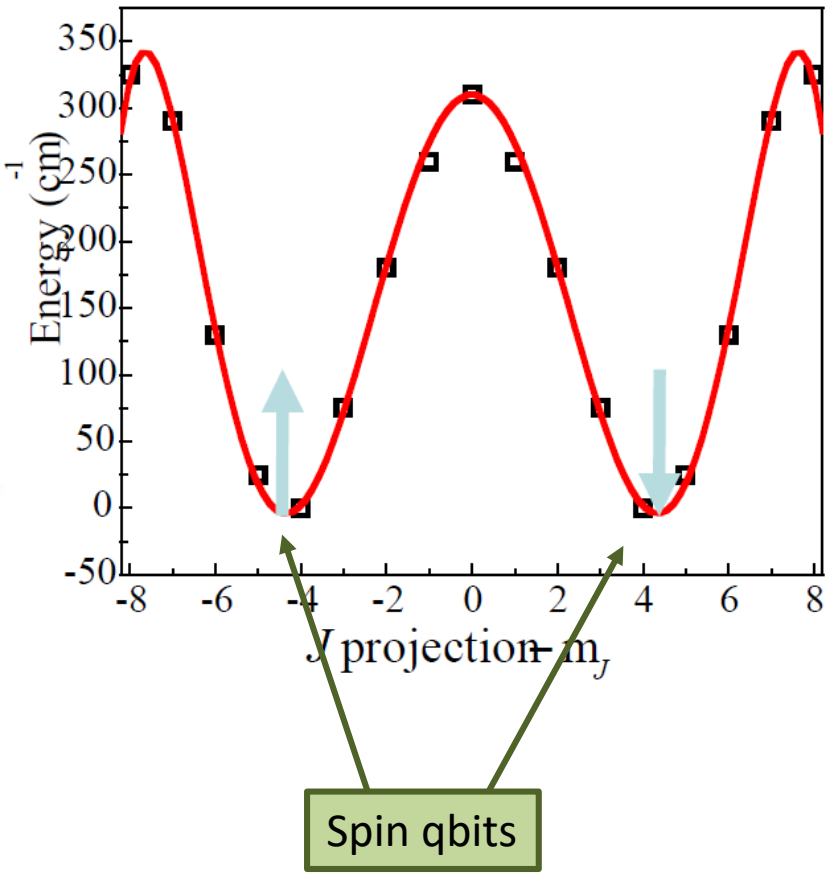

Ground state $m_J = \pm 4$

VNIVERSITAT DE VALÈNCIA

E. Coronado

Organic Spintronics

Long spin relaxation time due to the small spin-orbit couplin and small hyperfine interaaction ⇒ **spin qbits**

$Ho_{0.25}Y_{0.75}W_{10}$ Pulsed EPR (X-band)

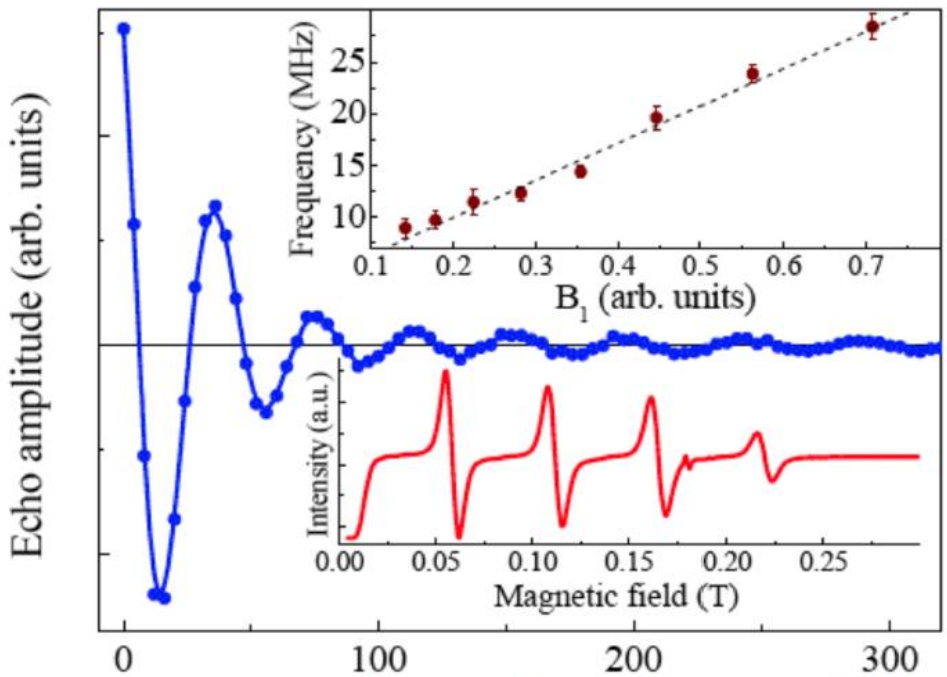

very robust spin qubit

Rabi oscillations
in a concentrated sample

$T_1 = 1\ \mu s$
$T_2 = 180$ ns

Long quantum coherence

M. Shiddiq, D. Komijani, Y. Duan, A. Gaita-Arino, E. Coronado, S. Hill "Enhancing coherence in molecular spin qubits via atomic clock transitions" Nature 531, 348 (2016).

Light

„Standard" spintronics

- There is a need for new materials (spin filters, spin transistors – Diluted Magnetic Semiconductors, Ferromagnetic Semiconductors, etc.)

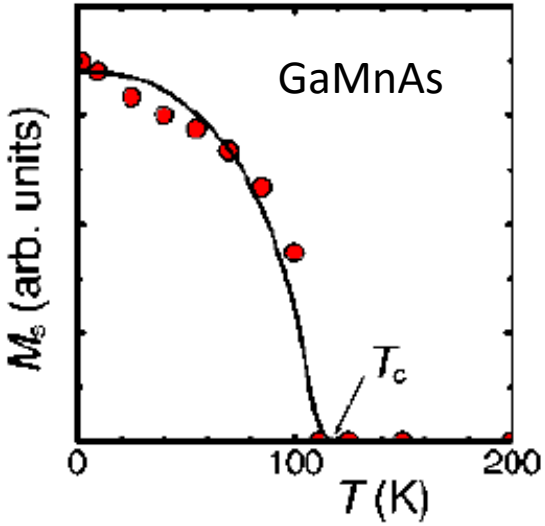

- There is a hope for new phenomena (light polarization, swithing magnetization on and off, etc.)

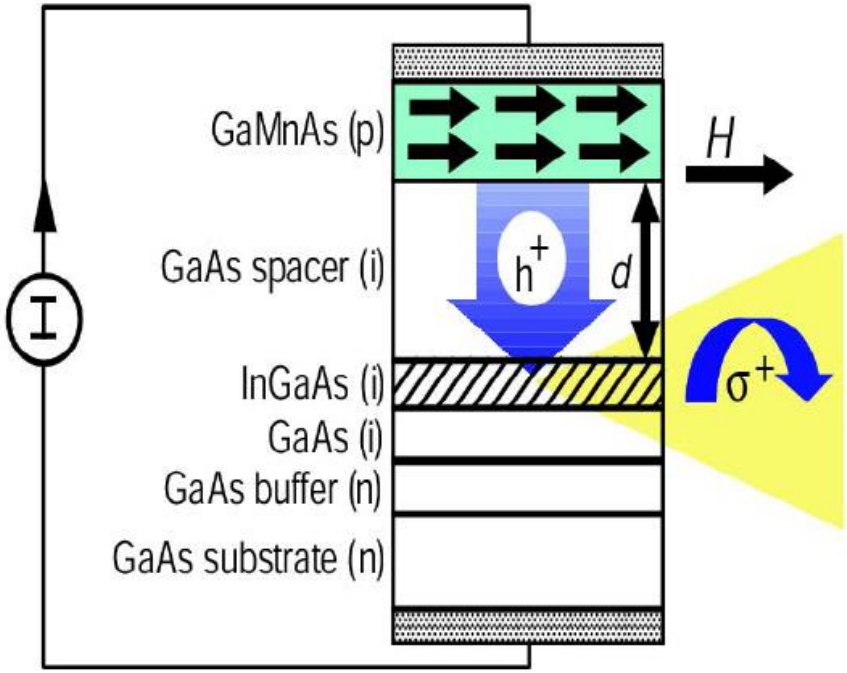

NATURE | VOL 402 | 16 DECEMBER 1999 | www.nature.com

Magnetic Semiconductors

NATURE | VOL 402 | 16 DECEMBER 1999 | www.nature.com

Electrical spin injection in a ferromagnetic semiconductor heterostructure

Y. Ohno*, D. K. Young†, B. Beschoten†, F. Matsukura*, H. Ohno* & D. D. Awschalom†

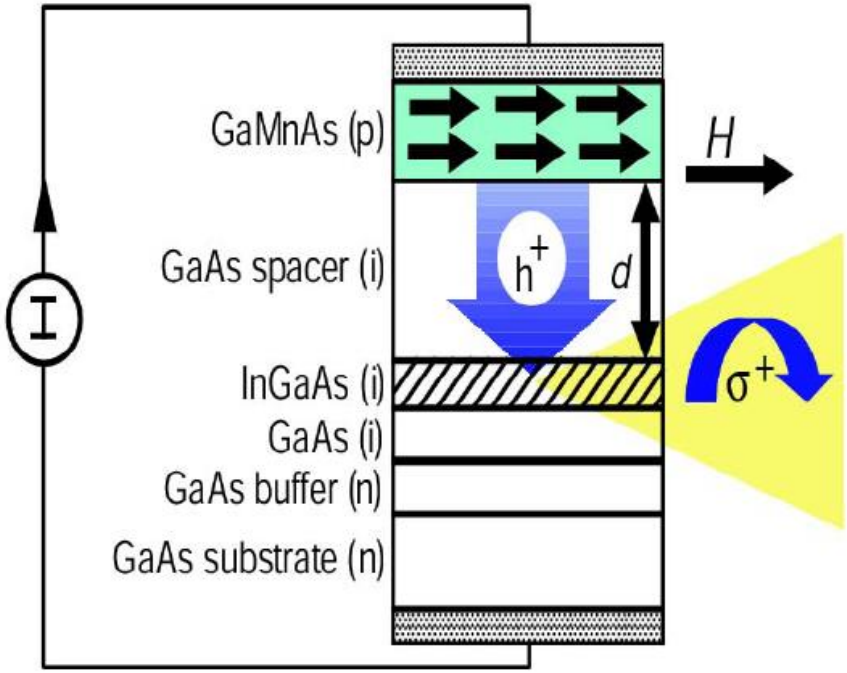

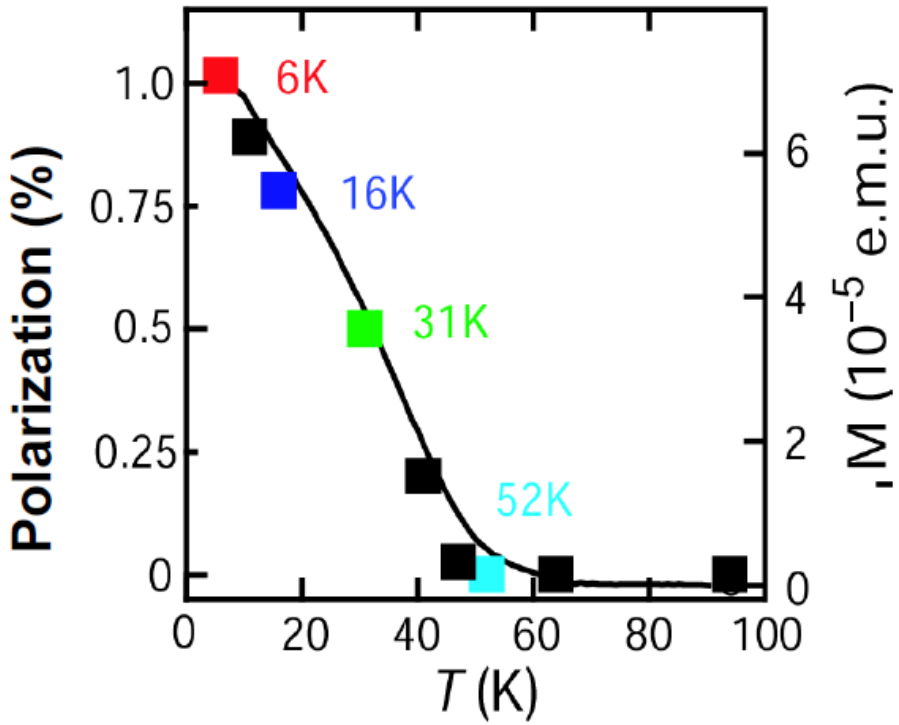

Organic Spintronics

Electroluminescence control using Magnetic field
(Magneto-Electro Luminescence (MEL) effect)

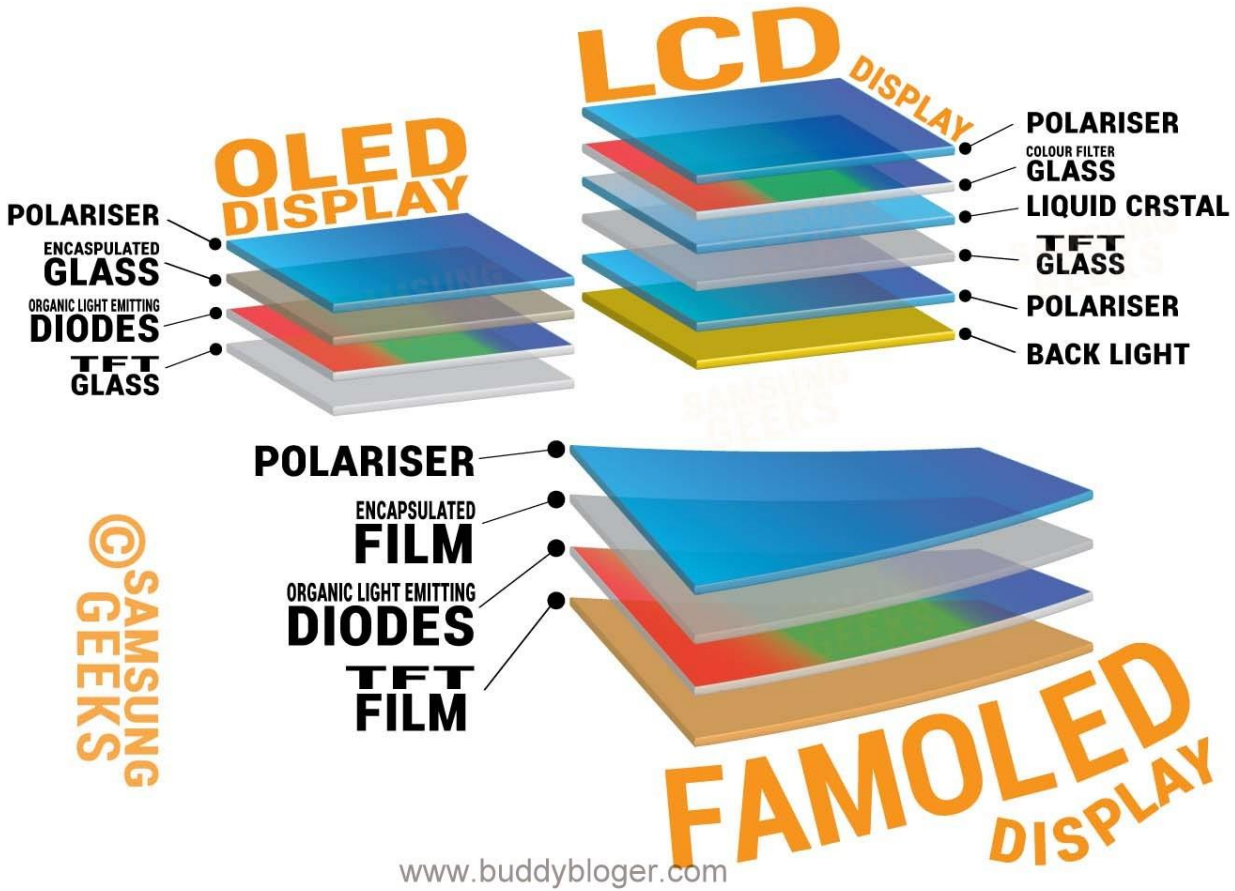

Organic Spintronics

Electroluminescence control using Magnetic field
(Magneto-Electro Luminescence (MEL) effect)

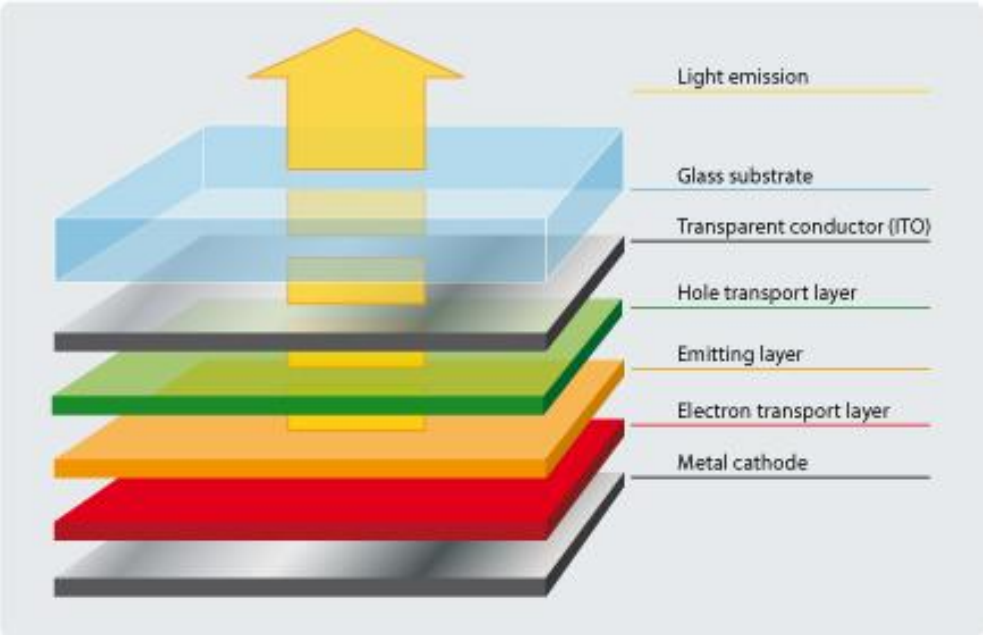

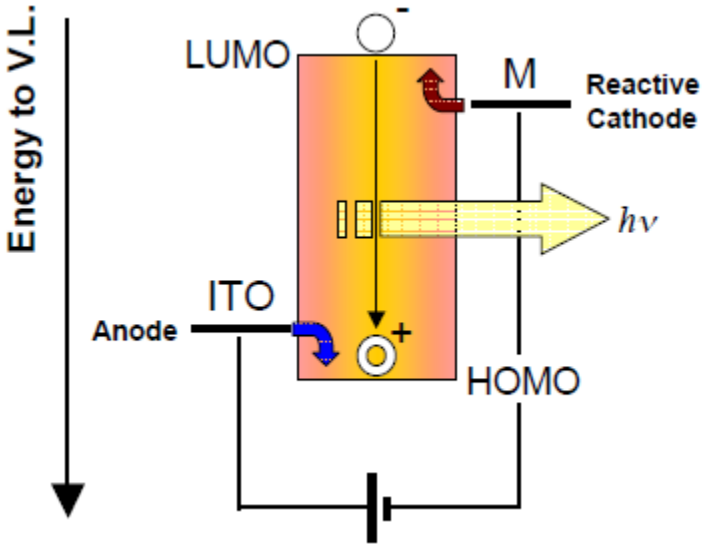

Organic Spintronics

Electroluminescence control using Magnetic field (Magneto-Electro Luminescence (MEL) effect)

Injection of chargé (e-, h+) in the EL device leads to the formation of two types of excitons

Singlet	Triplet
25%	75%
Bright	Dark

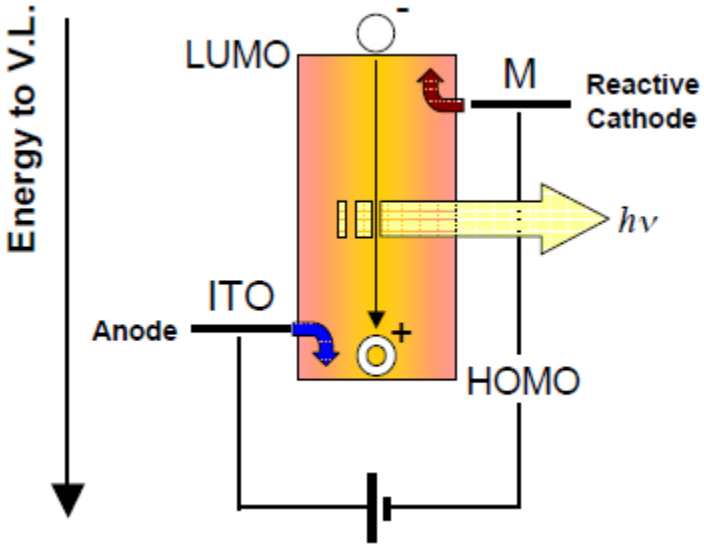

VNIVERSITAT DE VALÈNCIA

E. Coronado

Organic Spintronics

Electroluminescence control using Magnetic field
(Magneto-Electro Luminescence (MEL) effect)

Injection of chargé (e-, h+) in the EL device
leads to the formation of two types of excitons

Singlet	Triplet
25%	75%
Bright	Dark

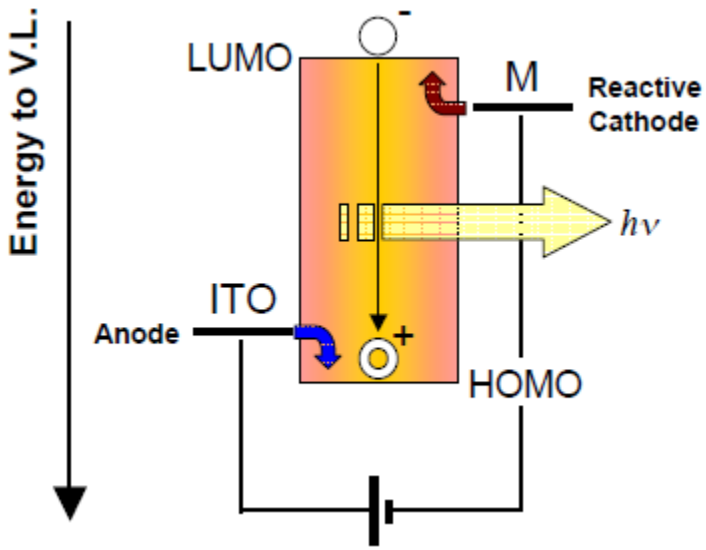

In a spin valve the current is spin polarized ⇒ by applying an external magnetic field the ratio single-triplet (and thus electroluminescence EL) should be controlled!

E. Coronado

Organic Spintronics

E. Coronado et al. Nature Chemistry 2, 1031–1036 (2010) doi:10.1038/nchem.898

Figure 1: Schematic representation of the layered components and the restacked material.

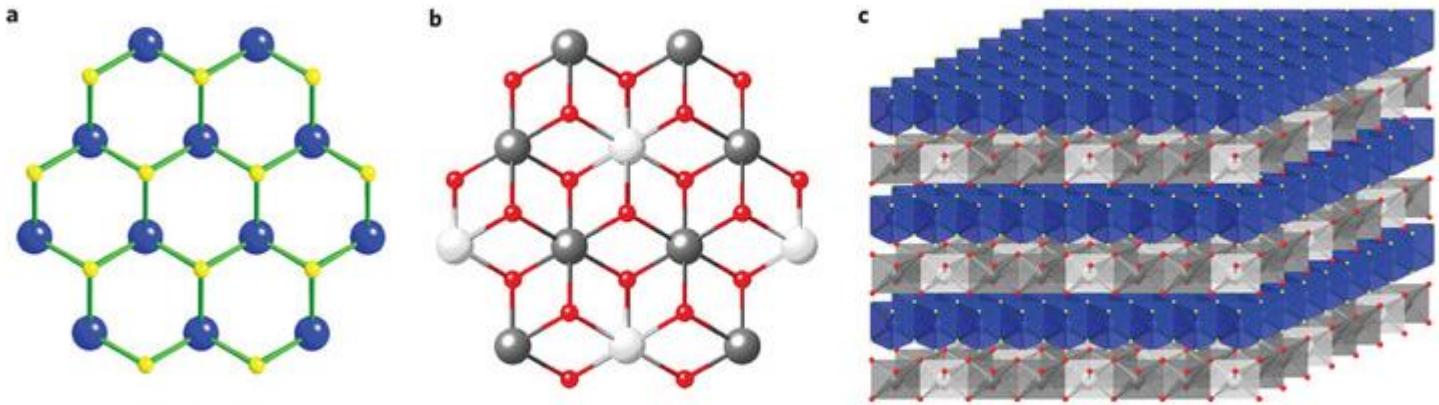

a, View of the $[TaS_2]^{-0.33}$ superconducting layer (Ta, blue spheres; S, yellow spheres). **b**, View of the $[Ni_{0.66}Al_{0.33}(OH)_2]^{+0.33}$ magnetic layer (Ni, grey spheres; Al, white spheres; O, red spheres). **c**, Representation of the restacked mat...

Organic Liquid Crystals Spintronics

Organic Spintronics

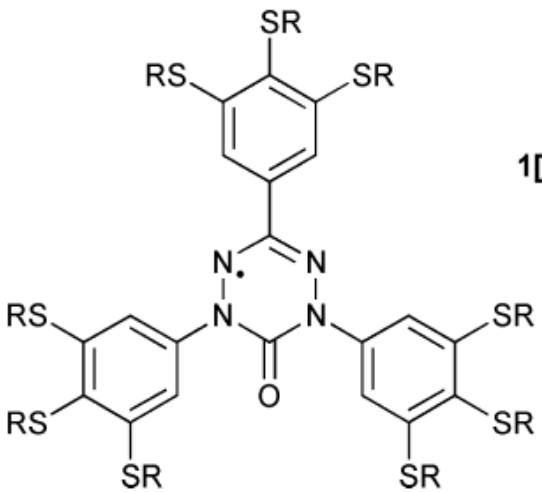

1[n] n = 6, R = C_6H_{13}
n = 8, R = C_8H_{17}
n = 10, R = $C_{10}H_{21}$
n = 12, R = $C_{12}H_{25}$

Scheme 1. Synthesis of Verdazyl Derivatives[a]

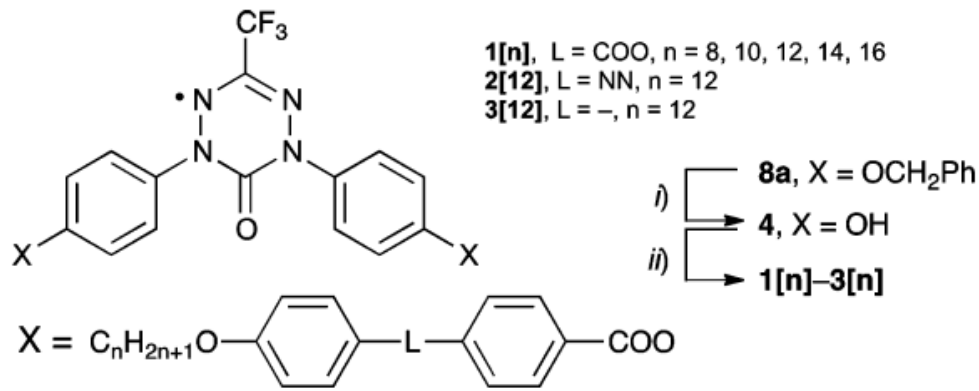

[a]Reagents and conditions: (*i*) H_2 (3 atm), Pd/C, THF-EtOH; (*ii*) RCOCl (5[n]–7[n]), DMAP, CH_2Cl_2, rt, 10 min.

Piotr Kaszyński, Jacek Szczytko et al.
JACS 134 (5), 2465-2468 (2012)
CHEM. COMMUN. 48, 7064-7066 (2012)
JACS 136 (42), pp 14658-14661 (2014)
LIQUID CRYSTALS 41, 1653-1660 (2014)
LIQUID CRYSTALS 41, 385-392 (2014)
J. OF MATERIALS CHEMISTRY C 2 319-324 (2014)

Organic Spintronics

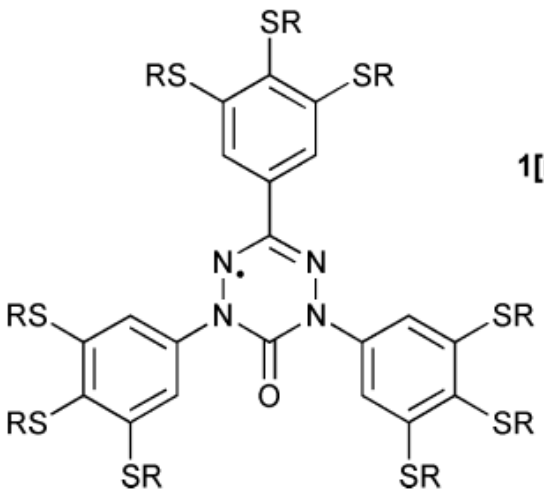

1[n] n = 6, R = C_6H_{13}
n = 8, R = C_8H_{17}
n = 10, R = $C_{10}H_{21}$
n = 12, R = $C_{12}H_{25}$

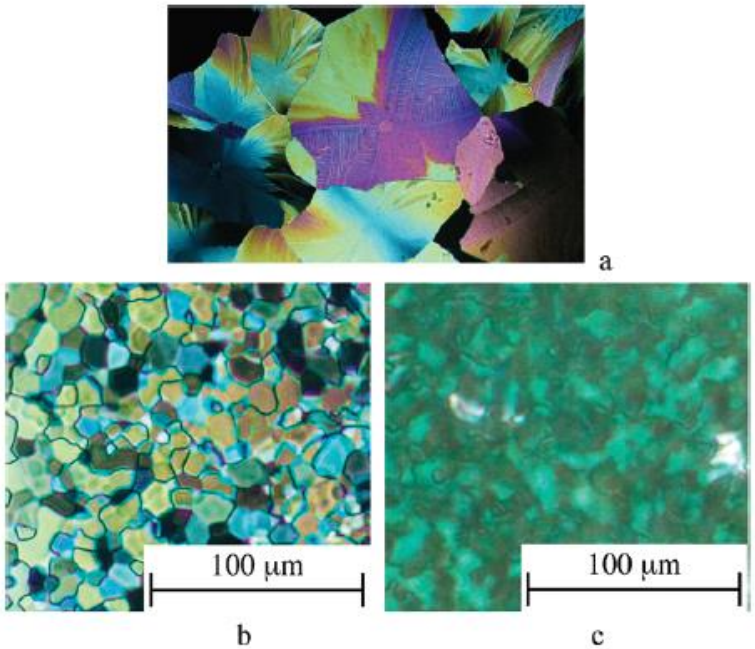

Figure 3. Optical textures of **1**[8] obtained upon (a) slow cooling, (b) fast cooling, and (c) after 2 h at 30 °C [8× longer exposure than in (b)].

Piotr Kaszyński, Jacek Szczytko et al.
JACS 134 (5), 2465-2468 (2012)
CHEM. COMMUN. 48, 7064-7066 (2012)
JACS 136 (42), pp 14658-14661 (2014)
LIQUID CRYSTALS 41, 1653-1660 (2014)
LIQUID CRYSTALS 41, 385-392 (2014)
J. OF MATERIALS CHEMISTRY C 2 319-324 (2014)

Organic Spintronics

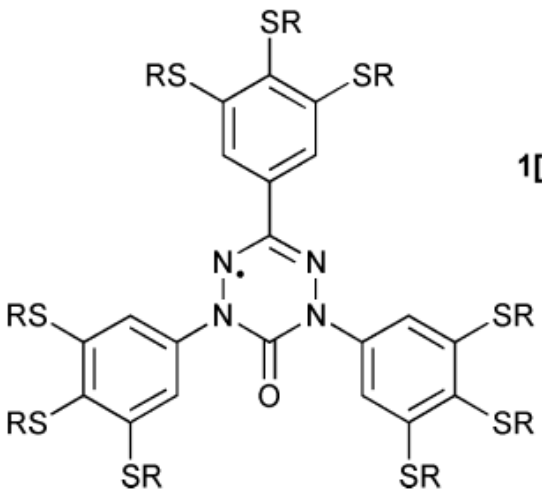

1[n]

n = 6, R = C_6H_{13}
n = 8, R = C_8H_{17}
n = 10, R = $C_{10}H_{21}$
n = 12, R = $C_{12}H_{25}$

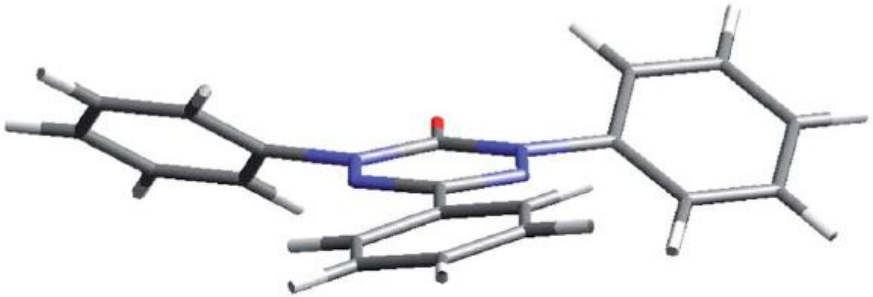

Fig. 9 B3LYP/6-31G(2d,p) optimized geometry for 7 with the imposed C_2 symmetry.

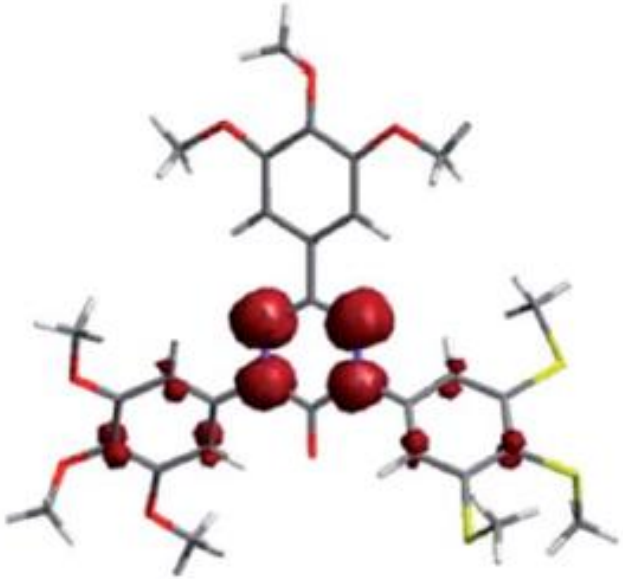

B3LYP/6-31G(d,p) derived total spin density in 1[1]c.

Organic Spintronics

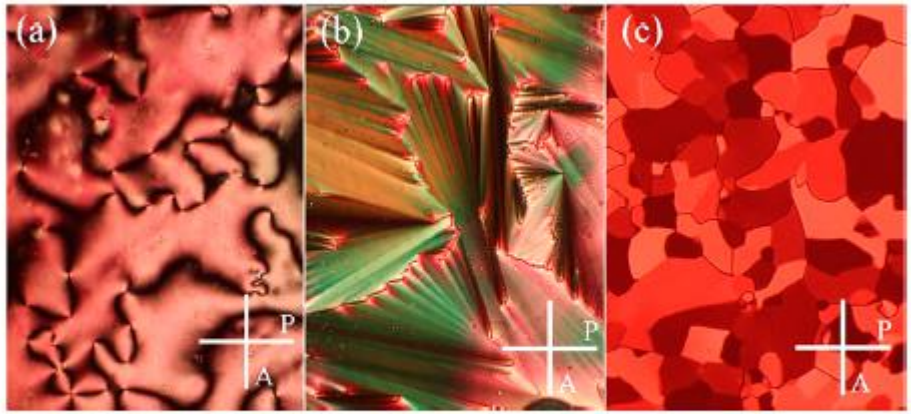

Figure 2. Optical textures of (a) N and (b) Sm phases in **1**[8] and (c) Tet phase in **1**[16].

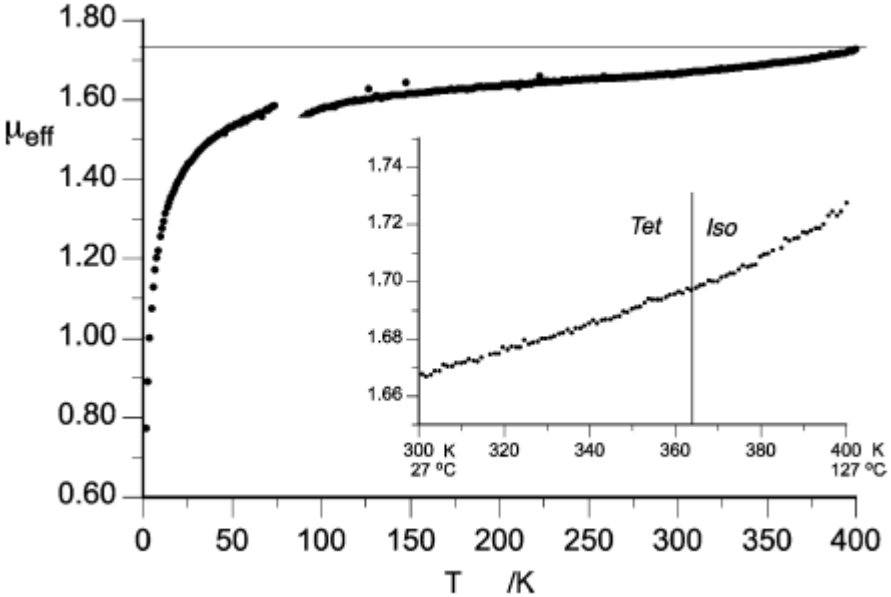

Organic Spintronics

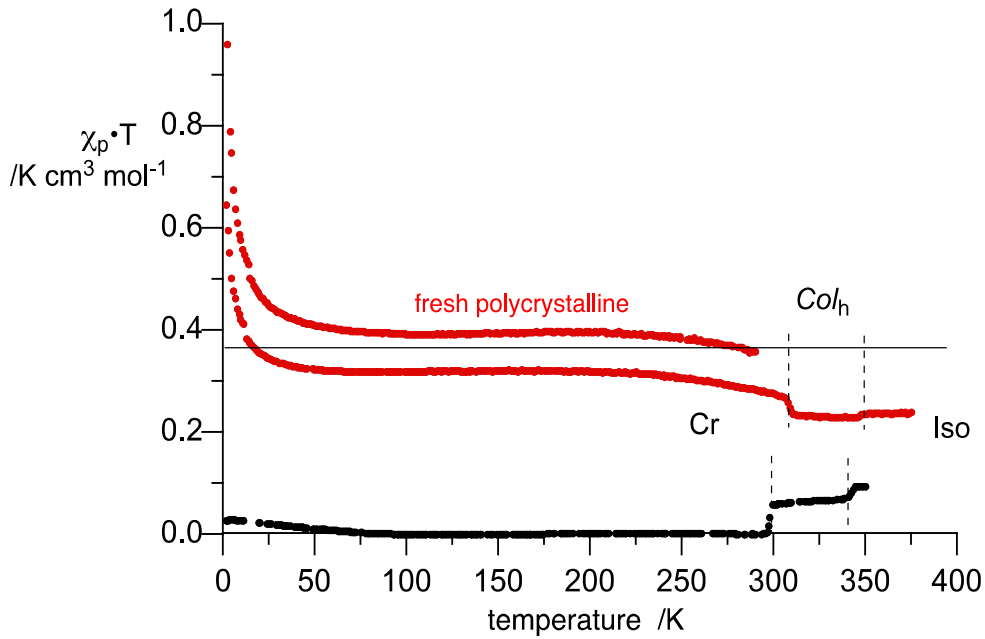

Organic Spintronics

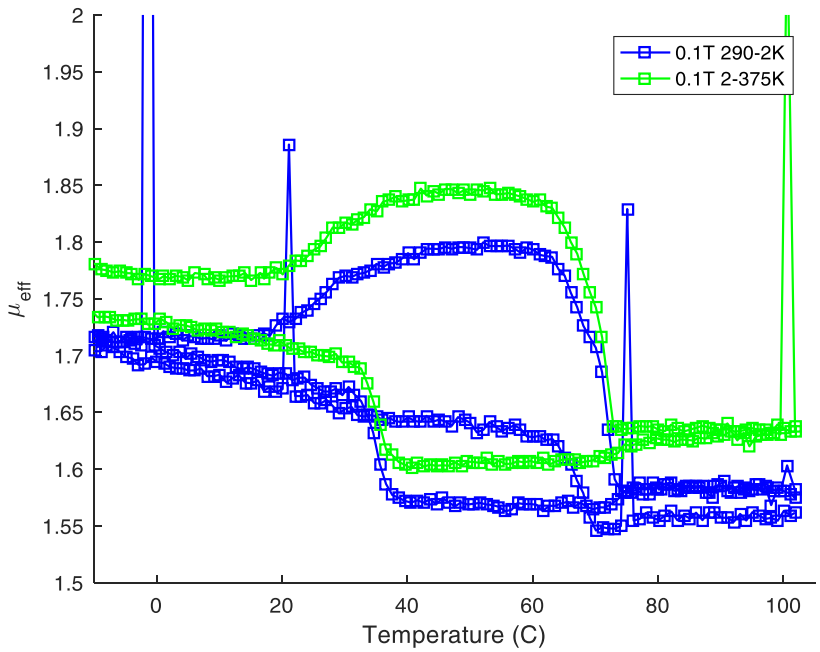

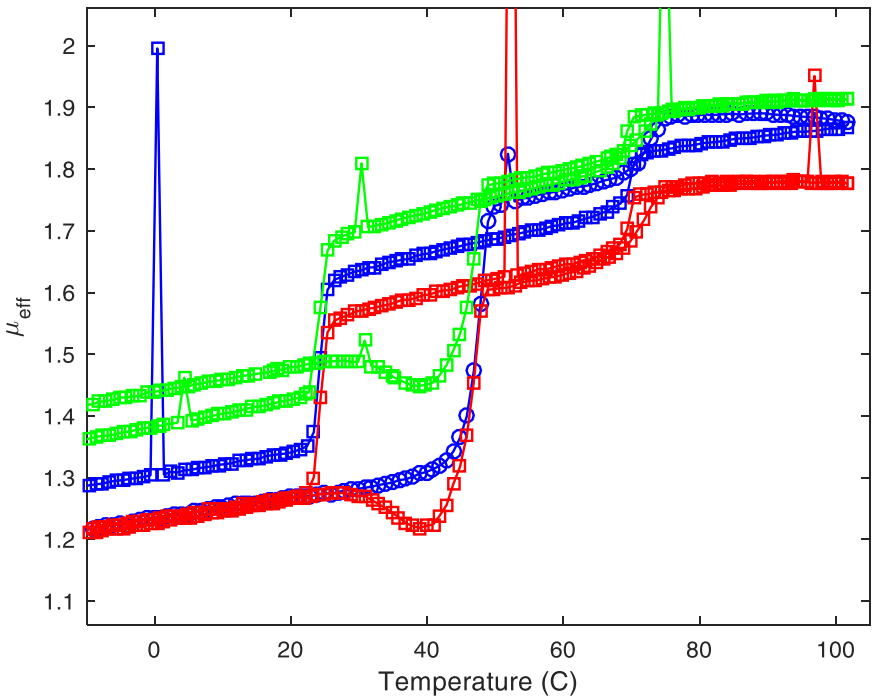

supercooled liquid

Spintronics

Semiconductor Devices

Transistors

IC, LSI, porcessors

Diodes (LED, Lasers)

Memory (RAM, EPROM, FLASH)

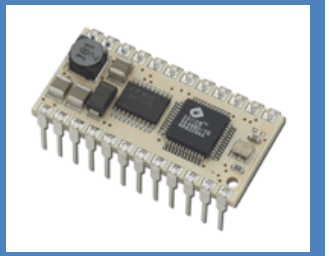

Magnetic Devices

Non-volatile memory

Storage (HDD, floppy, streamer)

Magneto-optical devices

Optical isolators (Faraday rotation)

charge

spin

High-speed high-density nonvolatile memory

Reconfigurable logic devices

Integrated magneto-optical devices

Quantum information processing with spin

SPINTRONICS

light

Optical Devices

Telecomunication (fibres, amplifiers)

Diodes (LED, Lasers)

Photo detectors

Organic Spintronics

Organic Semiconductor Devices

Transistors

IC, LSI, porcessors

Diodes (LED, Lasers)

Memory (RAM, EPROM, FLASH)

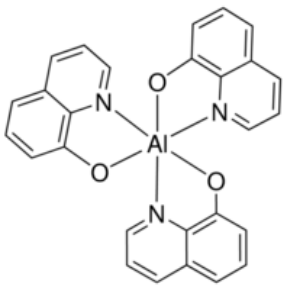

Organic Magnetic Devices

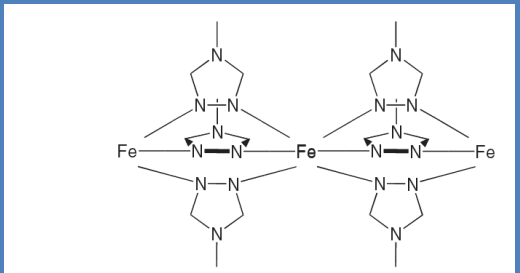

Scheme 1. Polymeric structure of the $[Fe(trz)_3]X_2$[15] family.

charge

spin

light

Optical Devices

Telecomunication (fibres, amplifiers)

Diodes (LED, Lasers)

Photo detectors